DESCRIBING THE ROLES OF MYELOID CELLS IN THE COMPARTMENTAL DEGENERATION OF RETINAL GANGLION CELLS IN THE NEURODEGENERATIVE DISEASE GLAUCOMA

by

Kevin Thomas Breen

A dissertation submitted to the faculty of
The University of Utah
in partial fulfillment of the requirements for the degree of

Doctor of Philosophy

in

Neuroscience

Department of Neurobiology and Anatomy

The University of Utah

December 2015

Copyright © Kevin Thomas Breen 2015

All Rights Reserved

The University of Utah Graduate School

STATEMENT OF DISSERTATION APPROVAL

The dissertation of **Kevin Thomas Breen**

has been approved by the following supervisory committee members:

Monica Lynn Vetter	, Chair	**5/11/2015** Date Approved
Scott Warren Rogers	, Member	**5/11/2015** Date Approved
Karen Sue Wilcox	, Member	**5/11/2015** Date Approved
Ning Tian	, Member	**5/11/2015** Date Approved
H. Joseph Yost	, Member	**5/11/2015** Date Approved

and by **Richard Dorsky** , Chair/Dean of

the Department/College/School of **Neuroscience**

and by David B. Kieda, Dean of The Graduate School.

ABSTRACT

The role that myeloid innate immune cells play in neurodegeneration has long fascinated researchers because of the apparent changes of these cells found in all neurodegenerative diseases. However, it has become clear that the different parts or compartments of a neuron that traverse different anatomical environments degenerate at different times. Since there are myeloid cells around all of these neuronal compartments, answering the question of how myeloid cells impact the process of compartmentalized neurodegeneration is challenging. Further complicating this question is the fact that these cells can rapidly change their morphology and function in a process termed activation. In these activated states, myeloid cells have the capacity to regulate many aspects of neuronal damage and repair. Lastly, these myeloid cells are derived from different lineages that may play different roles in neurodegeneration.

Many authors have manipulated myeloid cells by loss of the receptor (CX3CR1) for the chemokine fractalkine and arrived at contrasting and context-dependent results even within models of the same neurodegenerative disease. Few studies have examined loss of fractalkine signaling in multiple compartments and even fewer have collected these data for each animal. Therefore, it remains unknown how loss of fractalkine signaling affects compartmentalized neurodegeneration.

Since the chronic mouse model of glaucoma, the DBA/2J, grants easy access to different degenerating retinal ganglion cell (RGC) compartments, it is an ideal system to

determine how myeloid cells affect neuronal compartmentalized degeneration. The DBA/2J also features changes to myeloid cells, including microglial activation as early as 3 months and macrophage infiltration at 10 months. We generated DBA/2J mice lacking CX3CR1, and determined that this differentially affected RGC compartmentalized degeneration by increasing numbers of RGCs with a marker of disrupted axonal transport while not affecting RGC transcriptional dysregulation or optic nerve degeneration. Loss of CX3CR1 did not increase microglial activation overall but increased macrophage infiltration. However, numbers of infiltrating macrophage did not correlate with RGC pathology. We found that early microglial activation was composed of resident microglia and that high levels correlated strongly with later optic nerve degeneration. All together, these data implicate the resident microglia in disease progression in neurodegeneration.

TABLE OF CONTENTS

ABSTRACT iii

LIST OF FIGURES vii

ACKNOWLEDGEMENTS ix

Chapters

1. INTRODUCTION……1

    Challenges and fundamental aspects of neurodegeneration……1
    Compartmentalized neurodegeneration……...3
    Introduction to the myeloid innate immune system: resident microglia and macrophages……5
    New markers for resident microglia and peripheral macrophages……..8
    Involvement of the myeloid innate immune system in neurodegeneration…..….12
    Neurons communicate to myeloid cell through ligand-receptor systems including the fractalkine signaling system……15
    Phenotype of CX3CR1-deficient mice at baseline and in neurodegenerative models……17
    Myeloid functions regulated by fractalkine signaling……..…..….18
    Glaucoma as a model of neurodegeneration……..…20
    Acute and chronic animal models of glaucoma…….25
    Pathogenesis in the chronic mouse model of glaucoma, the DBA/2J mouse……26
    Changes to myeloid cells in the DBA/2J mouse……28
    Chapter overviews…….……...……..…….29
    References…….……30

2. DISRUPTED CX3CR1 SIGNALING DIFFERENTIALLY WORSENS NEURODEGENERATION IN DBA/2J GLAUCOMA AND INCREASES MACROPHAGE INFILTRATION…….38

    Credits……38
    Abstract……39
    Introduction……...……...……40
    Materials and methods……...42
    Results……....47

Discussion……..……..……..64
References……..67

3. NEURODEGENERATION SEVERITY IS ANTICIPATED BY EARLY MICROGLIA ALTERATIONS MONITORED IN VIVO IN A MOUSE MODEL OF CHRONIC GLAUCOMA…….72

Credits……72
Abstract……..74
Introduction……74
Results……75
Discussion……..80
Materials and methods.....…….....83
References……..84

4. DISCUSSION…….……..……...87

Research summary…….....87
Loss of CX3CR1 signaling differentially worsens RGC compartmentalized degeneration……...89
Future experiments examining how loss of CX3CR1 affects RGC compartmentalized degeneration……..92
Loss of CX3CR1 signaling increases macrophage infiltration but not myeloid activation overall……..…….....93
Future experiments examining how loss of CX3CR1 affects myeloid function and lineage specific roles in RGC neurodegeneration……..96
Early microgliosis correlates with later optic nerve degeneration and is composed of resident microglia ……..……....…….....99
Future experiments generating a time course of RGC degeneration in the DBA/2J …….....……..….....102
Conclusions……..…103
References……....105

LIST OF FIGURES

1.1. Neurodegenerative diseases have features in common. ……..4

1.2 Microglia change shape when they become activated……10

1.3 Retinal ganglion cell degeneration is compartmentalized in glaucoma.…….22

2.1 The density of Brn3+ nuclei does not change with loss of the CX3CR1…….…..49

2.2 More RGCs have accumulated pNF around the cell soma in retinas with disrupted fractalkine signaling…….51

2.3 There is no difference in the amount of gliosis and scarring in the optic nerve with loss of fractalkine signaling…….52

2.4 Loss of fractalkine signaling results in increased numbers of Brn3+ and Brn3- somal pNF+ RGCs……..55

2.5 Somal pNF+ RGCs are not entering apoptosis (do not express cleaved caspase 3)……. 56

2.6 Somal pNF+ RGCs do not have pyknotic nuclei…….57

2.7 Brn3+ somal pNF+ RGCs accumulate in retinas with higher Brn3+ nuclei densities with loss of fractalkine signaling……..58

2.8 There are similar percentages of samples with markers of RGC clearance (low Brn3+ nuclei and somal pNF+ RGC density and a high % non-axonal area in the optic nerve) with loss of fractalkine signaling……..59

2.9 Loss of fractalkine signaling results in greater numbers of amoeboid shaped Iba1+ cells……...61

2.10 Amoeboid Iba1+ cells are peripherally derived macrophages but they do not correlate with RGC pathology in either genotype……63

3.1 In vivo, monthly imaging of retinal and ONH microglia/peripheral monocytes during early stages of chronic glaucoma……..76

3.2 Induced decreases in local microgliosis are detectable by live imaging……...77

3.3 Eyes show large variability in their levels of ONH microgliosis at pre-neurodegenerative ages…….78

3.4 Late nerve damage is preceded by early microgliosis at the ONH……...79

3.5 Severity of nerve pathology and early microgliosis show a positive correlation….80

3.6 Early microgliosis is mainly driven by microglia resident in the ONH……...81

4.1 Proposed model for how loss of CX3CR1 affects retinal ganglion cell axonal transport, resident microglia, and CCR2+ infiltrating macrophages in the DBA/2J…….....95

ACKNOWLEDGEMENTS

I would like to acknowledge everyone in the Vetter lab for making it a great place to work. I would like to thank Monica and Ale for all the time spent mentoring me as well as inspiring me to be thoughtful and passionate about my science. I would like to especially thank Kathy Moore for her critique of my writing, her technical and intellectual acumen, and her in-depth knowledge of the Avengers. I would like to thank Mike Steele for many happy hours spent watching Teaching company lectures. I would like to thank Joy Corley for her great attitude, sense of humor, and patience when the grad student forgot it actually takes time for materials to arrive.

I would also like to thank my committee: Dr. Monica L. Vetter, Dr. Scott W. Rogers, Dr. Ning Tian, Dr. Karen S. Wilcox, and Dr. H. Joseph Yost, as well as former member Robert Marc, for sound criticism of my work and helpful advice.

Apart from the Vetter lab, I would like to thank Chris Rodesch to whom I am indebted for more than just microscopy. I would like to thank Don Ayer for having the patience of dealing with and inspiring a tech with more drive than planning skills as well as Chris Pickett, Chris Peterson, Mohan Kaadige, and Carrie Stoltzman for showing me that scientists can be normal grounded people. I would like to thank Keith Carney for channeling a Jewish mother and making me laugh through the hard times. Lastly, I would like to thank N.R.Vana for continued support and inspiration.

CHAPTER 1

INTRODUCTION

Challenges and fundamental aspects of neurodegeneration

For most of our adult life, we take for granted the intricate and many faceted control that the central nervous system has over so many life functions, which is why the relentless breakdown in neurodegeneration is such a betrayal. The cause of these diseases is unknown and with age as a common risk factor, the prevalence is increasing with the percentage of older individuals in the population. For example, the number of Alzheimer's disease cases is projected to triple by 2050 from its current number of 5 million cases (Hebert et al., 2013). Furthermore, patients can spend potentially a decade or more experiencing progressively worse symptoms. For all these reasons, neurodegenerative disease is a serious health concern now and even more so in the future. Diagnosis of these diseases is made when patients can't remember, can't move, or can't see, reflecting an irreversible loss of neurons. Therapies are variously efficacious at slowing the progress of symptoms speaking directly to a lack of biological knowledge of this process.

Despite many years of study, the biology driving neurodegeneration stubbornly remains a mystery. Still unanswered are the fundamental questions of when and where does neurodegeneration begin? A main reason for this is the increasing number of

observed pre-apoptotic changes that occur in different parts of a neuron before a final commitment to apoptosis. However, these observations also suggest that investigating these changes in a compartment-specific manner might facilitate a better understanding of pathogenic events that occur before neurons commit to cell death. Neurons are structurally unique cells, with >99% of their cell volume in their projections that can extend up to 1 meter in length (Morfini et al., 2009; Rishal and Fainzilber, 2014). In keeping with this amazing extension, neurons traverse a number of different physical environments and interact with many cellular systems making their study during neurodegeneration spatially challenging. Since neurodegeneration takes place over a protracted course with changes to these different cellular systems, there is an additional temporal challenge to studying this process. All together, these facts have transformed the study of neurodegeneration from examining the end readouts such as death or apoptosis of neurons, to investigating how and in what order a neuron systematically takes itself apart over time. A related question concerns defining what the cellular systems are that take part in this degeneration. In light of these challenges/obstacles, it is perhaps not surprising that mechanistic knowledge of neurodegenerative diseases is still elusive.

There are three fundamental questions that remain unanswered in neurodegeneration and the lack of answers has led to obstacles in detection, treatment, and potential prevention of neurodegenerative diseases: 1) when and how does neurodegeneration initiate?, 2) what is the subsequent sequence of neuronal degeneration?, and 3) what are the contributions of non-neural cells to the process of neurodegeneration? This last question is particularly intriguing, because understanding the roles of these surrounding support cells could be useful in designing new therapeutic

targets or might be harnessed to support ailing neurons, thus delaying or preventing the degenerative process.

Despite the fact that neurodegenerative diseases affect vastly different parts of the central nervous system (CNS), such as the spinal cord in amyotrophic lateral sclerosis (ALS), or the retina in glaucoma, they do share common features. A cardinal feature is the targeting of one particular neuronal type, such as the retinal ganglion cell (RGC) in glaucoma, while other types of neurons in the immediate vicinity are at first apparently unaffected but may degenerate secondarily later in the disease (see Figure 1.1A, Calkins, 2012). The pattern of decline and death in the affected neuronal type is both progressive (see Figure 1.1B, gets worse over time) and asynchronous (see Figure 1.1B, affects some but not all of the targeted neuronal type at a given time). Given its complexity, age is a common but poorly understood risk factor for all of these diseases. Whether this progressive and asynchronous pattern reflects unknown sensitivities of different subsets of these neurons at different locations or perhaps unknown disease insults occurring at different anatomical sites is unknown.

Compartmentalized neurodegeneration

In addition to the questions surrounding the degeneration of populations of neurons, there are many questions about the pattern of degeneration of an individual neuron. Since neurons are so structurally spread out in order to perform their function, compartments then sustain insults, signal those insults to other compartments, and can degenerate in a compartment-specific but finally overlapping manner. While the ability of different neuronal compartments to react autonomously to their environments lends

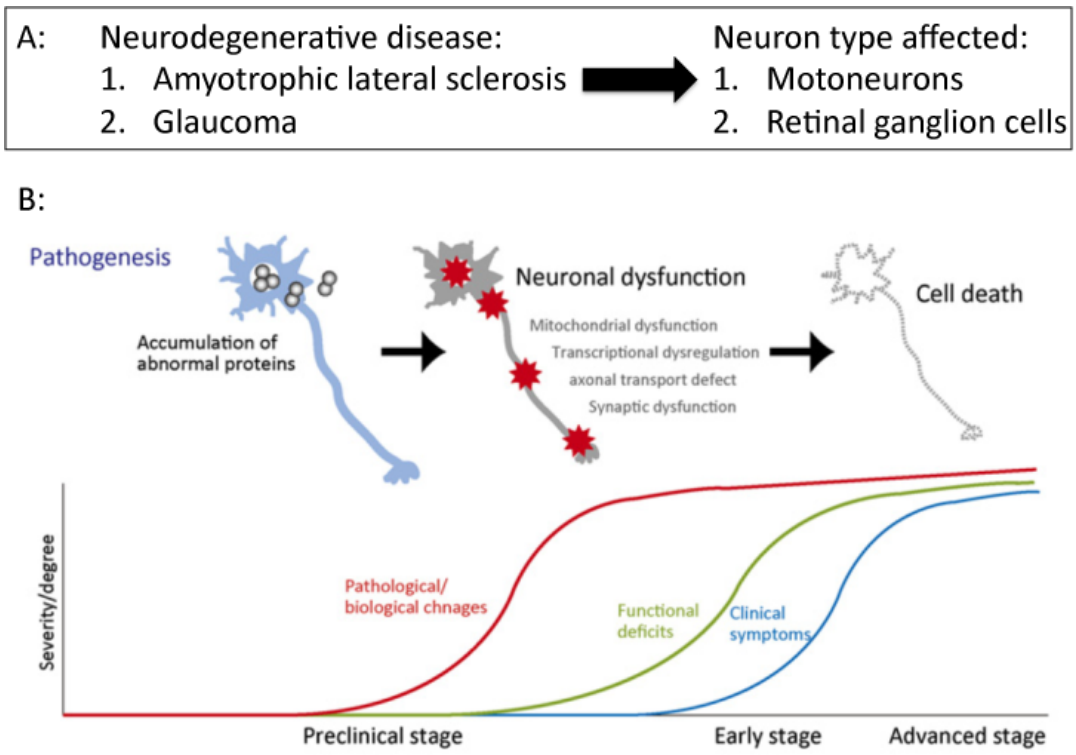

Figure 1.1: Neurodegenerative diseases have features in common. (A) Neurodegeneration affects one type of neuron but not others. On the left is listed the neurodegenerative disease and on the right the affected class of neurons (B) Neurodegeneration is progressive. Top – the progressive nature of neurodegeneration is illustrated as a neuron goes from declining to apoptotic. Damage to different parts of the neuron is indicated by red stars. Middle – a time course depicting pre-apoptotic neuronal changes preceding symptoms as disease advances from preclinical to an advanced stage. The shape of the curve reflects the asynchronous nature of neurodegeneration that does not proceed in a linear manner.
Reproduced from "Perspectives on molecular targeted therapies and clinical trials for neurodegenerative diseases", by Masahisa Katsuno, Fumiaki Tanaka, Gen Sobue, 83, 329-335, Copyright (2012) with permission from BMJ Publishing Group Ltd.

resiliency to the system, it makes it challenging to determine a sequence in neurodegeneration (Conforti et al., 2007). This process of neuronal compartmental degeneration makes it critical to study neurodegeneration in systems that grant access to these compartments so that degeneration can be assayed/examined in multiple compartments at the same time.

The different CNS environments through which a given neuronal compartment travels are made of cellular systems that include many components: vasculature, astrocytes, oligodendrocytes, and cells of the myeloid innate immune system. Elegant studies in ALS amongst others (Ilieva et al., 2009), have demonstrated that these components can greatly contribute to the progression of neurodegeneration. For example, expression of a mutated version of superoxide dismutase in mouse models of familial ALS in astrocytes or microglia drives disease progression but does not affect disease onset (Ilieva et al., 2009). Of these glial cells, the myeloid innate immune cells have fascinated investigators for over 100 years because of their morphologic and functional changes in all neurodegenerative diseases (Kettenmann et al., 2010). This then raises a set of interesting questions: how is the crosstalk between neurons and myeloid cells affected during neurodegeneration and how do changes in these cells affect the common features of neurodegenerative diseases (Jurgens and Johnson, 2012)?

Introduction to the myeloid innate immune system: resident microglia and macrophages

Amongst these glial cells, the role that cells of the myeloid innate immune system may play in neurodegeneration is particularly intriguing since these cells are very plastic

and have the capacity not only to contribute to neurodegeneration but also potentially to help ameliorate it. The innate immune system is composed of cells such as neutrophils, mast cells, and myeloid cells including microglia and macrophages that recognize conserved motifs of invading pathogens or molecules that indicate cellular stress. Specifically, the myeloid arm of the innate immune system is composed of cells of the myeloid lineage that take up residence in many tissues, including circulating monocytes in the blood, Langerhans cells in the skin, Kuppfer cells in the liver, and microglia in the CNS (Murray and Wynn, 2011). Collectively, these cells are referred to as the mononuclear phagocyte system (MPS). Monocytes in these different organs have multiple roles, they can be pro- or anti-inflammatory depending on the context, present antigen to stimulate adaptive immunity, clear away cell debris, and prevent autoimmune responses to this debris (Murray and Wynn, 2011). In particular, the ability to clear away debris has been hypothesized to be of benefit in neurodegenerative diseases, including Alzheimer's, where there is a prominent deposition of amyloid-β protein aggregates. However, despite the promise of this system to clear protein aggregates or cellular debris, there have been recent, spectacular, and expensive failures to ameliorate neurodegeneration by manipulating this process (Karran and Hardy, 2014), perhaps reflecting a lack of understanding of the MPS.

One possible reason for these failures has been the lack of specific markers to identify the origin of cells of the MPS. The MPS is composed of yolk sac-derived phagocytes born very early in embryogenesis as well as hematopoietically-derived macrophages that may be present during disease. For example, seminal studies from several authors (Ginhoux et al., 2010; Kierdorf et al., 2013; Mizutani et al., 2012)

determined that the resident myeloid cells of the CNS, microglia, are derived exclusively from yolk sac erythroid-myeloid progenitor cells born around E8 in the mouse. Thereafter, microglia establish a stable population in the retina and brain that is supplemented by a very low rate of local proliferation (Ransohoff and Perry, 2009) that can be increased in the event of microglia depletion by a resident, as yet unidentified, microglial stem cell (Elmore et al., 2014). In contrast, hematopoietically-derived macrophages originate in the aorta-gonad-mesonephros region before expanding in the fetal liver and finally within the bone marrow (Prinz and Priller, 2014). The existence of distinct origins for different cell types has led to the hypothesis that such cells play different roles in neurodegeneration (Prinz et al., 2011).

Microglia have been implicated in several neurodegenerative diseases, including ALS, Huntington's, and Parkinson's disease (Prinz et al., 2011). In the majority of cases, the mechanisms implicated in microglial-driven pathology involve toxic gains of function with increased secretion of pro-inflammatory cytokines like IL1β and subsequent generation of reactive oxygen species (ROS; Prinz et al., 2011). These cytokines and ROS then further damage neurons in a local manner potentially explaining why only some of the affected neuronal population die when toxic proteins are expressed in all of them. However, in addition to microglia, other studies have implicated peripheral macrophages in the disease progression of multiple sclerosis and Alzheimer's disease (Ajami et al., 2011; El Khoury et al., 2007).

Further complications come from studies in mouse models of ALS, showing that one branch of the myeloid innate immune system may affect the other. Butovsky et al. (2012) found in mouse models of ALS that resident microglia express the chemokine

CCL2 that summons CCR2-expressing macrophages. They also showed that once in the spinal cord, these CCR2 macrophages proliferated while the resident microglia underwent apoptosis. Observations such as these raise two questions in the neurodegenerative field: what arm of the MPS is responsible for what facet of neurodegeneration and how do these arms interact with or influence each other? Lack of complete understanding of these cells' roles may have contributed to the failure of attempts to manipulate these myeloid cells by anti-amyloid-β antibodies (Tayeb et al., 2013) either because they targeted the wrong branch of the MPS or because one branch was manipulating the activity of the other.

New markers for resident microglia and peripheral macrophages

In order to begin addressing which myeloid branch is responsible for disease, several authors have recently identified markers that can distinguish resident microglia from infiltrating macrophages in the adult mouse through extensive profiling experiments (Butovsky et al., 2014; Butovsky et al., 2012; Hickman et al., 2013; Saederup et al., 2010; Zhang et al., 2014). All resident microglia and macrophages express the cytoskeleton-associated gene Iba1 (see Figure 1.2A & 1.2B) and at some point during their development, express the receptor CX3CR1 for the chemokine, fractalkine (Jung et al., 2000; Prinz and Priller, 2014; Yona et al., 2013). In the case of some resident myeloid cells such as Kuppfer cells, CX3CR1 is expressed during development but subsequently turned off in adulthood, while in others such as circulating monocytes, there are subsets that express more or less CX3CR1 (Yona et al., 2013). Indeed, a mouse with GFP knocked into the CX3CR1 gene locus (CX3CR1 $^{gfp/+}$ mice) has become a crucial tool in

studying microglia under physiologic or pathologic conditions (Jung et al., 2000). The CX3CR1 $^{GFP/+}$ heterozygous and CX3CR1 $^{GFP/GFP}$ homozygous mouse has been used for live imaging of myeloid cells such as microglia (Bosco et al., 2015; Tremblay et al., 2010) as well as for testing the role of FKN in a wide variety of models of CNS injury or disease (Wolf et al., 2013). However, in this mouse, GFP labels all myeloid cells, as well as NK cells, and some subsets of T cells, making interpretation of results problematic (Jung et al., 2000). In contrast, the purinergic receptor, P2Y12, and the transforming-growth factor B receptor 1 (Tgfbr1) were found specifically to label resident microglia (Butovsky et al., 2014), while the expression of a different chemokine receptor, CCR2 is restricted to circulating macrophages (Saederup et al., 2010).

These markers are critical to the study of neurodegeneration because it has long been thought that these different lineages may play different roles in the healthy and diseased CNS (Prinz et al., 2011). Classically, the resident microglia were thought of as sentinels, patiently waiting for infection or injury to the CNS before they change their phenotype to address the problem (Kettenmann et al., 2010). This change in phenotype, termed microglial "activation", is best characterized by a change in microglial shape from a small cell body with many ramified processes, to a shape with shorter, stouter processes, and finally to an amoeboid shape under very activated conditions (see Figure 1.2C). In this amoeboid state, microglia are thought to phagocytose material and potentially secrete pro-inflammatory cytokines as well as reactive nitrogen and oxygen species to combat the problem and alert the peripheral immune system of ongoing infection or damage (Kettenmann et al., 2010). However, in this amoeboid state, a very activated microglia is morphologically indistinguishable from a macrophage. In contrast,

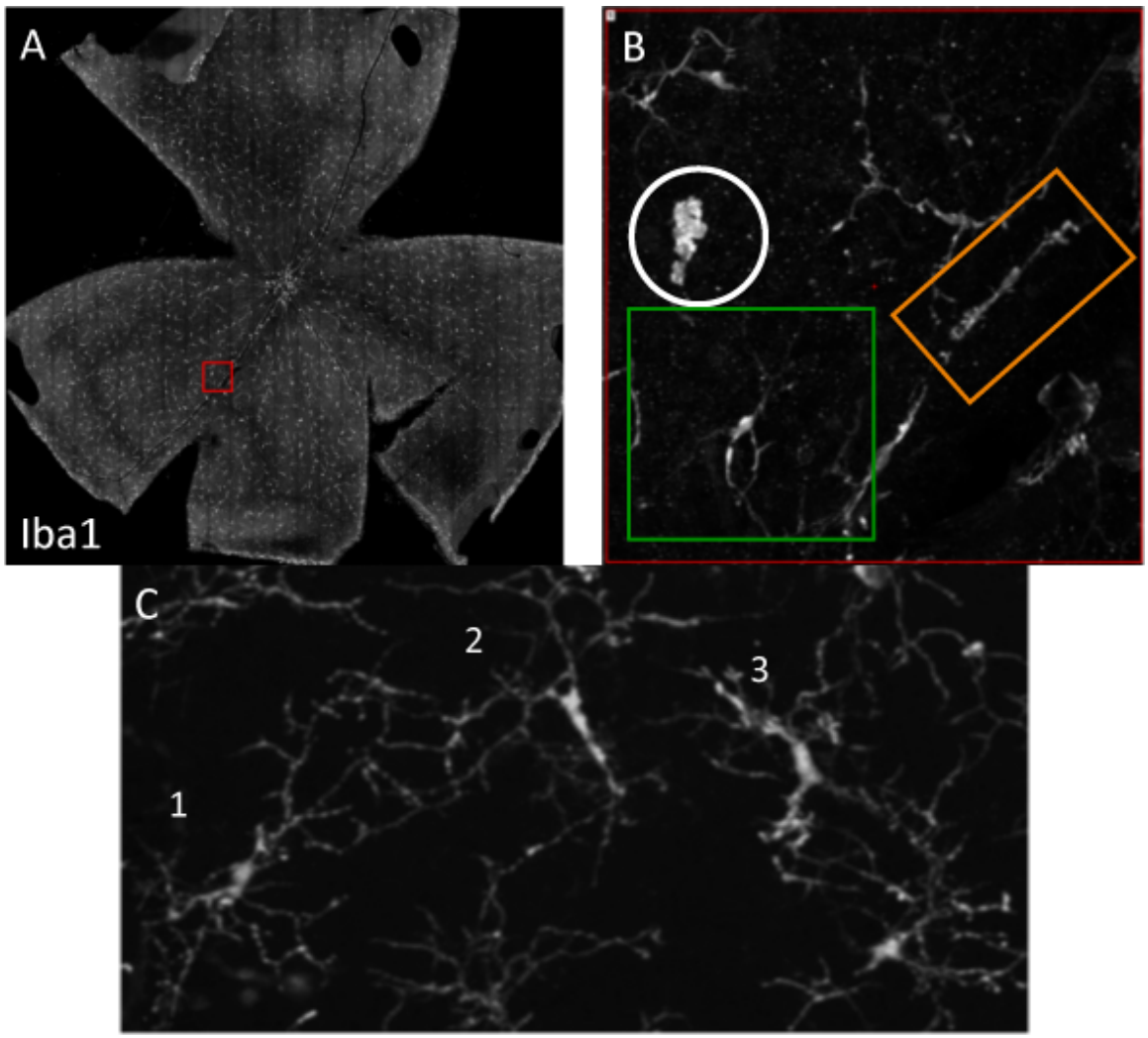

Figure 1.2: Microglia change shape when they become activated. (A) Retinal whole mount stained for Iba1. (B) Higher magnification view of the red box outlined in A. Depicted are the three easily distinguished Iba1+ elements. In the white circle is an amoeboid shaped cell distinguished by lacking all processes. In the green square is a branched cell with a small cell soma and branched processes. In the orange rectangle is a perivascular cell with two prominent processes on polar opposite sides of the cell. (C) Sequence of microglial activation from a small cell with many branches (1), to a cell with an enlarged soma (2), and then a cell with shorter processes as they are retracted (3). A fully activated microglia would resemble the amoeboid Iba1+ cell in the white circle depicted in 2.

macrophages infiltrate peripheral tissues under inflammatory conditions but once there, they too can display a number of different phenotypes. Furthermore, these macrophage phenotypes appear to change with time although it is not currently clear whether this is the result of infiltration of different macrophages subtypes over time or a change in the phenotype of the already present macrophage (Mosser and Edwards, 2008).

In addition to this simple scheme of resident microglia as sentinels and macrophages as responding effector cells, resident microglia play important roles in CNS development. During development, an excessive number of neurons and synapses are generated and the resident microglia with their phagocytic ability are key in clearing away these cells and connections so that an orderly circuit can be established. In this context as well, the dynamic nature of microglia has been recognized since they play not only a crucial phagocytic role but also can induce apoptosis of excess neurons, for example as with Purkinje neurons in the cerebellum (Ransohoff and Perry, 2009).

During the postnatal and adult periods, however, homeostatic roles for microglia are controversial. It has been demonstrated through sophisticated two-photon imaging experiments that the resident microglia constantly remodel and move their processes (Davalos et al., 2005; Nimmerjahn et al., 2005), suggesting a homeostatic role. Since microglia exist in an orderly, tiled mosaic in the CNS and retina wherein the cell body is thought to stay fixed and the arbor of processes from one microglia does not overlap the territory of another, the movement of these processes is estimated to screen the entire CNS every two hours (Hanisch and Kettenmann, 2007). The purpose of this movement under any given circumstance is unknown but Davolos et al. (2005) showed dramatic, real-time reaction of microglial processes towards a laser-induced injury within minutes

while Tremblay et al. (2010) demonstrated that this movement can be modified by visual activity.

Other authors have ablated microglia in order to determine if they play homeostatic roles but have so far come to conflicting conclusions. Parkhurst et al. (2013) depleted microglia by using the CX3CR1 promoter to drive expression of the diphtheria toxin receptor. After verifying robust CNS microglia depletion at one week (~85% depleted), they found disrupted synaptic plasticity, slower acquisition of motor and memory learning behaviors, and a reduction in proteins involved in excitatory glutamatergic synaptic transmission in the mice. A second study from Elmore et al. (2014) depleted microglia pharmacologically with a CSF1R antagonist and achieved nearly complete microglia depletion at 21 days that could be sustained up to 2 months with repeated dosing. In contrast to Parkhurst et al. (2013), mice depleted of microglia in this way displayed no behavioral deficits in terms of anxiety or hippocampal-dependent learning tasks. Though these two authors used different methods to deplete microglia, the debate on the physiologic role of resident microglia in the adult CNS continues. It remains unknown therefore whether depletion of microglia in the adult in any given disease context at the same time alter microglial homeostatic functions, thus confounding the interpretation. To date then, it remains unknown if neurodegeneration features a loss of microglial homeostatic functions.

Involvement of the myeloid innate immune system in neurodegeneration

Myeloid lineage-specific markers may open new avenues into studying the homeostatic roles of resident microglia and may enable researchers to more clearly define how these cells affect neurodegenerative disease. In fact, using tools such as the CX3CR1 $^{gfp/+}$ mouse has proven useful to describe changes in the different myeloid cell populations but understanding of cell-specific roles has remained elusive, in part due to technical challenges. For example, to answer the longstanding question of whether peripheral macrophages seed the CNS, Ajami et al. (2007) used elegant but complicated parabiosis and irradiation experiments involving the CX3CR1 $^{gfp/+}$ mouse and showed that peripheral macrophages do not seed the CNS even in a mouse model of multiple sclerosis. In contrast to requiring parabiosis and irradiation, El Khoury et al. (2007) used a mouse expressing RFP under the control of the peripheral macrophage marker CCR2, and were able to demonstrate that peripheral macrophages rather than the resident microglia were responsible for phagocytosing vascular amyloid-β plaques. Further, using the resident microglial specific marker CD39, Butovsky et al. (2012) were able to demonstrate that resident microglia may be recruiting macrophages through CCL2 expression and then dying by apoptosis once these cells arrive and proliferate in mouse models of ALS.

Myeloid lineage-specific markers may better define a crosstalk between resident microglia and macrophages and may help to address the question of whether microglia lose neuroprotective function with age that may contribute to neurodegeneration. The finding that resident microglia in the retina and brain are a stable population (Ransohoff

and Perry, 2009), in combination with age being a common risk factor in neurodegenerative diseases, has led some authors to suggest that resident microglia are in fact neuroprotective but that they lose function with age (Streit and Xue, 2014). In support of this microglia aging hypothesis, Streit and Xue, (2014) noted that with age, microglial processes appear dystrophic, and speculated that aged microglia are therefore less able to support ailing neurons.

In contrast to the microglia aging and loss of function hypothesis, other authors have noted an age-related increase in microglial activation albeit using general myeloid markers. For example, Mouton et al. (2002) described an increase in microglial number with age in mice, and Damani et al. (2011) showed that aged microglia appear more activated with reduced process arbors and remodel their processes more slowly. All of this suggests a toxic gain of function as well as a possible alteration in how microglia interact with peripheral macrophages. However, relying on microglia shape change to indicate altered function may be too simplistic since microglia need not change shape to change phenotype (Kettenmann et al., 2010).

The mechanism most frequently cited for a microglial toxic gain of function involves increased secretion of pro-inflammatory cytokines and reactive oxygen species. For example, increased secretion of pro-inflammatory cytokines like Il-1β and Tnf-α by activated myeloid cells has been described in animal models of neurodegenerative diseases such as Alzheimer's and Parkinson's disease (Prinz et al., 2011). Further, pro-inflammatory cytokines measured in serum have been used to identify Alzheimer's patients amongst blinded samples with 90% accuracy (Ray et al., 2007). However, the role of these cytokines in neurodegeneration remains unclear since they can act on

neuronal survival or death in a delicate balance (Smith et al., 2012). Lastly, as noted above, it is also unclear whether resident microglia or infiltrating macrophages are the source of these cytokines. All together then, whether neurodegeneration features a loss, gain of function, or both amongst myeloid cells remains unanswered.

Neurons communicate to myeloid cell through ligand-receptor systems including the fractalkine signaling system

Regardless of whether myeloid cells become neurotoxic or lose the ability to support neurons, it is clear that communication exists between myeloid cells and neurons and that this crosstalk is likely altered during neurodegeneration. Both resident microglia and infiltrating macrophages respond to neuronal stress and damage through ligand-receptor systems. These ligand receptor systems act in either a stimulatory or a repressive manner with respect to myeloid activation.

Microglia and macrophages express a wide array of receptors for neuronal stress or damage signals, including Toll-like receptors and purinergic receptors such as the various P2X receptors (Amor et al., 2010). In contrast, other ligand receptor systems act to repress aspects of myeloid activation but with different kinetics. For example, the neuronal CD200 to myeloid CD200R system keeps myeloid activation at baseline so that with loss of the CD200R, microglia become constitutively activated (Hoek et al., 2000). In contrast, the chemokine fractalkine (CX3CL1; FKN) signaling system represses microglial activation in response to an insult. Mice with a loss of the fractalkine receptor, CX3CR1, have normal appearing microglia at baseline in terms of shape and number (Jung et al., 2000). However, upon insult, ranging from injection of the bacterial cell wall

component lipopolysaccharide (LPS) or within mouse models of neurodegenerative diseases, the microglial activation response is enhanced, with microglia changing into an amoeboid shape as well as elevating secretion of pro-inflammatory cytokines (Cardona et al., 2006). Importantly for studies in neurodegeneration, FKN signaling has been shown to affect age-related changes to microglia. Lyons et al. (2009) showed the FKN mRNA and protein are downregulated with age in the mouse brain. Further, Wynne et al. (2010) demonstrated a prolonged downregulation of CX3CR1 upon LPS injection that correlated with a greater increase in secretion of IL1β in isolated microglia from aged versus adult mice. These data suggested that the microglia lacking CX3CR1 over-activated and secreted more pro-inflammatory cytokines in response to an insult.

The apparent lack of microglial activation at baseline and over-activation upon insult with loss of CX3CR1 makes this system attractive to study neuronal to microglial communication. Fractalkine is also well positioned to orchestrate neuron to myeloid cell communication because of its expression pattern in the CNS and unique structure. Consistent with a role in neuron to myeloid signaling, FKN is expressed constitutively and at high levels in the CNS (with highest levels of mRNA in the cortex, hippocampus, and striatum) and on the protein level, mostly on pyramidal, glutamatergic neurons (Tarozzo et al., 2003). The 373 amino acid ligand FKN is unique among chemokines because the chemokine-signaling domain sits atop a long mucin-like stalk, followed by a single pass transmembrane domain, and a short 37 amino acid cytoplasmic tail that has not been described to have any signaling motifs (Bazan et al., 1997). Another unique feature of FKN is that, because of its structure, FKN can signal in both a membrane-bound and secreted manner and was found to be a potent chemoattractant for monocytes

and lymphocytes but not neutrophils (Bazan et al., 1997).

The expression pattern and function of the FKN receptor, CX3CR1, is also consistent with a role in neuron to myeloid cell signaling. CX3CR1 is the only known receptor for FKN and is expressed by myeloid cells, NK cells, and subsets of T cells including microglia in the CNS (Jung et al., 2000). CX3CR1 is a 7 pass transmembrane Gα-i protein coupled receptor thought to mediate different effects depending upon binding by different forms of FKN. For example, the receptor modulates adhesion in concert with integrins (Fujita et al., 2012) when bound by membrane bound FKN and chemotaxis when bound by soluble FKN (Imai et al., 1997).

Phenotype of CX3CR1 deficient mice at baseline and in neurodegenerative models

Jung et al. (2000) generated a mouse that is frequently used to study FKN signaling by ablation of the CX3CR1 gene and protein through knock-in of the gene for EGFP. This strategy simultaneously removes CX3CR1 expression and labels the cells that were expressing or had expressed CX3CR1. CX3CR1 $^{gfp/gfp}$ mice are viable and fertile with normal lifespans (Jung et al., 2000). However, despite this seeming lack of effect of loss of fractalkine signaling at baseline, recently, Zhan et al. (2014) determined that mice deficient for CX3CR1 show delays in microglial population of the CNS. This delay correlated with a failure to appropriately prune synapses developmentally and autistic behaviors later in adulthood.

Most studies have examined FKN signaling in a wide range of neuronal injury and degeneration models and demonstrated context-dependent and contrasting results.

For example, ablation of CX3CR1 signaling increased neuronal loss in mouse models of Parkinson's disease and ALS (Cardona et al., 2006) but reduced infarct volume in models of stroke (Denes et al., 2008). In both of these examples, CX3CR1 null microglia appeared more activated in terms of shape and number. To date, not many studies have examined the physiologic role of FKN within nondiseased mice, but Liang et al. (2009) determined that microglia lacking CX3CR1 remodel their processes more slowly in the retina which could indicate that resident microglia may be somehow functionally compromised.

One caveat to all these experiments is that FKN signaling occurs throughout the entire animal and thus global loss of function may alter organ systems that communicate with the CNS. For example, Kim et al. (2011) showed that intestinal macrophages lacking CX3CR1 failed to form transendothelial dendrites used to sample the intestinal lumen while Landsman et al. (2009) showed that CX3CR1 $^{gfp/gfp}$ mice were deficient in the Ly6C^{lo} CX3CR1^{hi} subset of circulating macrophages. Lastly, Lee et al. (2013) found that FKN signaling can regulate insulin secretion. Since these systems may impact CNS, development or function global loss of FKN signaling may well confound interpretation of how loss of FKN signaling affects neurodegeneration. To date, studies involving the loss of FKN signaling (either in a membrane-bound or soluble manner) have relied on whole animal ablation of FKN signaling.

Myeloid functions regulated by fractalkine signaling

As is evident from the studies of Liang et al. (2009), Kim et al. (2011) , and Cardona et al. (2006), the list of myeloid functions regulated by FKN signaling has

grown beyond the originally described functions in adhesion and chemotaxis (Bazan et al., 1997). This could explain in part the contrasting results seen in different disease and injury models with manipulations to the FKN system since these additional functions of phagocytosis, secretion of pro-inflammatory cytokines, infiltration of macrophages, and others may differentially affect disease progression depending on the model. In particular, the ability of FKN signaling to affect infiltration of macrophages may have confounded earlier studies (Cardona et al., 2006) that described an increase in microglial activation, especially since it is now appreciated that macrophages can alter neurodegenerative progression (Ajami et al., 2011; El Khoury et al., 2007). Further, it has been determined that fractalkine signaling interferes with the signaling of another chemokine system: the CCL2/MCP1 to CCR2 chemokine system that is crucial in trafficking of infiltrating macrophages to sites of inflammation. In contrast to CX3CR1 that marks all myeloid cells, CCR2 labels peripherally-derived macrophages in the adult mouse (Mizutani et al., 2012; Saederup et al., 2010). Vitale et al. (2004) showed that soluble FKN reduces chemotaxis of a monocyte cell line to CCL2 and reduced the CCL2-stimulated increase in phospho-p38 that in turn stimulates the production of pro-inflammatory cytokines. Jacquelin et al. (2013) found that in the absence of CX3CR1, there was a more rapid increase of CCR2+ Ly6C^{hi} macrophages in the bloodstream and spleen post-myeloablation. Consistent with this, these authors also demonstrated that CX3CR1 reduced monocyte motility and subsequent release under normal conditions within the bone marrow. These studies are consistent with Sennlaub et al. (2013) who found that there was an increase of CCR2+ infiltrating macrophages in a mouse model of age-related macular degeneration and that ablation of these cells rescued neuronal

apoptosis. These studies suggest that with regard to infiltrating macrophages, one role of FKN signaling may be to limit the infiltration of a neurotoxic macrophage into the diseased CNS.

FKN signaling regulates not only macrophage infiltration but also phagocytosis by these cells which may be important in neurodegenerative diseases that feature cellular debris as neurons decline and die. However, conflicting results have been determined regarding FKN's ability to regulate phagocytosis. In particular, Fuller and Van Eldik (2008) found that fractalkine stimulates the clearance of apoptotic cells by stimulating myeloid cells to secrete the protein Mfg-E8 that tethers apoptotic cells to phagocytic cells. In apparent contrast to a pro-phagocytic role for FKN, Lee et al. (2010) found that CX3CR1-deficient microglia phagocytose more microspheres and amyloid-β material, leading to a reduction in the amyloid-β burden in Alzheimer's disease model mice. A possible explanation for these contrasting results is a differential effect of FKN signaling on the phagocytosis of different materials, in this case cell debris or apoptotic cells versus protein deposits. In agreement with the idea that FKN may enhance the removal of dead or dying cells, CX3CR1 deficiency in a mouse model of Alzheimer's disease enhanced Tau pathology amongst neurons (Bhaskar et al., 2010) while over-expression of FKN reduced tau pathology (Nash et al., 2013). Loss of CX3CR1 also prevented the loss of neurons at an earlier timepoint (Fuhrmann et al., 2010) in other Alzheimer's disease mice. These disparate results in Alzheimer's disease mouse models call for a more comprehensive examination of different neuronal compartments when the FKN signaling system has been perturbed. Ultimately, ablation of CX3CR1 in a myeloid-specific manner, within resident microglia or peripheral macrophages will best answer these

questions.

Glaucoma as a model of neurodegeneration

The issue of differential effects of fractalkine signaling on myeloid cell lineages is compounded in the neurodegenerative field when the concept of compartmentalized neurodegeneration is added into the mix (see Figure 1.3A and B). In addition to specific myeloid lineage markers, what is needed to unravel this mystery is a model of neurodegenerative disease that features easy access to multiple degenerating neuronal compartments from the same animal so that they can be compared to one another. In many cases, such as Alzheimer's disease, Parkinson's disease, and ALS, there are technical challenges in studying degenerating neurons that are located within bony structures and project axons to even deeper regions of the CNS. Furthermore, it may be difficult to get the entire picture when disease is spread over larger cortical areas, as is the case with Alzheimer's disease. In contrast, the neurodegenerative disease glaucoma affects neurons within the retina, an outgrowth of the CNS. The eye grants tremendous access to degenerating CNS neurons, as evidenced by live imaging studies (Bosco et al., 2015). In contrast to the cortex, the eye provides a contained, smaller anatomic area where all the degenerating neurons are contained as well as a single nerve containing all the projections.

Importantly, glaucoma is a classic neurodegenerative disease in that it is age-related, progressive, and targets one type of neuron in an asynchronous manner in the same way as Alzheimer's, Parkinson's, or ALS. Although glaucoma refers to a number of diseases with different times of onset and courses, all feature the primary degeneration of

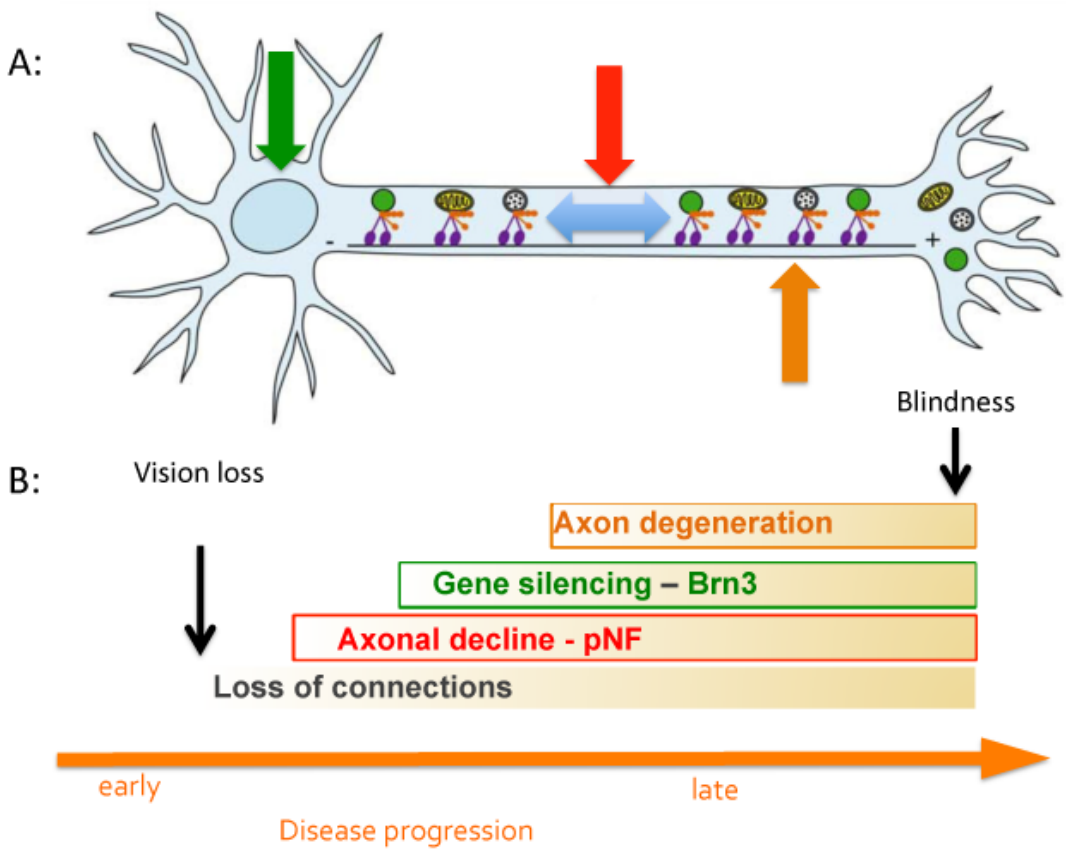

Figure 1.3: Retinal ganglion cell degeneration is compartmentalized in glaucoma. (A) A cartoon of a retinal ganglion cell is depicted with the green arrow indicating the cell soma, the red arrow transport within the axon, and the orange arrow the distal myelinated axon within the optic nerve. (B) Timeline of glaucoma progression from an early stage with vision loss to blindness in a late stage. The boxes around the readouts of compartmentalized degeneration correspond to the compartment depicted in A. Within the boxes are indicated the pathology readout used to measure neurodegeneration in that compartment. Within the retina RGCs accumulate axonal cytoskeleton proteins, phosphorylated neurofilaments, as a marker of disrupted RGC axonal transport (red box). Gene transcription in RGCs is dysregulated with glaucoma progression including downregulation of the RGC-specific transcription factor family Brn3 (a, b, and c; green box). With glaucoma progression, RGC axons in the optic nerve are lost with a subsequent increase in glia and extracellular matrix within the nerve (orange box).

Reprinted from Trends in Neurosciences, 33 /7, by Eran Perlson, Sandra Maday, Meng-meng Fu, Armen J. Moughamian, and Erika L.F. Holzbaur, in “Retrograde axonal transport: pathways to cell death?”, 335-344, Copyright (2010), with permission from Elsevier.

retinal ganglion cells (RGCs), while other retinal neurons degenerate secondarily. Since RGCs are the ultimate gatherer of visual information in the retina prior to transmission to the brain, damage to these cells leads to blindness. Therefore, the glaucomas are characterized by particular structural changes that reflect damage to RGCs, including loss of neural tissue at the optic nerve head (ONH), a region where all axons of RGCs coalesce to become the optic nerve behind the globe. The loss of this neural tissue is referred to as excavation of the ONH that deepens as a result of loss of RGC axons. As with other neurodegenerative diseases, loss of RGCs is asynchronous, seen as patients develop vision loss in particular arcing regions called arcuate scotomas that typically extend from the nasal pole to either the superior or inferior pole in an hourglass pattern. Reflecting the progressive nature of glaucoma, these arcuate scotomas coalesce, first leaving only central vision, and then proceeding to complete blindness (Quigley, 2011). Clinically, the ultimate diagnosis of glaucoma depends on two features of structural changes in the retina, ONH excavation and visual field loss. Unfortunately, because these changes are progressive, glaucoma is usually diagnosed when irreplaceable neuron loss has already occurred. Treatments at this stage cannot prevent the loss but can only slow the process and often not in all patients.

In an attempt to diagnose and treat glaucoma at earlier stages, a number of risk factors have been identified in order to screen patients for the disease. Important risk factors include age (as in all neurodegenerative diseases), elevated intraocular pressure, and family history (Cook and Foster, 2012). The mean age of glaucoma patients is 60 years old with a slight preponderance of women over men (55%) and some difference among ethnicities with Asians having the highest numbers of affected individuals for all

types of glaucoma (Cook and Foster, 2012). Elevated intraocular pressure (IOP; considered elevated at >21mmHg) has received much attention since it does increase therisk of getting glaucoma, is relatively easy and noninvasive to measure and treat, and since lowering IOP seems to delay vision loss in some but not all patients. For these reasons, IOP has become the main screening tool and therapeutic target in glaucoma. The idea behind elevated intraocular pressure as a pathogenic insult rests on the idea that the axons of RGCs traverse very different environments when they coalesce at the ONH with its intraocular pressure range of 10-20 mmHg, proceed through the glial lamina, and then exit the eye where the intracranial pressure is probably lower at 7-15 mmHg. This then creates a point of stress for RGC axons where they exit the back of the eye and it has been proposed that as intraocular pressure increases RGC axons become compressed. Additionally, RGC axons are not myelinated until a few mm behind the eye, leaving them unprotected from injury in this region.

However, there are many situations where IOP has been shown to be uncoupled from RGC degeneration. For example, there are patients who develop glaucoma despite having an IOP below 21 mmHg (normal tension glaucoma). Furthermore, patients with IOPs above 21 mmHg do not always progress to exhibit glaucomatous changes such as ONH excavation and visual field loss (Quigley, 2011). Lastly, in clinical trials, 50% of patients with IOPs above 21 mmHg given IOP lowering medications and verified to have had a reduction in IOP still progressed to glaucoma (Kass et al., 2002). There are genetic associations amongst glaucoma patients with genes that have a role in the front of the eye such as the myocilin and optineurin gene that might be consistent with a role in elevating IOP but these genes are also expressed in many ocular and nonocular tissues, making

interpretations difficult (Wiggs, 2007). It may be better, then, to consider glaucoma as a disease of susceptibility of RGCs to insults such as IOP and genetic mutations (Calkins, 2012), rather than solely focus on IOP as a causative agent.

Acute and chronic animal models of glaucoma

Nonetheless, in keeping with the focus on IOP in human glaucoma, animal models of glaucoma also have focused on elevating IOP within the mouse or rat eye. There are both acute and chronic/genetic models. The advantages of an acute model are that the onset, magnitude, and to some extent the duration of the insult to RGCs can be controlled. Elevated IOP has been accomplished by disruption of the veins draining the anterior chamber by cautery, photocoagulation, or injection of hypertonic saline. The acute model of glaucoma most often used currently involves injection of small polystyrene beads into the anterior chamber that physically block the outflow tracks (McKinnon et al., 2009) raising the IOP. While these acute models have been useful, they have the limitation of introducing an injury, and it remains unknown if this synchronous elevation of IOP models what occurs in glaucoma patients over a long time course. In contrast, the chronic/genetic models better capture the age-related aspects of neurodegeneration and have allowed researchers to study age-related changes to multiple systems that may well combine to influence glaucoma progression.

Pathogenesis in the chronic mouse model of glaucoma, the DBA/2J mouse

The most frequently used chronic, genetic mouse model of glaucoma is the DBA/2J mouse. This mouse develops a pigment dispersion glaucoma over a protracted time course as the result of spontaneously occurring loss of function mutations in two genes: tyrosinase related protein 1^b ($Tyrp1^b$) and glycoprotein in nonmetastasing melanoma b (Gpnmb). These two genes function in melanosome generation and maintenance pathways within the iris so their loss results in iris stromal atrophy and dispersion of melanosome debris into the anterior chamber. This debris then clogs outflow channels, resulting in increasing IOP over time (Anderson et al., 2002). The presence of both mutations as well as the DBA/2J background is necessary to induce glaucoma. Bl6 mice with both mutations develop an iris disease but are much less prone to glaucoma (Anderson et al., 2006). Importantly, there is a strain-matched control that features restoration of the wild type version of Gpnmb in the presence of the $Tyrp1^b$ mutation on the DBA/2J background that rescues the animals from glaucomatous neurodegeneration (Howell et al., 2007). Interestingly, as in human glaucoma, a greater percentage of female DBA/2J mice develop the disease than male mice (Libby et al., 2005). Importantly, this model mimics human glaucomas in many ways, including the fact that there are likely other genes that are modifying disease expression as well as potentially environmental influences on disease onset and severity.

Again similar to human glaucoma and despite this being a genetically identical inbred mouse strain, elevation in IOP, as well as every pathology readout examined in DBA/2J mice, occurs asynchronously within the population. This suggests a combination

of genetics and unknown environmental factors that results in glaucoma. Analysis of pathology in the DBA/2J therefore results in a percentage of mice displaying a given pathology at any selected timepoint with a greater percentage of animals being affected with time. For example, elevated IOP is first detected in some mice at 6 months with a majority (but not all) of animals having elevated IOP at 9 months (Libby et al., 2005). For this reason Libby et al. (2005) recommend 40 eyes for analysis of any pathology. While this is a fair number of samples and not always followed in the literature, it was determined that glaucoma progresses differently between the left and right eye of an individual animal in terms of the loss of axons in the optic nerve such that each animal is considered an n of 2 (Libby et al., 2005). In spite of some limitations, the DBA/2J is the best model of human glaucoma because pathology is age-related, progressive, and asynchronous.

As in human patients, RGCs are the primary neurons affected in the retina of DBA/2J mice (Calkins, 2012). RGCs traverse a number of cellular environments with dendrites, a cell soma, and unmyelinated axon within the retina that then becomes myelinated in the proximal optic nerve. Since each of these cellular compartments degenerate at different times, RGCs are an excellent model system in which to study compartmentalized degeneration. Importantly, there are structural and functional pathologic readouts directed at the RGC cell soma, axons, and CNS targets that have been characterized in the DBA/2J mouse, allowing us to assay the roles of myeloid innate immune cells on neurodegeneration in these different compartments (Dengler-Crish et al., 2014; Libby et al., 2005; Soto et al., 2008). Within the retina, these include measures of disrupted RGC gene transcription as well as immunostaining for structural axonal

proteins (Soto et al., 2008). Optic nerve degeneration has been characterized both structurally (Bosco et al., 2015; Crish et al., 2010; Libby et al., 2005) and functionally by assessing antero and retrograde axonal transport (Dengler-Crish et al., 2014). Therefore, within the DBA/2J mouse, analysis of the retina and optic nerve can be combined, providing a more complete picture of RGC compartmentalized degeneration.

Changes to myeloid cells in the DBA/2J mouse

The DBA/2J mouse is also an excellent model to explore the impact of changes in the myeloid innate immune system on neurodegeneration since alterations to both resident microglia and infiltrating macrophages occur alongside RGC decline and death. Microglia become activated by morphology, proliferate, and upregulate markers of activation, such as Iba1, in the DBA/2J as early as 3 months in some animals (Bosco et al., 2012; Bosco et al., 2011). Further, it was determined that peripheral macrophages infiltrate into the DBA/2J retina at 10 months (Howell et al., 2012), although the implication of this for disease progression is unknown. Interestingly, head-only irradiation targeting these proliferating microglia at 3 months rescued glaucoma pathology and prevented infiltration of macrophages (Bosco et al., 2012; Howell et al., 2012). These results suggested that this early microglial activation might play a role in later RGC pathology. Further implicating microglia in DBA/2J pathology, treating mice with the immunosuppressive drug minocycline reduced the loss of axonal transport (Bosco et al., 2008). Since good techniques for profiling myeloid cells now exist, unraveling the roles of these cells may lead to a targeted, more mechanistic understanding of how the innate immune system affects compartmentalized neuronal degeneration.

In sum, the DBA/2J mouse offers an excellent model of neuronal (RGC) degeneration because it grants relatively easy access to different degenerating compartments, the retina and optic nerve. Furthermore, an impact of myeloid cells in RGC degeneration within DBA/2J mice has been hinted at but not manipulated in a targeted manner. With the tools in hand to examine RGC compartmentalized degeneration, I manipulated the myeloid innate immune cell compartment by loss of CX3CR1 on the DBA/2J background.

Chapter overviews

This dissertation details my work in describing how loss of FKN signaling affects compartmentalized RGC neurodegeneration, myeloid cell activation, and the identity of the myeloid cells that change early and later in glaucoma progression.

In Chapter 2 of this dissertation, I detail the phenotypic characterization of loss of CX3CR1 on RGC compartmentalized degeneration and changes to myeloid innate immune cells versus control DBA/2J mice. I found that loss of CX3CR1 affects some RGC compartments but not others. Loss of CX3CR1 on the DBA/2J background increased the number of RGCs with a marker of axonal transport defects, but changes in RGC gene transcription or optic nerve degeneration were unaffected. Furthermore, by analyzing multiple RGC compartments in each sample, I was able to propose a logical sequence of RGC degeneration, reflecting the readouts measured here, consistent with the hypothesis that loss of FKN signaling generates more sick RGCs rather than delaying their clearance.

Loss of FKN signaling has been shown to result in over-activation of microglia,

but interestingly, I found that while the myeloid Iba1+ cells were morphologically more activated, with more amoeboid shapes, they were not more activated as measured molecularly by determination of Iba1 mRNA levels in CX3CR1 null DBA/2J retinas. Instead I showed that the amoeboid-shaped Iba1+ cells were infiltrating macrophages based on their location in the neurofibrillary layer and the presence of the peripheral macrophage marker CCR2. In contrast, the numbers and morphological appearance of branched Iba1+ myeloid cells (presumed resident microglia) were unchanged. Thus, loss of FKN signaling increased macrophage infiltration but not myeloid activation. Interestingly, the numbers of these infiltrating macrophages did not correlate with RGC pathology readouts, suggesting that they do not contribute to these processes but might be playing some other role in RGC degeneration. What specifically this role(s) is and whether this role is detrimental or beneficial has yet to be directly demonstrated.

Chapter 3 details the use of early microglial activation as a predictive tool in the DBA/2J mouse. Given the variable onset of disease in the DBA/2J mouse described above, the use of in vivo monitoring of microglial activation used in this study was highly innovative. A very high correlation between early microgliosis in the DBA/2J and later optic nerve degeneration was determined by novel in vivo imaging and tissue analysis techniques. Further, by immunostaining using new markers of myeloid cell origin, the early microgliosis was comprised of resident microglia rather than infiltrating macrophages.

References

Ajami, B., Bennett, J.L., Krieger, C., McNagny, K.M., and Rossi, F.M. (2011). Infiltrating monocytes trigger EAE progression, but do not contribute to the resident

microglia pool. Nat. Neurosci. *14*, 1142-1149.

Ajami, B., Bennett, J.L., Krieger, C., Tetzlaff, W., and Rossi, F.M. (2007). Local self-renewal can sustain CNS microglia maintenance and function throughout adult life. Nat. Neurosci. *10*, 1538-1543.

Amor, S., Puentes, F., Baker, D., and Valk, P.v.d. (2010). Inflammation in neurodegenerative diseases. Immunology *129*, 154-169.

Anderson, M.G., Libby, R.T., Mao, M., Cosma, I.M., Wilson, L.A., Smith, R.S., and John, S.W. (2006). Genetic context determines susceptibility to intraocular pressure elevation in a mouse pigmentary glaucoma. BMC Biol. *4*, 20.

Anderson, M.G., Smith, R.S., Hawes, N.L., Zabaleta, A., Chang, B., Wiggs, J.L., and John, S.W.M. (2002). Mutations in genes encoding melanosomal proteins cause pigmentary glaucoma in DBA/2J mice. Nat. Gen. *30*, 81-85.

Bazan, J.F., Bacon, K.B., Hardiman, G., Wang, W., Soo, K., Rossi, D., Greaves, D.R., Zlotnik, A., and Schall, T.J. (1997). A new class of membrane-bound chemokine with a CX3C motif. Nature *385*, 640-644.

Bhaskar, K., Konerth, M., Kokiko-Cochran, O.N., Cardona, A., Ransohoff, R.M., and Lamb, B.T. (2010). Regulation of tau pathology by the microglial fractalkine receptor. Neuron *68*, 19-31.

Bosco, A., Crish, S.D., Steele, M.R., Romero, C.O., Inman, D.M., Horner, P.J., Calkins, D.J., and Vetter, M.L. (2012). Early reduction of microglia activation by irradiation in a model of chronic glaucoma. PLoS One *7*, e43602.

Bosco, A., Inman, D.M., Steele, M.R., Wu, G., Soto, I., Marsh-Armstrong, N., Hubbard, W.C., Calkins, D.J., Horner, P.J., and Vetter, M.L. (2008). Reduced retina microglial activation and improved optic nerve integrity with minocycline treatment in the DBA/2J mouse model of glaucoma. Invest. Ophthalmol. Vis. Sci. *49*, 1437-1446.

Bosco, A., Romero, C.O., Breen, K.T., Chagovetz, A.A., Steele, M.R., Ambati, B.K., and Vetter, M.L. (2015). Neurodegeneration severity is anticipated by early microglia alterations monitored in vivo in a mouse model of chronic glaucoma. Dis. Mod. & Mech. *8*, 443-455.

Bosco, A., Steele, M.R., and Vetter, M.L. (2011). Early microglia activation in a mouse model of chronic glaucoma. J. Comp. Neurol. *519*, 599-620.

Butovsky, O., Jedrychowski, M.P., Moore, C.S., Cialic, R., Lanser, A.J., Gabriely, G., Koeglsperger, T., Dake, B., Wu, P.M., Doykan, C.E*., et al.* (2014). Identification of a unique TGF-beta-dependent molecular and functional signature in microglia. Nat. Neurosci. *17*, 131-143.

Butovsky, O., Siddiqui, S., Gabriely, G., Lanser, A.J., Dake, B., Murugaiyan, G., Doykan, C.E., Wu, P.M., Gali, R.R., Iyer, L.K.*, et al.* (2012). Modulating inflammatory monocytes with a unique microRNA gene signature ameliorates murine ALS. J. Clin. Invest. *122*, 3063-3087.

Calkins, D.J. (2012). Critical pathogenic events underlying progression of neurodegeneration in glaucoma. Prog. Retin. Eye Res. *31*, 702-719.

Cardona, A.E., Pioro, E.P., Sasse, M.E., Kostenko, V., Cardona, S.M., Dijkstra, I.M., Huang, D., Kidd, G., Dombrowski, S., Dutta, R.*, et al.* (2006). Control of microglial neurotoxicity by the fractalkine receptor. Nat. Neurosci. *9*, 917-924.

Conforti, L., Adalbert, R., and Coleman, M. (2007). Neuronal death: where does the end begin? TRENDS Neurosci. *30*, 159-166.

Cook, C., and Foster, P. (2012). Epidemiology of glaucoma: what's new? Can. J. Ophthalmol. *47*, 223-226.

Crish, S.D., Sappington, R.M., Inman, D.M., Horner, P.J., and Calkins, D.J. (2010). Distal axonopathy with structural persistence in glaucomatous neurodegeneration. Proc. Natl. Acad. Sci. USA *107*, 5196-5201.

Damani, M.R., Zhao, L., Fontainhas, A.M., Amaral, J., Fariss, R.N., and Wong, W.T. (2011). Age-related alterations in the dynamic behavior of microglia. Aging Cell *10*, 263-276.

Davalos, D., Grutzendler, J., Yang, G., Kim, J.V., Zuo, Y., Jung, S., Littman, D.R., Dustin, M.L., and Gan, W.B. (2005). ATP mediates rapid microglial response to local brain injury in vivo. Nat. Neurosci. *8*, 752-758.

Denes, A., Ferenczi, S., Halasz, J., Kornyei, Z., and Kovacs, K.J. (2008). Role of CX3CR1 (fractalkine receptor) in brain damage and inflammation induced by focal cerebral ischemia in mouse. J. Cere. Blood Flow & Metab. *28*, 1707-1721.

Dengler-Crish, C.M., Smith, M.A., Inman, D.M., Wilson, G.N., Young, J.W., and Crish, S.D. (2014). Anterograde transport blockade precedes deficits in retrograde transport in the visual projection of the DBA/2J mouse model of glaucoma. Front. Neurosci. *8*, 290.

El Khoury, J., Toft, M., Hickman, S.E., Means, T.K., Terada, K., Geula, C., and Luster, A.D. (2007). Ccr2 deficiency impairs microglial accumulation and accelerates progression of Alzheimer-like disease. Nat. Med. *13*, 432-438.

Elmore, M.R., Najafi, A.R., Koike, M.A., Dagher, N.N., Spangenberg, E.E., Rice, R.A., Kitazawa, M., Matusow, B., Nguyen, H., West, B.L.*, et al.* (2014). Colony-stimulating factor 1 receptor signaling is necessary for microglia viability, unmasking a microglia

progenitor cell in the adult brain. Neuron *82*, 380-397.

Fuhrmann, M., Bittner, T., Jung, C.K., Burgold, S., Page, R.M., Mitteregger, G., Haass, C., LaFerla, F.M., Kretzschmar, H., and Herms, J. (2010). Microglial Cx3cr1 knockout prevents neuron loss in a mouse model of Alzheimer's disease. Nat. Neurosci. *13*, 411-413.

Fujita, M., Takada, Y.K., and Takada, Y. (2012). Integrins alphavbeta3 and alpha4beta1 act as coreceptors for fractalkine, and the integrin-binding defective mutant of fractalkine is an antagonist of CX3CR1. J. Immunol. *189*, 5809-5819.

Fuller, A.D., and Van Eldik, L.J. (2008). MFG-E8 regulates microglial phagocytosis of apoptotic neurons. J. Neuroimm Pharmacol: Soc. NeuroImm. Pharmacol. *3*, 246-256.
Ginhoux, F., Greter, M., Leboeuf, M., Nandi, S., See, P., Gokhan, S., Mehler, M.F., Conway, S.J., Ng, L.G., Stanley, E.R*., et al.* (2010). Fate mapping analysis reveals that adult microglia derive from primitive macrophages. Science *330*, 841-845.

Hanisch, U.K., and Kettenmann, H. (2007). Microglia: active sensor and versatile effector cells in the normal and pathologic brain. Nat. Neurosci. *10*, 1387-1394.

Hebert, L.E., Weuve, J., Scherr, P.A., and Evans, D.A. (2013). Alzheimer disease in the United States (2010-2050) estimated using the 2010 census. Neurology *80*, 1778-1783.

Hickman, S.E., Kingery, N.D., Ohsumi, T.K., Borowsky, M.L., Wang, L.C., Means, T.K., and El Khoury, J. (2013). The microglial sensome revealed by direct RNA sequencing. Nat. Neurosci. *16*, 1896-1905.

Hoek, R.M., Ruuls, S.R., Murphy, C.A., Wright, G.J., Goddard, R., Zurawski, S.M., Blom, B., Homola, M.E., Streit, W.J., Brown, M.H*., et al.* (2000). Down-Regulation of the Macrophage Lineage Through Interaction with OX2 (CD200). Science *290*, 1768-1771.

Howell, G.R., Libby, R.T., Marchant, J.K., Wilson, L.A., Cosma, I.M., Smith, R.S., Anderson, M.G., and John, S.W.M. (2007). Absence of glaucoma in DBA/2J mice homozygous for wild-type versions of Gpnmb and Tyrp1. BMC Gen. *8*, 1-10.

Howell, G.R., Soto, I., Zhu, X., Ryan, M., Macalinao, D.G., Sousa, G.L., Caddle, L.B., MacNicoll, K.H., Barbay, J.M., Porciatti, V*., et al.* (2012). Radiation treatment inhibits monocyte entry into the optic nerve head and prevents neuronal damage in a mouse model of glaucoma. J. Clin. Invest. *122*, 1246-1261.

Ilieva, H., Polymenidou, M., and Cleveland, D.W. (2009). Non-cell autonomous toxicity in neurodegenerative disorders: ALS and beyond. J. Cell Biol. *187*, 761-772.

Imai, T., Hieshima, K., Haskell, C., Baba, M., Nagira, M., Nishimura, M., Kakizaki, M., Takagi, S., Nomiyama, H., Schall, T.J*., et al.* (1997). Identification and molecular

characterization of fractalkine receptor CX3CR1, which mediates both leukocyte migration and adhesion. Cell *91*, 521-530.

Jacquelin, S., Licata, F., Dorgham, K., Hermand, P., Poupel, L., Guyon, E., Deterre, P., Hume, D.A., Combadiere, C., and Boissonnas, A. (2013). CX3CR1 reduces Ly6Chigh-monocyte motility within and release from the bone marrow after chemotherapy in mice. Blood *122*, 674-683.

Jung, S., Aliberti, J., Graemmel, P., Sunshine, M.J., Kreutzberg, G.W., Sher, A., and Littman, D.R. (2000). Analysis of Fractalkine Receptor CX3CR1 Function by Targeted Deletion and Green Fluorescent Protein Reporter Gene Insertion. Mol. Cell. Biol. *20*, 4106-4114.

Jurgens, H.A., and Johnson, R.W. (2012). Dysregulated neuronal–microglial cross-talk during aging, stress and inflammation. Exp. Neurol. *1*, 40-48.

Karran, E., and Hardy, J. (2014). Antiamyloid therapy for Alzheimer's disease--are we on the right road? N. Engl. J. Med. *370*, 377-378.

Kass, M.A., Heuer, D.K., Higginbotham, E.J., Johnson, C.A., Keltner, J.L., Miller, J.P., Parrish, R.K., 2nd, Wilson, M.R., and Gordon, M.O. (2002). The Ocular Hypertension Treatment Study: a randomized trial determines that topical ocular hypotensive medication delays or prevents the onset of primary open-angle glaucoma. Arch. Ophthalmol. *120*, 701-713.

Kettenmann, H., Hanisch, U.K., Noda, M., and Verkhratsky, A. (2010). Physiology of microglia. Physiol. Rev. *91*, 461-553.

Kierdorf, K., Erny, D., Goldmann, T., Sander, V., Schulz, C., Perdiguero, E.G., Wieghofer, P., Heinrich, A., Riemke, P., Holscher, C*., et al.* (2013). Microglia emerge from erythromyeloid precursors via Pu.1- and Irf8-dependent pathways. Nat. Neurosci. *16*, 273-280.

Kim, K.W., Vallon-Eberhard, A., Zigmond, E., Farache, J., Shezen, E., Shakhar, G., Ludwig, A., Lira, S.A., and Jung, S. (2011). In vivo structure/function and expression analysis of the CX3C chemokine fractalkine. Blood *118*, e156-167.

Landsman, L., Bar-On, L., Zernecke, A., Kim, K.W., Krauthgamer, R., Shagdarsuren, E., Lira, S.A., Weissman, I.L., Weber, C., and Jung, S. (2009). CX3CR1 is required for monocyte homeostasis and atherogenesis by promoting cell survival. Blood *113*, 963-972.

Lee, S., Varvel, N.H., Konerth, M.E., Xu, G., Cardona, A.E., Ransohoff, R.M., and Lamb, B.T. (2010). CX3CR1 Deficiency Alters Microglial Activation and Reduces Beta-Amyloid Deposition in Two Alzheimer's Disease Mouse Models. Am. J. Pathol. *177*, 2549-2562.

Lee, Y.S., Morinaga, H., Kim, J.J., Lagakos, W., Taylor, S., Keshwani, M., Perkins, G., Dong, H., Kayali, A.G., Sweet, I.R.*, et al.* (2013). The fractalkine/CX3CR1 system regulates beta cell function and insulin secretion. Cell *153*, 413-425.

Liang, K.J., Lee, J.E., Wang, Y.D., Ma, W., Fontainhas, A.M., Fariss, R.N., and Wong, W.T. (2009). Regulation of Dynamic Behavior of Retinal Microglia by CX3CR1 Signaling. Invest. Ophthalmol. Vis. Sci. *50*, 4444-4451.

Libby, R.T., Anderson, M.G., Pang, I.-H., Robinson, Z.H., Savinova, O.V., Cosma, I.M., Snow, A., Wilson, L.A., Smith, R.S., Clark, A.F.*, et al.* (2005). Inherited glaucoma in DBA02J mice: Pertinent disease features for studying the neurodegeneration. Vis. Neurosci. *22*, 637-648.

Lyons, A., Lynch, A.M., Downer, E.J., Hanley, R., O'Sullivan, J.B., Smith, A., and Lynch, M.A. (2009). Fractalkine-induced activation of the phosphatidylinositol-3 kinase pathway attentuates microglial activation in vivo and in vitro. J. Neurochem. *110*, 1547-1556.

McKinnon, S.J., Schlamp, C.L., and Nickells, R.W. (2009). Mouse models of retinal ganglion cell death and glaucoma. Exp. Eye. Res. *88*, 816-824.

Mizutani, M., Pino, P.A., Saederup, N., Charo, I.F., Ransohoff, R.M., and Cardona, A.E. (2012). The fractalkine receptor but not CCR2 is present on microglia from embryonic development throughout adulthood. J. Immunol. *188*, 29-36.

Morfini, G.A., Burns, M., Binder, L.I., Kanaan, N.M., LaPointe, N., Bosco, D.A., Brown, R.H., Jr., Brown, H., Tiwari, A., Hayward, L.*, et al.* (2009). Axonal transport defects in neurodegenerative diseases. J. Neurosci. *29*, 12776-12786.

Mosser, D.M., and Edwards, J.P. (2008). Exploring the full spectrum of macrophage activation. Nat. Rev. Immunol. *8*, 958-969.

Mouton, P.R., Long, J.M., Lei, D.L., Howard, V., Jucker, M., Calhoun, M.E., and Ingram, D.K. (2002). Age and gender effects on microglia and astrocyte numbers in brains of mice. Brain Res. *956*, 30-35.

Murray, P.J., and Wynn, T.A. (2011). Protective and pathogenic functions of macrophage subsets. Nat. Rev. Immunol. *11*, 723-737.

Nash, K.R., Lee, D.C., Hunt, J.B., Jr., Morganti, J.M., Selenica, M.L., Moran, P., Reid, P., Brownlow, M., Guang-Yu Yang, C., Savalia, M.*, et al.* (2013). Fractalkine overexpression suppresses tau pathology in a mouse model of tauopathy. Neurobiol. Aging *34*, 1540-1548.

Nimmerjahn, A., Kirchhoff, F., and Helmchen, F. (2005). Resting microglial cells are highly dynamic surveillants of brain parenchyma in vivo. Science *308*, 1314-1318.

Parkhurst, C.N., Yang, G., Ninan, I., Savas, J.N., Yates, J.R., 3rd, Lafaille, J.J., Hempstead, B.L., Littman, D.R., and Gan, W.B. (2013). Microglia promote learning-dependent synapse formation through brain-derived neurotrophic factor. Cell *155*, 1596-1609.

Perry, R.B., and Fainzilber, M. (2014). Local translation in neuronal processes--in vivo tests of a "heretical hypothesis". Dev. Neurobiol. *74*, 210-217.

Prinz, M., and Priller, J. (2014). Microglia and brain macrophages in the molecular age: from origin to neuropsychiatric disease. Nat. Rev. Neurosci. *15*, 300-312.

Prinz, M., Priller, J., Sisodia, S.S., and Ransohoff, R.M. (2011). Heterogeneity of CNS myeloid cells and their roles in neurodegeneration. Nat. Neurosci. *14*, 1227-1235.
Quigley, H.A. (2011). Glaucoma. Lancet *377*, 1367-1377.

Ransohoff, R.M., and Perry, V.H. (2009). Microglial Physiology: Unique Stimuli, Specialized Responses. Ann. Rev. Immunol. *27*, 119-145.

Ray, S., Britschgi, M., Herbert, C., Takeda-Uchimura, Y., Boxer, A., Blennow, K., Friedman, L.F., Galasko, D.R., Jutel, M., Karydas, A.*, et al.* (2007). Classification and prediction of clinical Alzheimer's diagnosis based on plasma signaling proteins. Nat. Med. *13*, 1359-1362.

Rishal, I., and Fainzilber, M. (2014). Axon-soma communication in neuronal injury. Nat. Rev. Neurosci. *15*, 32-42.

Saederup, N., Cardona, A.E., Croft, K., Mizutani, M., Cotleur, A.C., Tsou, C.L., Ransohoff, R.M., and Charo, I.F. (2010). Selective chemokine receptor usage by central nervous system myeloid cells in CCR2-red fluorescent protein knock-in mice. PLoS One *5*, e13693.

Sennlaub, F., Auvynet, C., Calippe, B., Lavalette, S., Poupel, L., Hu, S.J., Dominguez, E., Camelo, S., Levy, O., Guyon, E.*, et al.* (2013). CCR2(+) monocytes infiltrate atrophic lesions in age-related macular disease and mediate photoreceptor degeneration in experimental subretinal inflammation in Cx3cr1 deficient mice. EMBO Mol. Med. *5*, 1775-1793.

Smith, J.A., Das, A., Ray, S.K., and Banik, N.L. (2012). Role of pro-inflammatory cytokines released from microglia in neurodegenerative diseases. Brain Res. Bull. *87*, 10-20.

Soto, I., Oglesby, E., Buckingham, B.P., Son, J.L., Roberson, E.D.O., Steele, M.R., Inman, D.M., Vetter, M.L., Horner, P.J., and Marsh-Armstrong, N. (2008). Retinal Ganglion Cells Downregulate Gene Expression and Lose Their Axons within the Optic Nerve Head in a Mouse Glaucoma Model. J. Neurosci. *28*, 548-561.

Streit, W.J., and Xue, Q.S. (2014). Human CNS immune senescence and neurodegeneration. Curr. Opin. Immunol. *29*, 93-96.

Tarozzo, G., Bortolazzi, S., Crochemore, C., Chen, S.C., Lira, A.S., Abrams, J.S., and Beltramo, M. (2003). Fractalkine protein localization and gene expression in mouse brain. J. Neurosci. Res. *73*, 81-88.

Tayeb, H.O., Murray, E.D., Price, B.H., and Tarazi, F.I. (2013). Bapineuzumab and solanezumab for Alzheimer's disease: is the 'amyloid cascade hypothesis' still alive? Expert Opin. Biol. Therapy *13*, 1075-1084.

Tremblay, M.E., Lowery, R.L., and Majewska, A.K. (2010). Microglial interactions with synapses are modulated by visual experience. PLoS Biol. *8*, e1000527.
Vitale, S., Schmid-Alliana, A., Breuil, V., Pomeranz, M., Millet, M.A., Rossi, B., and Schmid-Antomarchi, H. (2004). Soluble fractalkine prevents monocyte chemoattractant protein-1-induced monocyte migration via inhibition of stress-activated protein kinase 2/p38 and matrix metalloproteinase activities. J. Immunol. *172*, 585-592.

Wiggs, J.L. (2007). Genetic etiologies of glaucoma. Arch. Ophthalmol. *125*, 30-37.

Wolf, Y., Yona, S., Kim, K.W., and Jung, S. (2013). Microglia, seen from the CX3CR1 angle. Front. Cell. Neurosci. *7*, 26.

Wynne, A.M., Henry, C.J., Huang, Y., Cleland, A., and Godbout, J.P. (2010). Protracted downregulation of CX3CR1 on microglia of aged mice after lipopolysaccharide challenge. Brain Behav. & Imm. *24*, 1190-1201.

Yona, S., Kim, K.W., Wolf, Y., Mildner, A., Varol, D., Breker, M., Strauss-Ayali, D., Viukov, S., Guilliams, M., Misharin, A.*, et al.* (2013). Fate mapping reveals origins and dynamics of monocytes and tissue macrophages under homeostasis. Immunity *38*, 79-91.
Zhan, Y., Paolicelli, R.C., Sforazzini, F., Weinhard, L., Bolasco, G., Pagani, F., Vyssotski, A.L., Bifone, A., Gozzi, A., Ragozzino, D.*, et al.* (2014). Deficient neuron-microglia signaling results in impaired functional brain connectivity and social behavior. Nat. Neurosci. *17*, 400-406.

Zhang, Y., Chen, K., Sloan, S.A., Bennett, M.L., Scholze, A.R., O'Keeffe, S., Phatnani, H.P., Guarnieri, P., Caneda, C., Ruderisch, N.*, et al.* (2014). An RNA-sequencing transcriptome and splicing database of glia, neurons, and vascular cells of the cerebral cortex. J. Neurosci. *34*, 11929-11947.

CHAPTER 2

DISRUPTED CX3CR1 SIGNALING DIFFERENTIALLY WORSENS NEURODEGENERATION IN DBA/2J GLAUCOMA AND INCREASES MACROPHAGE INFILTRATION

Credits

Monica Vetter and Alejandra Bosco conceived the original idea for this project, but thereafter, the creative direction was mine. I performed all of the experiments with the exception of embedding and sectioning optic nerves, for which I would like to thank both David J. Calkins for kindly providing some of these nerves and Michael R Steele for generating the rest. I would like to thank Cesar Romero for assistance in tissue collection and mouse colony maintenance. I performed the bulk of the data analysis and quantification but would also like to thank Sarah R Anderson for help in quantifying the density of somal pNF+ RGCs. I would also like to thank Brian Dalley from the microarray core at the University of Utah for assistance with RNA quality assessment and Derek Warner and Mike Kline from the genomics core for their assistance in qRT-PCR experiments. I performed the statistical analysis on the data, prepared the figures, and wrote the resulting manuscript. I would like to thank the entire Vetter lab for their critical input in this process.

Abstract

There is a paucity of chronic and genetic models in which myeloid cells including microglia and macrophages are manipulated and effects on compartmentalized neurodegeneration examined. We determined how ablating fractalkine signaling affected retinal ganglion cell (RGC) compartmentalized degeneration and myeloid cell activation in a chronic model of glaucoma, the DBA/2J mouse.

We generated CX3CR1 $^{gfp/gfp}$ DBA/2J mice and analyzed RGC degeneration and neuroimmune responses in retina and optic nerve at 10-11 months of age, versus parental DBA/2J mice. To assess RGC degeneration, we quantified density of Brn3+ nuclei, density of RGCs with somal accumulation of phosphorylated neurofilament (pNF), and quantified the extent of axonal loss in the proximal optic nerve. To assess microglial activation, we quantified the density of retinal Iba1+ cells by morphology and measured Iba1 mRNA. We determined that amoeboid Iba1+ cells were macrophages by CCR2 immunostaining.

CX3CR1 $^{gfp/gfp}$ DBA/2J mice had increased numbers of RGCs with somal pNF, although Brn3+ nuclei density and degeneration of the optic nerve were unaffected. Only amoeboid but not ramified Iba1+ cells were increased in number, although Iba1 mRNA levels were similar between genotypes. Amoeboid Iba1+ cells were identified as peripheral macrophages by localization and CCR2 expression, yet numbers of these cells did not correlate with measured RGC pathology.

Loss of fractalkine signaling selectively increased somal pNF accumulation without altering other aspects of RGC neurodegeneration in the retina or optic nerve, suggesting specific effects on axon transport. Notably, CX3CR1 $^{gfp/gfp}$ DBA/2J retinas did

not show altered activation of resident microglial cells, but had significant increased macrophage infiltration, although these may not be coupled to glaucoma progression.

Introduction

The myeloid innate immune system has long been of interest in the field of neurodegeneration because of its reactivity to neuronal stress and damage, but also its tantalizing ability to support neurons (Czeh et al., 2011; Ilieva et al., 2009). However, since it has become apparent that different compartments of a neuron (i.e., the cell soma, axons, or dendrites) degenerate along different timelines (Conforti et al., 2007), it has been difficult to determine the role of myeloid cells in each of these compartments. Further complicating this issue is the possibly different roles of yolk sac originating resident microglia or hematopoietically-derived macrophages in neurodegeneration (Prinz et al., 2011). Recently, it has become possible to distinguish between resident microglia and infiltrating macrophages (Butovsky et al., 2014; Butovsky et al., 2012; Hickman et al., 2013; Saederup et al., 2010; Zhang et al., 2014) allowing the roles in neurodegeneration of these different myeloid lineage cells to be addressed.

In order to address the role of myeloid cells in neurodegeneration, many studies have manipulated the fractalkine (FKN) signaling system that serves as a major neuron to myeloid cell communication system. However, this has led to conflicting results, not just between diseases (Wolf et al.), but between animal models of the same neurodegenerative disease. For example, loss of FKN signaling is able to reduce amyloid-β burden in one model of Alzheimer's disease (Lee et al., 2010), while increasing Tau pathology in another (Bhaskar et al., 2010). At least part of the source of these conflicting results may

be the diverse myeloid functions that are regulated by FKN signaling, as well as an inability to identify myeloid lineage. For example, FKN signaling regulates cytokine secretion, microglia activation, dynamics and migration, survival of subsets of circulating monocytes, phagocytosis, and more recently has also been shown to impact infiltration of CCR2+ macrophages (Cardona et al., 2006; Landsman et al., 2009; Lee et al., 2010; Liang et al., 2009; Sennlaub et al., 2013).

However, there is a paucity of studies that examine how loss of FKN signaling affects multiple degenerating neuronal compartments within the same model of neurodegeneration. The DBA/2J mouse model of glaucoma is an excellent experimental tool to determine how loss of FKN signaling affects retinal ganglion cell (RGC) compartmentalized neurodegeneration, since many quantitative readouts within the retina and optic nerve have been well characterized (Bosco et al., 2015; Dengler-Crish et al., 2014; Libby et al., 2005a; Schlamp et al., 2006; Soto et al., 2008). These include downregulation of RGC genes such as the transcription factor Brn3b, accumulation of axonal proteins such as phosphorylated neurofilament (pNF) within RGC somata in the retina, and loss of myelinated axons with subsequent increase in glia in the optic nerve. Furthermore, alterations to both resident microglia and infiltrating macrophages have been noted in this model, although the impact of these on RGC compartmentalized degeneration remains poorly understood (Bosco et al., 2015; Bosco et al., 2011; Howell et al., 2012).

We therefore ablated FKN signaling on the DBA/2J background by loss of the sole FKN receptor, CX3CR1, and determined how this affected RGC compartmentalized neurodegeneration, as well as numbers and activation of microglia versus peripheral

macrophages within the retina. We find that loss of CX3CR1 affected some neuronal compartments but not others by increasing somal pNF accumulation, suggesting reduced axonal transport, but not affecting loss of RGC gene transcription or optic nerve degeneration. In addition, while microglia numbers and activation appeared unaffected, we observed that loss of CX3CR1 increased the infiltration of CCR2+ macrophages into the DBA/2J retina, although the numbers of these cells correlated poorly with RGC disease readouts.

Materials and methods

Mice

Homozygous CX3CR1 $^{gfp/gfp}$ DBA/2J mice were generated by breeding an existing colony of CX3CR1 $^{gfp/+}$ DBA/2J mice to homozygosity (Bosco et al., 2015). Control DBA/2J mice were originally obtained from Jackson Labs, bred in-house, and were refreshed with new breeders every 3 to 4 generations. Experiments and mouse care were performed in compliance with the ARVO Statement for the Use of Animals in Ophthalmic and Vision Research, and with the guidelines of the University of Utah Institutional Animal Care and Use Committee.

Tissue collection

Perfusion and dissection of retinal tissue and optic nerves for both immunohistochemistry and RNA collection were performed as in Bosco et al. (2011). Retinal whole mounts were stored in chilled 0.1M PBS overnight at 4^{o}C and utilized the next day for immunohistochemistry. Retinal eyecups were cast in gelatin, stored at -80^{o}C,

cut at 16um thickness, and placed on Superfrost Plus Slides (Fisher Scientific, Pittsburgh, PA) as in Bosco et al. (2011). Optic nerves were reserved for PPD staining.

Immunohistochemistry

Triple immunofluoresent staining was performed as in Bosco et al. (2011). Primary antibodies used in this study included: goat anti-Brn3 (Santa Cruz sc-6026 at 1:50), mouse anti-phosphorylated neurofilament (NFM and NFH; Dako M0762 at 1:100), rabbit anti-Iba1 (Wako at 1:1000), rat anti-CCR2 APC conjugated (R&D Systems FAB5538A at 1:10), and rabbit anti-cleaved caspase 3 (BD Biosciences BDB559565 at 1:500). All Alexa Fluor-conjugated (488, 568, or 647) donkey secondary antibodies were used at 1:400 (Invitrogen); Alexa-Fluor 594-conjugated donkey anti-Rat secondary was used at 1:200 (Jackson ImmunoResearch Lab). Whole mounts were incubated with primary antibodies for 3 days at 4^{o}C and incubated with appropriate AlexaFluor conjugated secondary antibodies for 2 hrs.

Microscopy

All samples were imaged on an inverted confocal microscope (Nikon A1 with NIS-Elements software 4.2) using a 20x objective and resonance scanning. Entire retinas were imaged using a multipoint acquisition macro of the software, collecting 25 x 25 fields at 60x magnification (0.41 nm/pixel), each spanning 30-40 μm of the retinal inner surface through a step size of 0.8 μm. Maximum intensity projections of stitched, high-resolution images were then generated for each retina, and all images were identically and minimally adjusted for brightness and contrast for analysis. Optic nerves were

imaged on a compound BX51 Olympus light microscope using a 60X objective and analyzed using cellSens software as 36 high-resolution multipoint images.

Quantification of Brn3+ nuclei

Brn3+ nuclei were sampled within the central 1.77 μm^2 of the retina by dividing a circle centered on the optic disc into 8 parts (2 dorsal, 2 ventral, 2 nasal, and 2 temporal). A 250-μm^2 box was placed in each of these areas and the proper plane was verified by the presence of blood vessels. When any of these 8 parts of retina visibly differed in Brn3 density, i.e., had a sector of RGC degeneration within it, a second box was placed. The total number of Brn3+ nuclei were tallied and normalized to the area sampled (# of boxes). To be counted, nuclei had to be spherical/elliptical in shape, greater than 1.5x the intensity of the background, and not be hyperintense as debris.

Quantification of somal pNF+ RGCs

Cell somas with accumulated phosphorylated neurofilament were quantified in the central 1.77 μm^2 of the retina. These cells were quantified based on shape (reflecting either somatic or somato-dendritic accumulation), intensity being greater than 1.5x the background, and size (being greater than 10 μm in diameter). By toggling on the Brn3 channel the number of Brn3+ or Brn3- phosphorylated neurofilament positive cells was determined.

Quantification of Iba1+ cells

Three categories of Iba1+ cell were determined based on morphology: branched Iba1+ cells with a small cell soma and many branches, perivascular Iba1+ cells having 2 main branches at polar opposite sides of the cell, and amoeboid Iba1+ cells having no branches. Branched Iba1+ and perivascular Iba1+ cells were quantified in the central 1.77 um^2 of the retina, excluding the optic disc. Amoeboid Iba1+ cells, being fewer in number, were quantified in the entire retina, excluding the optic disc and blood vessels.

Quantification of % axon-free nerve area

The % area within an optic nerve cross-section comprised of glia and extracellular matrix but devoid of axons or dystrophic axons was generated by automatic thresholding to create binary masks on 8 bit, RGB images as in Bosco et al. (2015). Images were minimally adjusted for contrast (0-10 on a scale to 0-100) and sharpness (Gauss Laplace between 1.0-1.1 on a scale of 0-2). A mask encompassing the area of the optic nerve minus meninges and blood vessels was generated. Non-axonal elements were then masked based on their different grey values. The % non-axonal area was then calculated by determining the percent of the total optic nerve mask (minus meninges and blood vessels) covering by non-axonal elements.

Optic nerve PPD staining

Optic nerve cross-sections were embedded and PPD stained for 28 min using a modified protocol as in Bosco et al. (2015) (Calkins et al., 2005; Libby et al., 2005a). 1um sections were cut on an ultramicrotome with a glass knife, transferred to slides, and

mounted under coverslips with Permount (Fisher).

qRT-PCR

Sample preparation, cDNA synthesis, and qRT-PCR were performed as in Bosco et al. (2011). Whole retinas were aspirated through a 22-gauge needle and RNA was isolated using a Qiagen RNeasy micro kit according to manufacturer's instructions. The mRNA quality was determined on an Agilent Bioanalyzer and samples with RINs less than 8 were discarded. First strand cDNA was synthesized using an Invitrogen Superscript III First Strand cDNA synthesis kit according to manufacturer's recommendations and quantities determined on a Nano-drop spectrophotometer. qRT-PCR was performed on an Applied Biosystems 7900HT instrument with QuantStudio 12K Flex software using an Invitrogen Platinum Sybr Green qPCR supermix-UDG kit according to manufacturer's instructions. A standard curve was generated based on serial one-half dilutions from the pooled expression of cDNAs from a large number of 1 to 12 month DBA/2J animals between 1.0 and 0.03125 all relative to the 1.0 standard. Genes were thus analyzed in the linear range based on these curves and normalized to GAPDH.

Primers

GAPDHF: TGCACCACCAACTGCTTAGC; GAPDHR: GGCATGGACTGTGGTCATGAG; IBA1F: CCTGATTGGAGGTGGATGTCA; IBA1R: GGCTCACGACTGTTTCTTTTTTCC; KIF1BF: TTATTGATACATCCATGGGGTC; KIF1BR: TCTCCTGAATACTGGTCACA ATP8A2F: CTTTGTGTTTTGTTTTCCCCGC; ATP8A2R:

CGCTGTACTTGGCCGTACTGA

Statistics

Normality of the data was examined both by histogram distribution and by percentage of data falling 1 and 2 standard deviations away from the mean. Individual data points are showed, and the means indicated with a solid horizontal bar, with dashed horizontal bars denoting +1 and -1 standard deviations. We therefore used a Wilcoxon ranked sum test to determine significance with * being a $p<.05$. Normalized qRT-PCR results were compared by Student's t test.

Results

Loss of the CX3CR1 in the DBA/2J mouse does not alter Brn3 downregulation

Since disruption of Cx3CR1 has been reported to influence neuronal decline in other models of neurodegeneration, we sought to determine whether the course of RGC decline would be impacted by loss of fractalkine signaling in a model of glaucoma. We generated DBA/2J mice homozygous for a *CX3CR1*-GFP knock-in allele (Bosco et al., 2015; Jung et al., 2000), and aged these animals, as well as standard DBA/2J mice, to 10-11 months of age, when a majority of DBA/2J eyes typically show clear glaucoma pathology (Libby et al., 2005a). Since RGC degeneration in the DBA/2J involves downregulation of RGC genes, including the transcription factor family, Brn3 (Domenici et al., 2014; Soto et al., 2008), we assessed whether loss of fractalkine signaling altered expression of Brn3 in *CX3CR1*-GFP DBA/2J retinas ($n = 36$) relative to DBA/2J retinas

(*n =31*) (Fig. 2.1 A). We quantified the density of Brn3+ nuclei in 8 sectors for each retina (Fig. 2.1 A), and found that regardless of genotype, there were areas with high and low numbers of Brn3+ nuclei (Fig. 2.1B-E), consistent with sectorial downregulation in both. We then calculated average densities of Brn3+ nuclei for each retina (Fig. 2.1 F). There were similar maximum densities of Brn3+ nuclei in each genotype (Fig. 2.1 F; 2,400 in DBA/2J and 2,300/mm^2 in CX3CR1 null DBA/2J), and similar distribution of retinas with varying levels of Brn3 depletion (Fig. 2.1 F), consistent with the varying levels of disease severity typically observed in the DBA/2J model. In addition, the population mean density of Brn3+ nuclei for each genotype was not significantly different (Fig. 2.1F). Therefore, we conclude that at this timepoint, loss of fractalkine signaling did not affect the characteristic downregulation of Brn3 that occurs in the DBA/2J with age.

Loss of Cx3CR1 increases the number of RGCs with somal accumulation of axonal proteins in the DBA/2J retina

Deficits in axonal transport progressively affect RGC axon and somal integrity in the DBA/2J (Crish et al., 2010; Dengler-Crish et al., 2014). One marker of disrupted axonal transport in DBA/2J retinas is the build-up of phosphorylated neurofilament (pNF; medium and heavy) proteins within the proximal axon segment, cell body, and dendrites of RGCs (Soto et al., 2008). Within the central retina of both wild type and CX3CR1 $^{gfp/gfp}$ DBA/2J mice at 10-11 months of age, we found regions with both high and low numbers of somal pNF+ RGCs (Fig. 2.2 A-C), consistent with the variable levels of pathology in the DBA/2J model. When we quantified the density of somal pNF+ RGCs

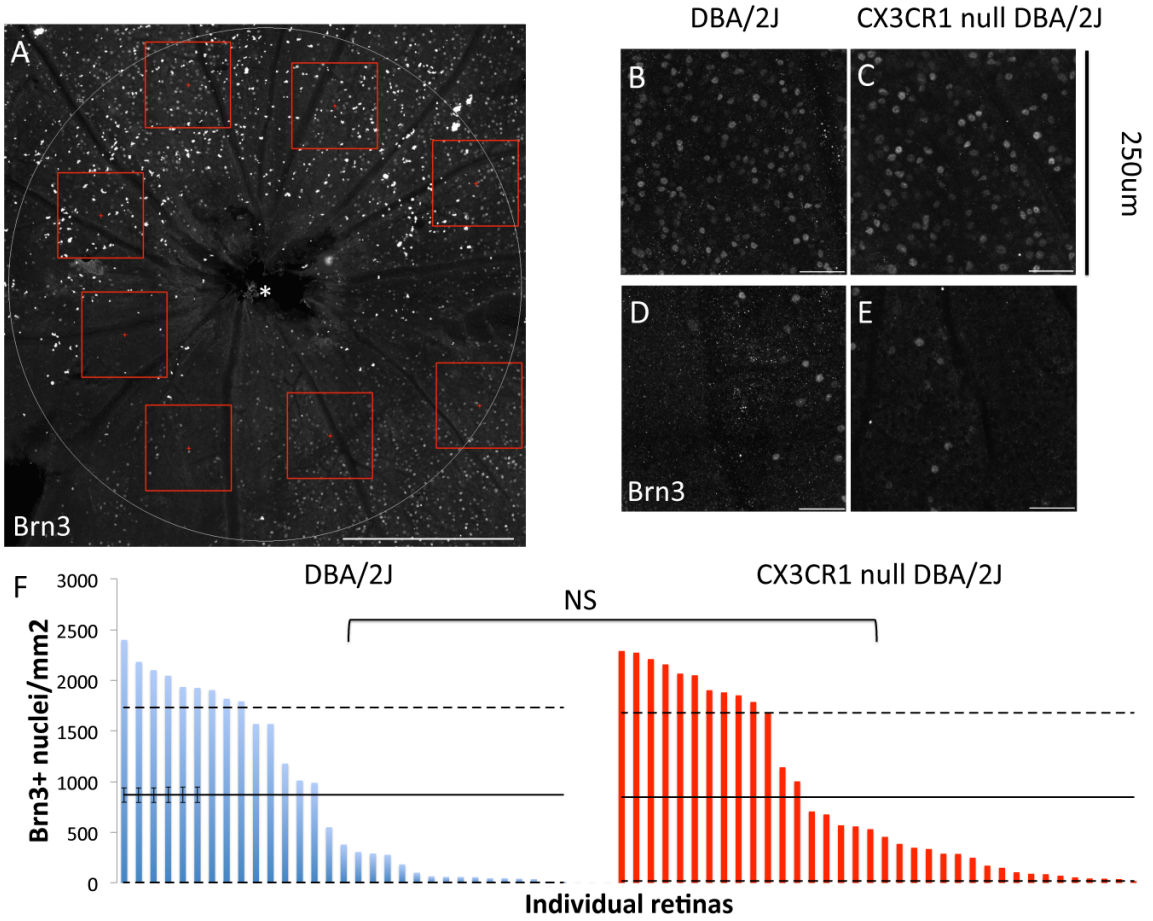

Figure 2.1: The density of Brn3+ nuclei does not change with loss of the CX3CR1. (A) Confocal image of a representative CX3CR1 null DBA/2J retinal flat mount showing the Brn3 immunofluorescence in the central retinal area (1.77mm^2). Red boxes depict example 0. 06mm^2 areas sampled. Sectors of Brn3+ nuclei depletion are apparent in this retina. (B,D) Higher magnification images of 0.06 mm^2 fields from a DBA/2J flat mount retina comparing/contrasting high (C) and low (E) Brn3+ nuclei density. (C,E) Higher magnification images of 0.06 mm^2 fields from a CX3CR1 null DBA/2J contrasting high (B) and low (D) Brn3+ nuclei density. (F) Distribution of Brn3+ nuclei densities per retina in DBA/2J (blue) and CX3CR1 null DBA/2J (red). Solid horizontal line indicates the population mean, dashed lines indicate 1 standard deviation above and below the mean. Error bars represent the SEM. * indicates optic nerve head, Scale bars: 500um (A); 50um (B-E).

for each retina, we observed a shift in the distribution of retinas towards a higher density of somal pNF+ RGCs with loss of Cx3CR1, which resulted in a statistically significant mean increase in somal pNF+ RGCs in Cx3CR1$^{gfp/gfp}$ DBA/2J retinas as compared to DBA/2J (Fig. 2.2 D).

Since somal accumulation of pNF suggests deficits in axonal transport, we isolated whole retina mRNA and performed quantitative RT-PCR to determine whether there is altered expression of genes involved in transport. Previous work has shown Kif1b reduction within sectors of DBA/2J retinas depleted of the retrograde tracer fluorogold positive RGCs (Panagis et al., 2010). Compared to DBA/2J, we found that expression of the anterograde transport motor Kif1b was significantly reduced in Cx3CR1$^{gfp/gfp}$ DBA/2J retinas (25% reduction; n=9 retinas Cx3CR1$^{gfp/gfp}$ DBA/2J n=8 DBA/2J; $p<0.05$-consistent by Student's t-test).

Loss of CX3CR1 in DBA/2J mice does not exacerbate optic nerve degeneration

RGC degeneration in the DBA/2J model is well characterized within the optic nerve to include a progressive loss of RGC axons and a subsequent replacement by glia and extracellular matrix (Bosco et al., 2015; John et al., 1998; Libby et al., 2005b; Schlamp et al., 2006). To determine whether this optic nerve degeneration is impacted by loss of fractalkine signaling, we quantified the extent of non-axonal area using binary masks as in Bosco et al. (2015). For DBA/2J and Cx3CR1$^{gfp/gfp}$ DBA/2J genotypes at 10-11 months, we observed a similar distribution of nerves with relative axonal versus glial coverage, ranging from ~10% to above 95% of axon-free area in individual nerves (Fig. 2.3 A-E). We did not observe a statistically significant difference in the mean non-axonal

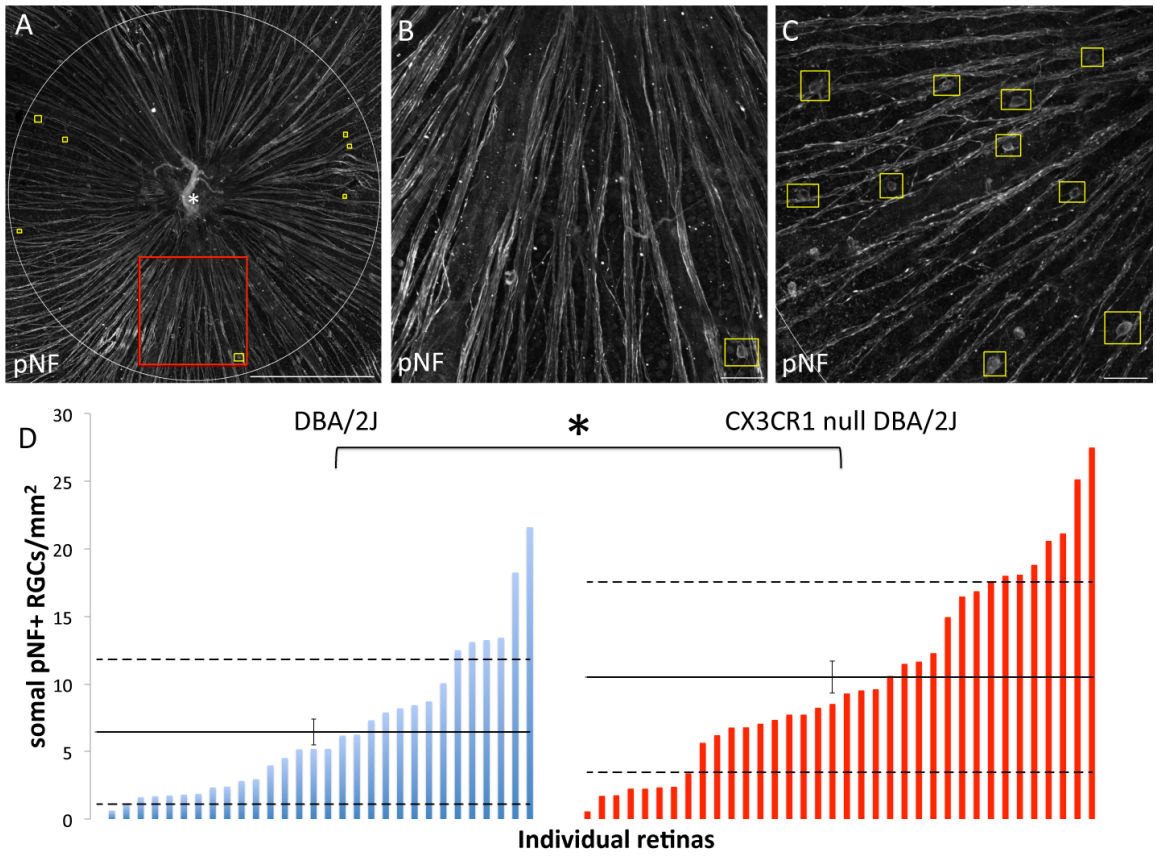

Figure 2.2: More RGCs have accumulated pNF around the cell soma in retinas with disrupted fractalkine signaling.(A) Confocal image of a retinal flat mount immunostained for phosphor-neurofilament (pNF) with few somal pNF+ RGCs and smooth, fasciculated axons, depicting the sampled central retinal area (1.77mm^2) . Yellow boxes indicate cells that show pNF accumulated around the cell soma.(B) Higher magnification view of an area in A (red box), depicting a cell with accumulated somal pNF (yellow box in the bottom right hand corner).(C) Higher magnification of the central retinal area from a different retina (same dimensions as in B) depicting many more somal pNF+ RGCs (yellow boxes) as well as beaded and de-fasciculated axons.(D) Distribution of the number of cells with somal pNF within the central retina in DBA/2J (blue) and CX3CR1 null DBA/2J (red). There are significantly more of these cells in CX3CR1 null retinas (*: $p<.05$; Wilcoxon ranked sum test). Solid horizontal line indicates the population mean, dashed lines indicate 1 standard deviation above and below the mean. Error bars represent the SEM. Scale bars: 500 um (A); 50 um (B&C).

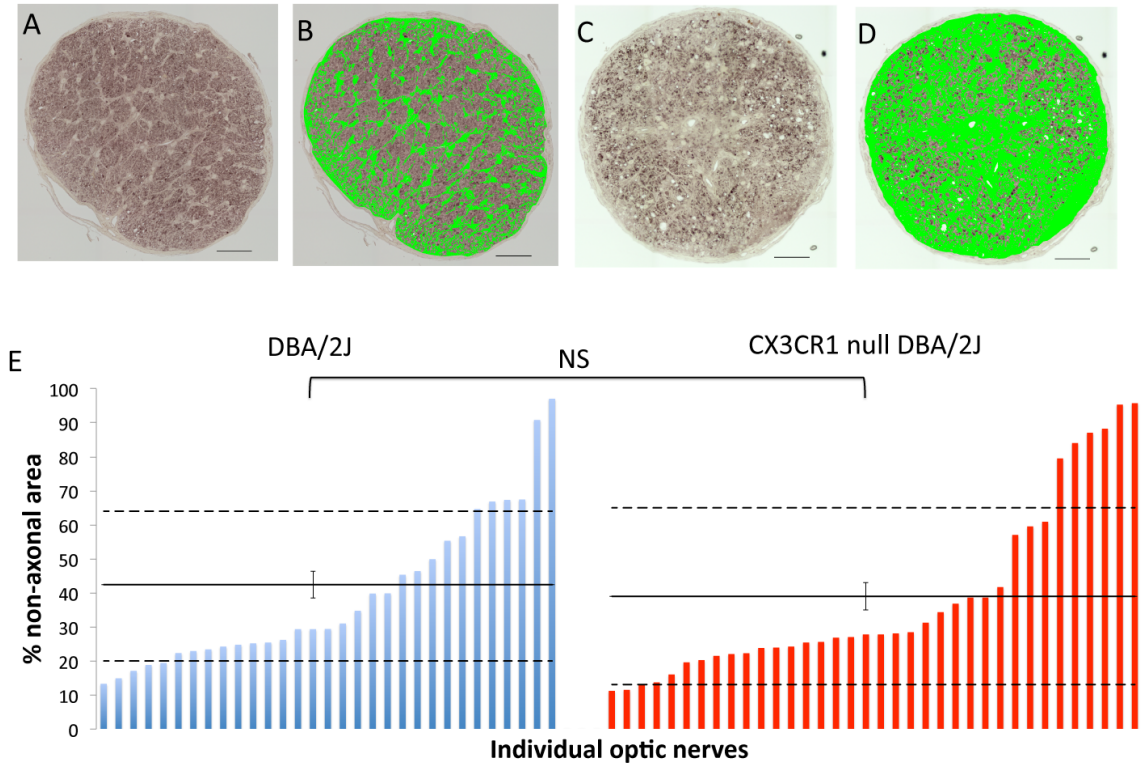

Figure 2.3: There is no difference in the amount of gliosis and scarring in the optic nerve with loss of fractalkine signaling. (A) Low magnification view of a healthy optic nerve cross-section with low gliosis and few dystrophic axonal profiles used for subsequent image analysis. (B) Low magnification view of the nerve in A with a binary mask including the glia and extracellular matrix indicated in green. The division of the area of this mask by the entire optic nerve minus meninges and blood vessels yields the % non-axonal area. (C) Low magnification view of a highly affected optic nerve cross-section with high gliosis and many dystrophic axonal profiles used for subsequent image analysis. (D) Low magnification view of the nerve in D with a binary mask including the glia and extracellular matrix indicated in green. (E) Distribution of the non-axonal area percentages per optic nerve in DBA/2J (blue) and FKNR null DBA/2J (red) showing no difference between the genotypes. Horizontal lines indicate the population mean. Error bars represent the SEM. Samples that define the limits of 1 standard deviation above and below the mean are indicated by bold outlines. Scale bars: 50 um (A); 10 um (B&C)

area for Cx3CR1$^{gfp/gfp}$ DBA/2J optic nerves as compared to DBA/2J (Fig. 2.3 E). Therefore, we conclude that loss of fractalkine signaling did not alter optic nerve degeneration on the DBA/2J background at this timepoint within the proximal segment of the nerve.

Loss of CX3CR1 increases the number of early declining RGCs

Loss of fractalkine signaling may be generating newly affected RGCs, impairing the clearance of sick RGCs, or both. Therefore, to identify individual RGCs at earlier and later stages of decline, we quantified subsets of somal pNF+ RGCs with or without nuclear Brn3 expression. While both a reduction in Brn3+ nuclei density and an increase in somal pNF+ RGC density occur at 9 months in some DBA/2J animals (Soto et al., 2008), these readouts have not been examined in combination. We found Brn3+ somal pNF+ RGCs and Brn3- somal pNF+ RGCs in both DBA/2J and Cx3CR1$^{gfp/gfp}$ DBA/2J genotypes at 10-11 months. This suggests that healthy RGCs express Brn3, but lack somal pNF (Brn3+/pNF-), early declining RGCs express Brn3 but accumulate somal pNF (Brn3+/pNF+), while RGCs in later stages of decline lose Brn3 expression and retain somal pNF (Brn3-/pNF+) before ultimately being eliminated (Fig. 2.4 A-C; Soto et al., 2008). If there is a failure of clearance of sick RGCs, there should be a selective increase in RGCs in the late stage of decline (Brn3-/pNF+).

We next quantified the density of RGCs in an early stage of decline (Brn3+/pNF+) versus late stages of decline (Brn3-/pNF+) for DBA/2J and Cx3CR1$^{gfp/gfp}$ DBA/2J retinas. We found a higher proportion of Cx3CR1$^{gfp/gfp}$ DBA/2J retinas that had RGCs double positive for Brn3 and somal pNF compared to age-matched DBA/2J mice,

and a significant increase in the mean number of RGCs double positive for Brn3 and somal pNF (Fig. 2.4 D), suggesting an increase in early declining RGCs. We also observed a significant increase in the mean number of RGCs in late stages of decline (Brn3-/pNF+), consistent with the overall increase in pNF+ RGCs (Fig. 2.4 E). Since there is not a selective increase in this population, we conclude that there is not simply a failure to clear sick RGCs in Cx3CR1$^{gfp/gfp}$ DBA/2J retinas.

We next sought to determine whether somal pNF+ cells were actively dying or dead RGCs that had not yet been cleared. We performed immunostaining for cleaved caspase 3, and found that none of the pNF+ cells were positive (0 out of 40 somal pNF+ RGCs, n = 2 retinas; Fig. 2.5 A-C). In addition, we observed that the nuclei of RGCs with somal pNF+ accumulation were not pyknotic (Fig. 2.6 A-C), suggesting they are not yet undergoing apoptosis.

Notably, DBA/2J retinas rarely contained both high density of Brn3+ nuclei and high density of Brn3+, somal pNF+ RGCs (Fig. 2.7 B). In contrast, high numbers of Brn3+ somal pNF+ RGCs occurred much more frequently in Cx3CR1$^{gfp/gfp}$ DBA/2J retinas regardless of Brn3+ nuclei density, and even in retinas with a high overall density of Brn3+ nuclei (Fig. 2.7 C). In contrast, with regards to clearance, we found that both genotypes had the same percentage (13%) of retinas with below average Brn3+ and somal pNF+ density as well as matching optic nerves with above average % non-axonal area (Fig. 2.8). Further with respect to clearance, fractalkine has been shown to induce the opsonin Mfge8 that stimulates myeloid cells to clear apoptotic neurons (Fuller and Van Eldik, 2008). We assessed levels of Mfge8 mRNA in Cx3CR1$^{gfp/gfp}$ DBA/2J (n=3) versus DBA/2J (n=3) retinas, but found no significant difference ($p>.05$, t-test). Together,

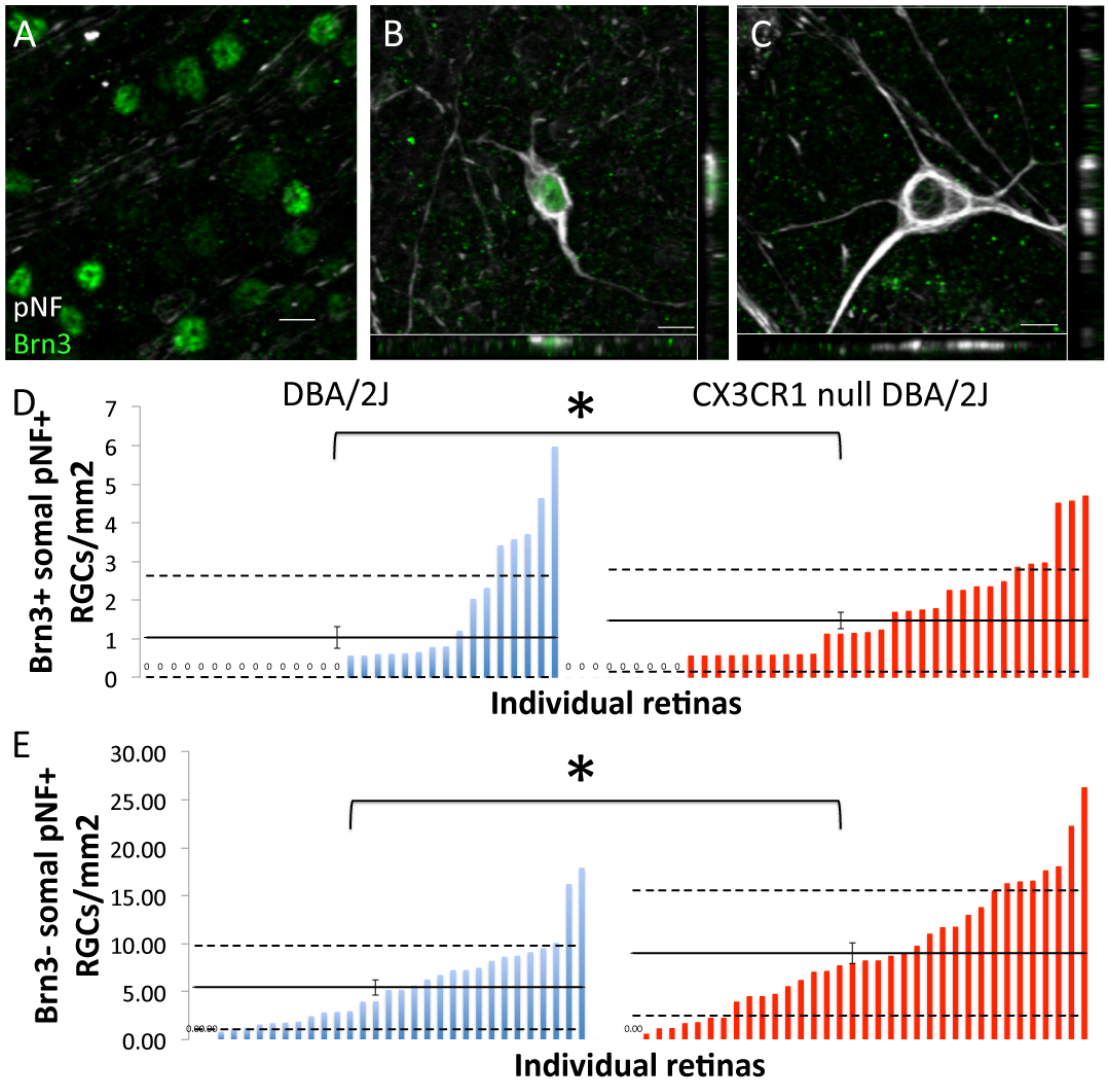

Figure 2.4: Loss of fractalkine signaling results in increased numbers of Brn3+ and Brn3- somal pNF+ RGCs. (A) High magnification view of a field of Brn3+ nuclei without accumulation of somal pNF. (B) Example of a cell with a Brn3+ nucleus and accumulated somal pNF. Orthogonal views in the x-y (bottom) and y-z (side) planes are shown. (C) Example of a cell with a Brn3- nucleus and accumulated somal pNF. Orthogonal views in the x-y (bottom) and y-z (side) planes are shown. (D) Distribution of the number of Brn3+ somal pNF+ cells within the central retina in DBA/2J (blue) and CX3CR1 null DBA/2J (red) mice. There are significantly more of these cells in CX3CR1 null retinas than in the DBA/2J retinas (*: $p<.05$; Wilcoxon ranked sum test). Solid horizontal line are the population mean, dashed lines are 1 standard deviation above and below the mean. (E) Distribution of the number of Brn3- somal pNF+ cells within the central retina in DBA/2J (blue) and CX3CR1 null DBA/2J (red). There are significantly more of these cells in CX3CR1 null retinas (*: $p<.05$; Wilcoxon ranked sum test). Solid horizontal line indicates the population mean, dashed lines indicate 1 standard deviation above and below the mean. Error bars represent the SEM. Scale bars: 10 um (A-C)

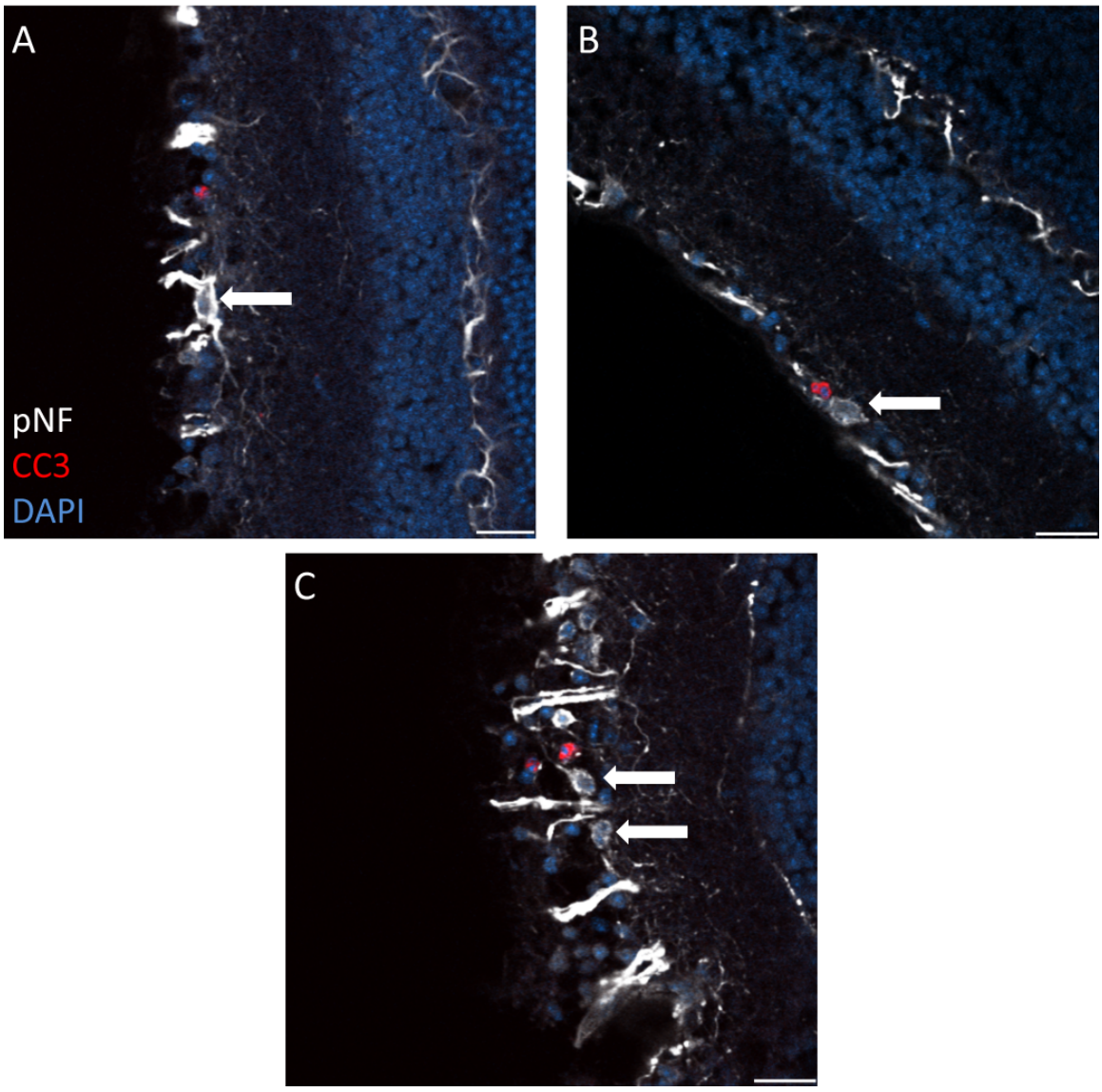

Figure 2.5: Somal pNF+ RGCs are not entering apoptosis (do not express cleaved caspase 3). (A-C) Radial cryosections through a CX3CR1 null DBA/2J retina stained for phosphorylated neurofilament (white) and cleaved caspase 3(red) with a DAPI nuclear counterstain. White arrows indicate somal pNF+ RGCs that are cleaved caspase 3 negative. Scale bar: 10um (A-C)

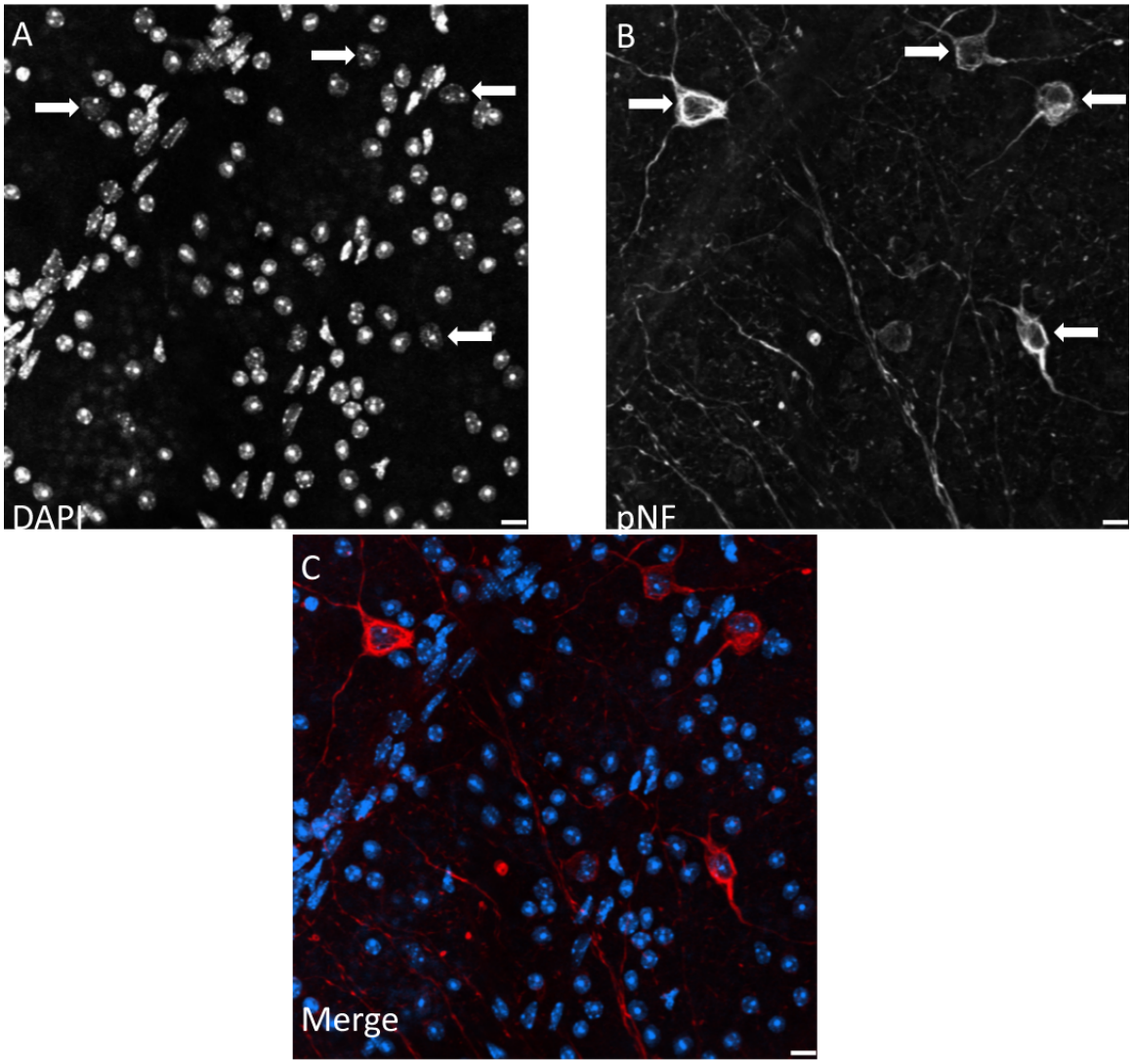

Figure 2.6: Somal pNF+ RGCs do not have pyknotic nuclei. (A) Normal appearing nuclei from a CX3CR1 null DBA/2J retinal whole mount in the DAPI channel. Arrows represent cells in B and C. (B) The same field showing the immunostaining for phosphorylated neurofilament. (C) Merge of the two channels showing overlap between the nuclei indicated in A and the somal pNF+ cells in B. Scale bar: 10um (A-C)

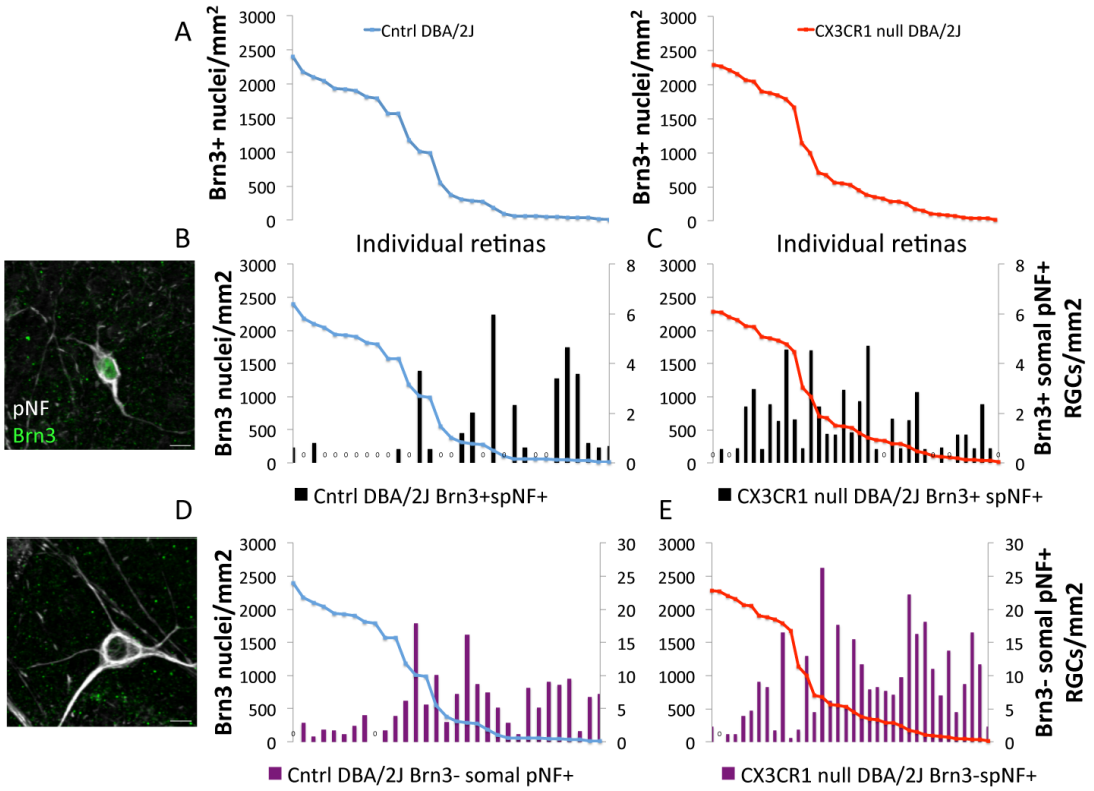

Figure 2.7: Brn3+ somal pNF+ RGCs accumulate in retinas with higher Brn3+ nuclei densities with loss of fractalkine signaling. (A) Distribution of Brn3+ nuclei densities in control DBA/2J (blue line) and CX3CR1 null DBA/2J (red line) retinas with retinas sorted in descending order. (B,D) Distribution of Brn3+ somal pNF+ RGCs (B) or Brn3- somal pNF+ RGCs (D) amongst control DBA/2J retinas (same retinas as in A, blue line), with the total Brn3+ nuclei/mm^2 density overlaid. Next to B is an example of a Brn3+ somal pNF+ retinas. Next to D is an example of a Brn3- somal pNF+ RGC. (C,E) Distribution of Brn3+ somal pNF+ RGCs (C) or Brn3- somal pNF+ RGCs (E) amongst CX3CR1 null DBA/2J retinas (same retinas as in A, red line), with the total Brn3+ nuclei/mm^2 density overlaid. Scale bars: 10 um (B&D)

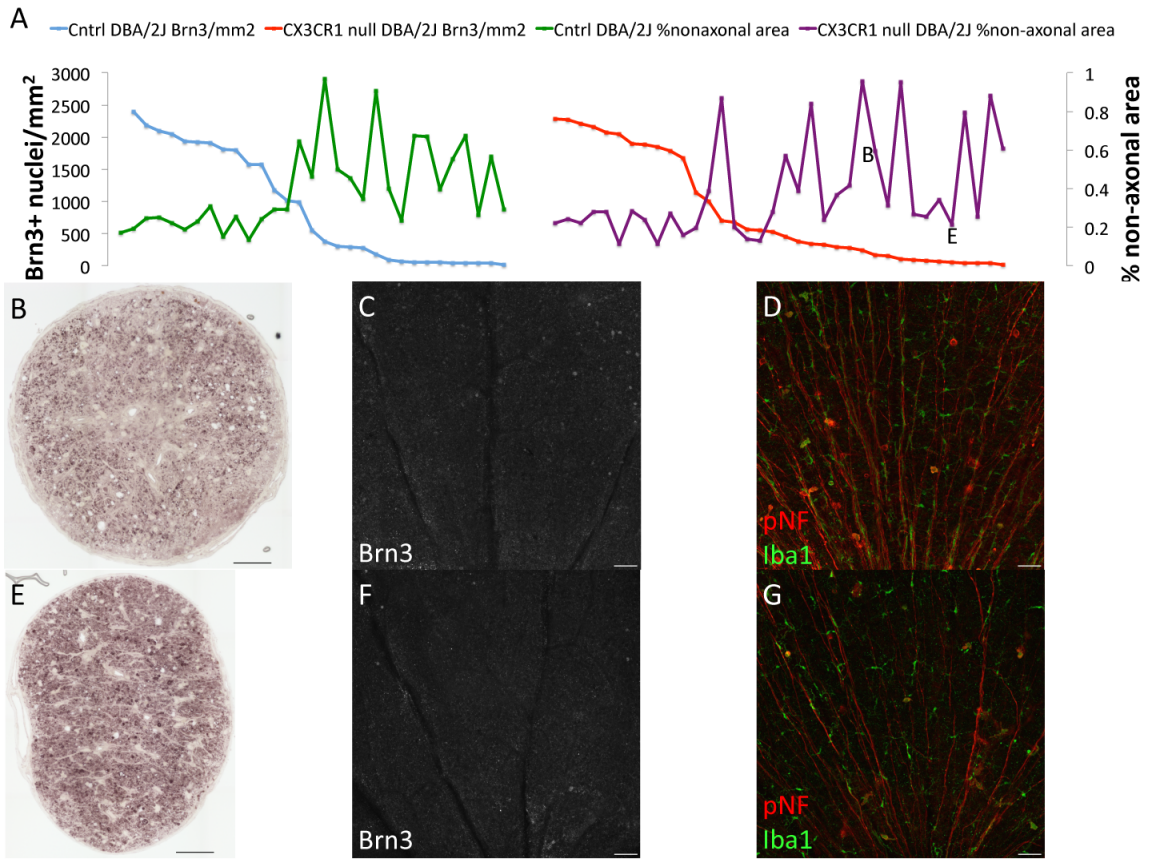

Figure 2.8: There are similar percentages of samples with markers of RGC clearance (low Brn3+ nuclei and somal pNF+ RGC density and a high % non-axonal area in the optic nerve) with loss of fractalkine signaling. (A) Distribution of Brn3+ nuclei densities in control DBA/2J (blue line) and CX3CR1 null DBA/2J (red line) sorted in descending order with the % non-axonal area in the corresponding optic nerve for control DBA/2J (green line) and CX3CR1 null DBA/2J (purple line) overlaid for each sample. Samples depicted in B-D and E-G are shown on the curve. (B-D) Representative example of an optic nerve with extensive scarring (B) with a matching retina depleted of Brn3+ nuclei (C) and few somal pNF+ RGCs (D). (E-G) Representative example of an optic nerve with little scarring (E) with a matching retina depleted of Brn3+ nuclei (F) and few somal pNF+ RGCs (G). Note the increased number of dystrophic axonal profiles within optic nerves that have a low density of Brn3+ nuclei in the retina. Amoeboid Iba1+ cells also nonspecifically label with pNF. Scale bar: 50 um

these findings suggest that loss of fractalkine signaling is amplifying the generation of dystrophic RGCs rather than impairing their clearance.

There are more infiltrating macrophages in Cx3CR1$^{gfp/gfp}$ DBA/2J retinas

Given that fractalkine signaling regulates many myeloid cell responses, including microglial activation, distribution, and recruitment of peripheral monocytes (Cardona et al., 2006; Wolf et al., 2013), we examined how loss of fractalkine signaling affected myeloid cell activation in terms of morphology, number, and levels of the activation associated gene, Iba1 (Inman and Horner, 2007) in CX3CR1 null DBA/2J mice.
We observed three distinct morphological subtypes of Iba1+ cells within the retina: cells with a small soma and many branches ("branched"), cells with two main branches on polar opposite sides typically outlining blood vessels ("perivascular"), and spherical cells with no branches ("amoeboid") (Fig. 2.9 A-C). We presume these cell subtypes to respectively represent resident microglia, perivascular macrophages, and either infiltrating macrophages or highly activated resident microglia. We found no change in the numbers of branched Iba1+ cells (Fig. 2.9 D-F) within Cx3CR1$^{gfp/gfp}$ DBA/2J retinas, suggesting no change in the resident microglia population. We observed a trend towards significance ($p< 0.1$) in the number of perivascular cells, but quantified a significant increase in the number of amoeboid Iba1+ cells. We found equal levels of Iba1 mRNA between the genotypes by qRT-PCR, suggesting no significant changes in the levels of myeloid cell activation.

To determine whether the amoeboid Iba1+ cells were infiltrating macrophages, we confirmed by volumetric view of confocal image stacks that the amoeboid Iba1+ cells

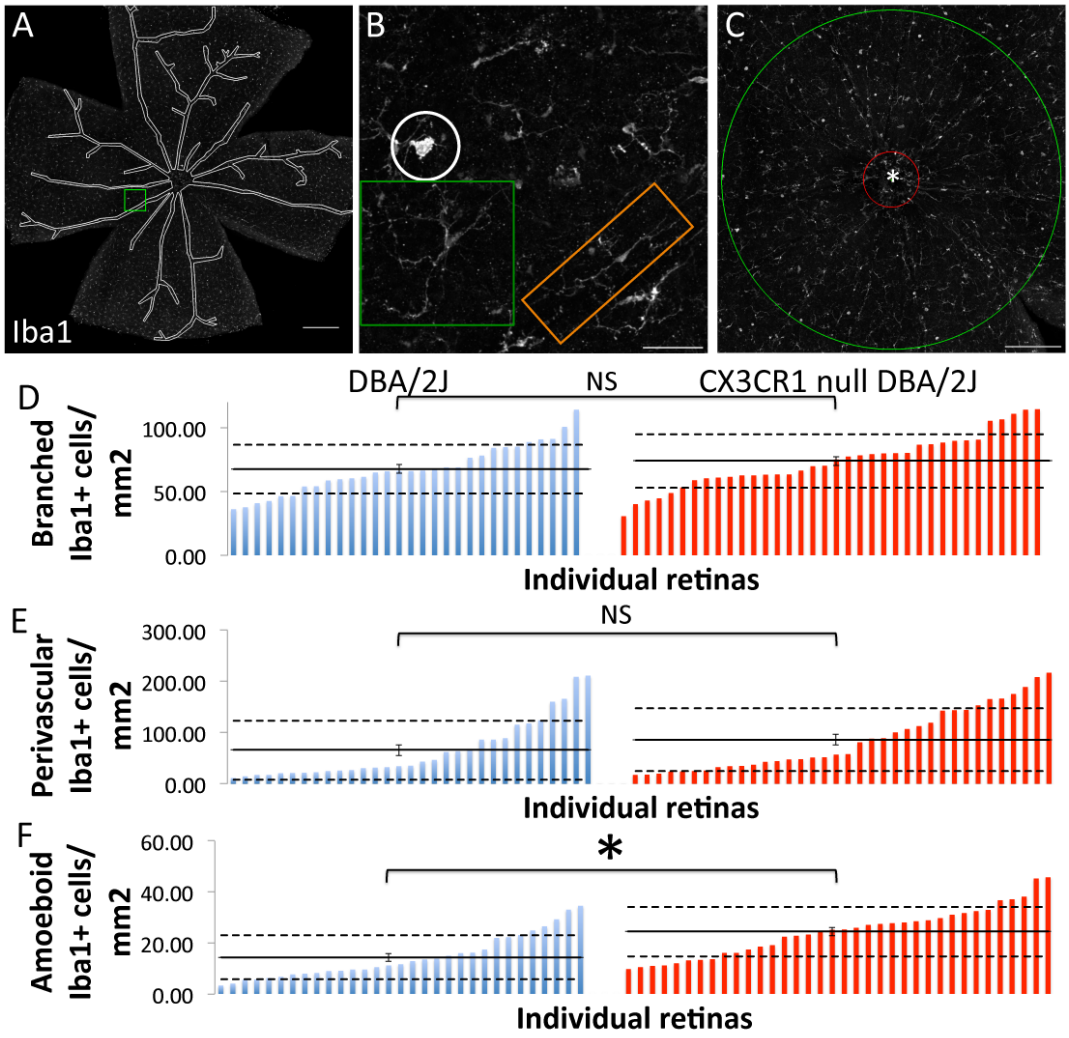

Figure 2.9: Loss of fractalkine signaling results in greater numbers of amoeboid shaped Iba1+ cells. (A) Low magnification view of an entire retinal flat mount that was sampled for Iba1+ cells showing amoeboid morphology. Blood vessels (traced) were excluded from analysis. (B) Higher magnification view of the area indicated in A demonstrating the 3 categories of shapes for Iba1+ cells. The white circle depicts a cell with amoeboid morphology , the green box depicts a cell with branched morphology, and the orange box indicates a perivascular-shaped Iba1+ cell. (C) Low magnification image of the central retina ($1.77mm^2$) depicting the area sampled for branched and perivascular shaped Iba1+ cells excluding the optic nerve head (marked by an asterisk and traced by the red circle). (D-F) Distribution of the number of branched (D), perivascular (E), and amoeboid shaped Iba1+ cells (F) within the central retina in DBA/2J (blue) and CX3CR1 null DBA/2J (red). There are significantly more amoeboid Iba1+ cells (*: $p<.05$; Wilcoxon ranked sum test) in CX3CR1 null retinas. There are no statistically significant changes in the numbers of branched or perivascular Iba1+ cells ($p<.3$ and $p<.1$ respectively). Horizontal lines indicate the population mean. Error bars represent the samples that define the limits of 1 standard deviation above and below the mean are indicated by bold outlines. Scale bars: 500 um (A), 50um (B), 250um (C)

were exclusively located in the nerve fiber layer (Fig. 2.10 A), as reported for infiltrating macrophages in retinal injury paradigms (Garcia-Valenzuela and Sharma, 1999) and macrophages that patrol the vitreous body (Vagaja et al., 2012). However, we wanted tomore definitively determine if these cells were infiltrating macrophages, so we immunostained for the peripheral macrophage marker CCR2 (Saederup et al., 2010). We determined that the amoeboid shaped Iba1+ cells stained positive for the peripheral macrophage marker CCR2 in whole mounts from control DBA/2J retinas (Fig. 2.10 B) and in cryosections from CX3CR1 null DBA/2J retinas (Fig. 2.10 C&D).

To determine whether the amoeboid Iba1+ cells were involved in driving the enhanced RGC pathology that we observed in $Cx3CR1^{gfp/gfp}$ DBA/2J retinas, we examined whether numbers of amoeboid Iba1+ cells correlated with RGC pathology in the retina. Surprisingly, we found a poor correlation between numbers and distribution of spherical Iba1+ cells and density of either Brn3+ nuclei or somal pNF+ RGCs in both DBA/2J and $Cx3CR1^{gfp/gfp}$ DBA/2J retinas (Fig. 2.10 E). Together, our data support a model in which loss of fractalkine signaling primarily increased macrophage infiltration in aged retinas rather than increasing resident microglia activation, consistent with the findings of Sennlaub et al. (2013). Surprisingly, the lack of correlation between these peripherally derived macrophages and RGC pathology suggests that the blood-derived monocytes may not be driving the differences in RGC pathology that we detected in $Cx3CR1^{gfp/gfp}$ DBA/2J retinas.

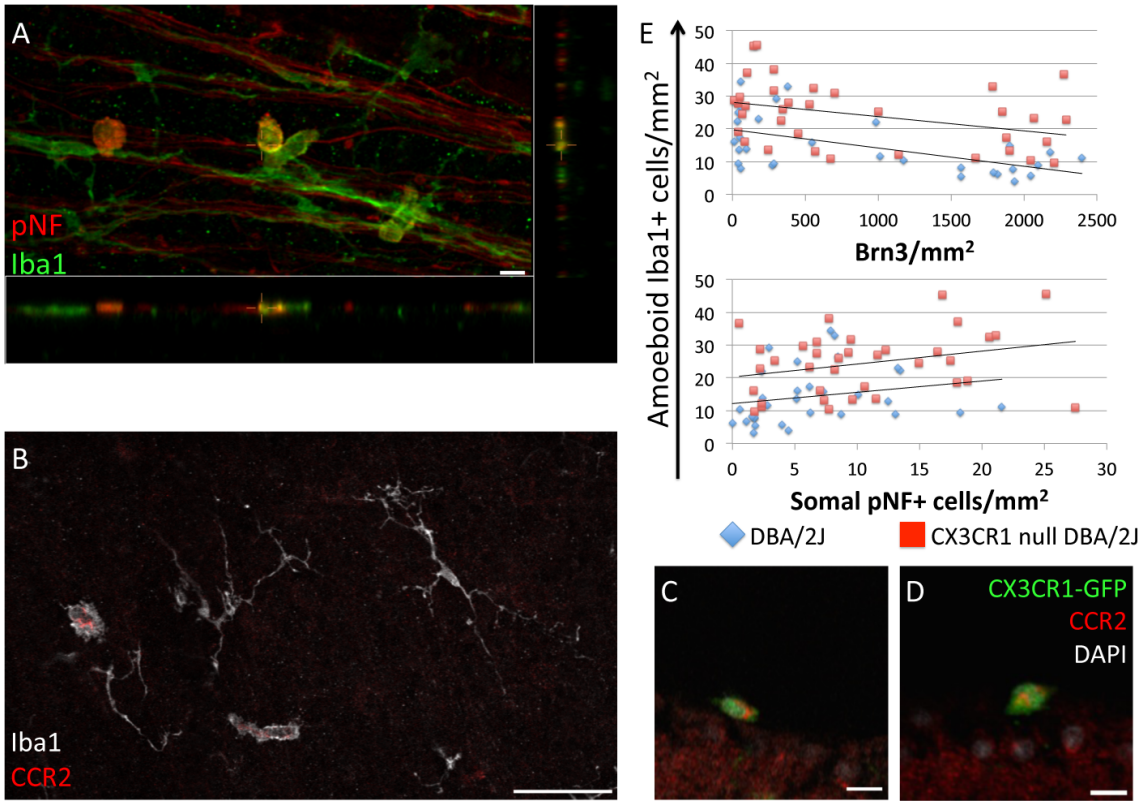

Figure 2.10: Amoeboid Iba1+ cells are peripherally derived macrophages but they do not correlate with RGC pathology in either genotype. (A) Amoeboid Iba1+ cells localize to the neurofibrillary layer. Volume view of CX3CR1 null DBA/2J retinal whole mount stained for the axonal marker pNF and the microglia/macrophage marker Iba1. Orthogonal views shown below and to the right. Amoeboid Iba1+ cells showed non-specific reactivity with the donkey anti-mouse secondary antibody used to detect pNF. (B) Single z-plane from a control DBA/2J retinal whole mount immunostained for the peripheral macrophage marker CCR2 (red) and Iba1. The amoeboid shaped Iba1+ cells are positive for CCR2 while branched Iba1+ cells are negative. (C & D) Single z-plane of a radial section from a CX3CR1 null DBA/2J retina immunostained for the peripheral macrophage marker CCR2 (red) and showing gfp expressed by cells expressing the CX3CR1 gene. Dapi (white) denotes the ganglion cell layer (GCL). Amoeboid CX3CR1+ cells above the GCL are CCR2 positive. (E) There is no correlation between the number of amoeboid Iba1+ cells and either the density of Brn3+ nuclei or somal pNF+ RGCs, regardless of genotype. R^2 value for amoeboid Iba1+ cells vs Brn3+ nuclei density (top) is .32 and .14 for DBA/2J and CX3CR1 null DBA/2J mice, R^2 value density of somal pNF+ cells (middle) is .05 and .08, R2 value for % non-axonal area (not shown) in the optic nerve is .08 and .1. Scale bars: 50 um (B) 10um (A, C, & D)

Discussion

We found that loss of CX3CR1 in the DBA/2J background had a selective effect on RGC somal integrity, likely due to deficient axonal transport, but did not affect other aspects of RGC neurodegeneration, including loss of gene transcription or optic nerve histopathology. These changes were concomitant with increased infiltration of CCR2+ peripheral macrophages but not myeloid activation overall, since levels of Iba1 mRNA were unaffected. This study reveals a selective role for FKN signaling on one aspect of RGC degeneration, and demonstrates that loss of FKN signaling primarily increased macrophage infiltration.

Loss of CX3CR1 affects compartmentalized RGC degeneration

Our compartmental approach to analyze RGC neurodegeneration in the DBA/2J model of chronic glaucoma revealed that disruption of CX3CR1 has selective effects on RGC axonal transport that are uncoupled from other RGC degenerative changes. While decline of RGC axons has clearly been shown to be crucial in degeneration (Howell et al., 2007), degenerative changes in other compartments also contribute to RGC demise (Fernandes et al., 2014). Our findings suggest that distinct mechanisms may drive these diverse degenerative changes in RGCs, and implicate myeloid cells specifically in modulating the decline of axon transport that is a hallmark of many neurodegenerative diseases.

It is unknown whether during the course of neurodegeneration somal decline and axonal degeneration are linked. Our findings suggest that these events can be uncoupled since we were able to find retinas severely depleted of Brn3+ nuclei that nonetheless had

few somal pNF+ RGCs, and an optic nerve with relatively intact axons and little gliosis (Fig. 2.8). The existence of such samples suggests very important pathological events are taking place in the retina prior to histologic degeneration of the optic nerve. These findings suggest that in the absence of being able to derail the initiating event in neurodegeneration, treatment directed to multiple neuronal compartments may be necessary to delay or halt progression.

Interestingly, loss of CX3CR1 is not the only instance of somal accumulation of pNF in RGCs being uncoupled from optic nerve degeneration. Another example is the wabbler-lethal mutant mouse that has a loss of function mutation in the phosphatidyl-serine flippase, Atp8a2, which is involved in apoptosis and vesicle trafficking (van der Mark et al., 2013; Zhu et al., 2012). This mutant mouse shows disrupted axonal transport with an increase in RGCs with somal pNF, without increased damage to the optic nerve. We found a significant (15%) reduction in mRNA levels of Atp8a2 in our CX3CR1 null DBA/2J retinas versus the control DBA/2J retinas, suggesting that this pathway may be in part responsible for reducing RGC axonal transport. These results raise the question of whether exposed phosphatidyl-serine signaling to receptors on microglia or macrophages affects RGC degeneration, or if a cell autonomous role in membrane fluidity affects axonal transport.

An early step in the decline of RGCs is downregulation of RGC genes, such as the transcription factor family Brn3 (Domenici et al., 2014; Welsbie et al., 2013). In our study, Brn3 downregulation was evident in both DBA/2J and CX3CR1 null DBA/2J retinas, but we did not see a difference in the number of Brn3 positive nuclei, either in the central retina or in a set of 35 control and 40 CX3CR1 null DBA/2Js sampled throughout

the retina (data not shown). This suggests that numbers of RGCs were not significantly different with loss of CX3CR1 in a chronic disease setting, and that this aspect of early RGC decline is not influenced by CX3CR1 signaling in myeloid cells. In contrast, Wang et al. (2014) found significant reductions in beta tubulin III labeled RGCs in a transient ocular hypertension model of glaucoma. Although different markers of RGCs were assessed, it is possible that CX3CR1 signaling has different effects in an acute injury versus chronic model of RGC degeneration. It is unknown whether similar mechanisms are driving RGC decline in these distinct models, but our findings suggest differential roles for myeloid cells. In general, it is unclear whether the myeloid system is phenotypically similar between acute and chronic models of neurodegeneration.

Potential roles of infiltrating macrophages and resident microglia in neurodegeneration

Since Cx3CR1 in the retina is selectively expressed by myeloid cells, our findings indicate that alterations in these cells drove a selective increase in somal pNF+ RGCs. FKN signaling has been assumed to be a brake on microglial activation in many models of neurodegeneration (Bhaskar et al., 2010; Cardona et al., 2006; Wang et al., 2014). However, we found that the activation of the presumed resident microglia (branched Iba1+ cells) remained unchanged in terms of morphology and Iba1 mRNA levels with loss of CX3CR1. However, other aspects of microglia function may be affected. For example, CX3CR1 null microglia have been noted to more slowly remodel their processes (Liang et al., 2009), suggesting functional impairment. Whether there is a functional change in resident microglia in our model remains unclear.

Our findings rather suggest that some of the previously reported effects on microglia activation and neurodegeneration may be due to enhanced macrophage infiltration. Increased CCR2+ macrophage infiltration on a CX3CR1 null background is consistent with the findings of (Sennlaub et al., 2013) in age and light damage models of subretinal inflammation that clearly showed a pathogenic role for these infiltrating macrophages. While we did not directly test this possibility, the lack of correlation between numbers of these macrophages and measured RGC pathology suggests that infiltrating macrophages may be involved in other aspects of glaucoma. Since macrophages have been implicated in RGC regeneration (Cui et al., 2009), it is entirely possible that their role in RGC compartmentalized degeneration may be either beneficial or detrimental. Whatever the mechanism, the data presented here suggest that myeloid dysfunction may contribute to the impaired axonal transport seen early in many neurodegenerative diseases (Morfini et al., 2009).

All together, this study demonstrates the value in examining neurodegeneration in a compartmentalized manner and determining the lineages of myeloid cells involved. There is a longstanding question in the literature as to what extent a toxic gain of function in myeloid cells, a loss of myeloid supportive functions, or both contribute to neurodegeneration (Rivest, 2009; Streit and Xue, 2014). Perhaps myeloid lineage specific loss of CX3CR1 may better answer these questions.

References

Bhaskar, K., Konerth, M., Kokiko-Cochran, O.N., Cardona, A., Ransohoff, R.M., and Lamb, B.T. (2010). Regulation of tau pathology by the microglial fractalkine receptor. Neuron *68*, 19-31.

Bosco, A., Romero, C.O., Breen, K.T., Chagovetz, A.A., Steele, M.R., Ambati, B.K., and Vetter, M.L. (2015). Neurodegeneration severity is anticipated by early microglia alterations monitored in vivo in a mouse model of chronic glaucoma. Dis. Mod. & Mech. *8*, 443-455.

Bosco, A., Steele, M.R., and Vetter, M.L. (2011). Early microglia activation in a mouse model of chronic glaucoma. J. Comp. Neurol. *519*, 599-620.

Butovsky, O., Jedrychowski, M.P., Moore, C.S., Cialic, R., Lanser, A.J., Gabriely, G., Koeglsperger, T., Dake, B., Wu, P.M., Doykan, C.E.*, et al.* (2014). Identification of a unique TGF-beta-dependent molecular and functional signature in microglia. Nat. Neurosci. *17*, 131-143.

Butovsky, O., Siddiqui, S., Gabriely, G., Lanser, A.J., Dake, B., Murugaiyan, G., Doykan, C.E., Wu, P.M., Gali, R.R., Iyer, L.K.*, et al.* (2012). Modulating inflammatory monocytes with a unique microRNA gene signature ameliorates murine ALS. J. Clin. Invest. *122*, 3063-3087.

Calkins, D.J., Sappington, R.M., and Hendry, S.H. (2005). Morphological identification of ganglion cells expressing the alpha subunit of type II calmodulin-dependent protein kinase in the macaque retina. J. Comp. Neurol. *481*, 194-209.

Cardona, A.E., Pioro, E.P., Sasse, M.E., Kostenko, V., Cardona, S.M., Dijkstra, I.M., Huang, D., Kidd, G., Dombrowski, S., Dutta, R.*, et al.* (2006). Control of microglial neurotoxicity by the fractalkine receptor. Nat. Neurosci. *9*, 917-924.

Conforti, L., Adalbert, R., and Coleman, M. (2007). Neuronal death: where does the end begin? TRENDS Neurosci. *30*, 159-166.

Crish, S.D., Sappington, R.M., Inman, D.M., Horner, P.J., and Calkins, D.J. (2010). Distal axonopathy with structural persistence in glaucomatous neurodegeneration. Proc. Natl. Acad. Sci. USA *107*, 5196-5201.

Cui, Q., Yin, Y., and Benowitz, L.I. (2009). The role of macrophages in optic nerve regeneration. Neurosci. *158*, 1039-1048.

Czeh, M., Gressens, P., and Kaindl, A.M. (2011). The yin and yang of microglia. Dev. Neurosci *33*, 199-209.

Dengler-Crish, C.M., Smith, M.A., Inman, D.M., Wilson, G.N., Young, J.W., and Crish, S.D. (2014). Anterograde transport blockade precedes deficits in retrograde transport in the visual projection of the DBA/2J mouse model of glaucoma. Front. Neurosci. *8*, 290.

Domenici, L., Origlia, N., Falsini, B., Cerri, E., Barloscio, D., Fabiani, C., Sanso, M., and Giovannini, L. (2014). Rescue of retinal function by BDNF in a mouse model of glaucoma. PLoS One *9*, e115579.

Fernandes, K.A., Harder, J.M., John, S.W., Shrager, P., and Libby, R.T. (2014). DLK-dependent signaling is important for somal but not axonal degeneration of retinal ganglion cells following axonal injury. Neurobiol. Dis. *69*, 108-116.

Fuller, A.D., and Van Eldik, L.J. (2008). MFG-E8 regulates microglial phagocytosis of apoptotic neurons. J. Neuroimm Pharmacol: Soc. NeuroImm. Pharmacol. *3*, 246-256.

Garcia-Valenzuela, E., and Sharma, S.C. (1999). Laminar restriction of retinal macrophagic response to optic nerve axotomy in the rat. J. Neurobiol. *40*, 55-66.
Hickman, S.E., Kingery, N.D., Ohsumi, T.K., Borowsky, M.L., Wang, L.C., Means, T.K., and El Khoury, J. (2013). The microglial sensome revealed by direct RNA sequencing. Nat. Neurosci. *16*, 1896-1905.

Howell, G.R., Libby, R.T., Jakobs, T.C., Smith, R.S., Phalan, F.C., Barter, J.W., Barbay, J.M., Marchant, J.K., Mahesh, N., Porciatti, V.*, et al.* (2007). Axons of retinal ganglion cells are insulted in the optic nerve early in DBA/2J glaucoma. J. Cell Biol. *179*, 1523-1537.

Howell, G.R., Soto, I., Zhu, X., Ryan, M., Macalinao, D.G., Sousa, G.L., Caddle, L.B., MacNicoll, K.H., Barbay, J.M., Porciatti, V.*, et al.* (2012). Radiation treatment inhibits monocyte entry into the optic nerve head and prevents neuronal damage in a mouse model of glaucoma. J. Clin. Invest. *122*, 1246-1261.

Ilieva, H., Polymenidou, M., and Cleveland, D.W. (2009). Non-cell autonomous toxicity in neurodegenerative disorders: ALS and beyond. J. Cell Biol. *187*, 761-772.

Inman, D.M., and Horner, P.J. (2007). Reactive Nonproliferative Gliosis Predominates in a Chronic Mouse Model of Glaucoma. Glia *55*, 942-953.

John, S.W., Smith, R.S., Savinova, O.V., Hawes, N.L., Chang, B., Turnbull, D., Davisson, M., Roderick, T.H., and Heckenlively, J.R. (1998). Essential iris atrophy, pigment dispersion, and glaucoma in DBA/2J mice. Invest. Ophthalmol. Vis. Sci. *39*, 951-962.

Jung, S., Aliberti, J., Graemmel, P., Sunshine, M.J., Kreutzberg, G.W., Sher, A., and Littman, D.R. (2000). Analysis of fractalkine receptor CX(3)CR1 function by targeted deletion and green fluorescent protein reporter gene insertion. Mol. Cell. Biol. *20*, 4106-4114.

Landsman, L., Bar-On, L., Zernecke, A., Kim, K.W., Krauthgamer, R., Shagdarsuren, E., Lira, S.A., Weissman, I.L., Weber, C., and Jung, S. (2009). CX3CR1 is required for monocyte homeostasis and atherogenesis by promoting cell survival. Blood *113*, 963-972.

Lee, S., Varvel, N.H., Konerth, M.E., Xu, G., Cardona, A.E., Ransohoff, R.M., and Lamb, B.T. (2010). CX3CR1 Deficiency Alters Microglial Activation and Reduces Beta-Amyloid Deposition in Two Alzheimer's Disease Mouse Models. Am. J. Pathol. *177*,

2549-2562.

Liang, K.J., Lee, J.E., Wang, Y.D., Ma, W., Fontainhas, A.M., Fariss, R.N., and Wong, W.T. (2009). Regulation of Dynamic Behavior of Retinal Microglia by CX3CR1 Signaling. Invest. Ophthalmol. Vis. Sci. *50*, 4444-4451.

Libby, R.T., Anderson, M.G., Pang, I.-H., Robinson, Z.H., Savinova, O.V., Cosma, I.M., Snow, A., Wilson, L.A., Smith, R.S., Clark, A.F.*, et al.* (2005a). Inherited glaucoma in DBA02J mice: Pertinent disease features for studying the neurodegeneration. Vis. Neurosci. *22*, 637-648.

Libby, R.T., Li, Y., Savinova, O.V., Barter, J., Smith, R.S., Nickells, R.W., and John, S.W.M. (2005b). Susceptibility to Neurodegeneration in a Glaucoma Is Modified by Bax Gene Dosage. PLoS Gen. *1*, e4.

Morfini, G.A., Burns, M., Binder, L.I., Kanaan, N.M., LaPointe, N., Bosco, D.A., Brown, R.H., Jr., Brown, H., Tiwari, A., Hayward, L.*, et al.* (2009). Axonal transport defects in neurodegenerative diseases. J. Neurosci. *29*, 12776-12786.

Panagis, L., Zhao, X., Ge, Y., Ren, L., Mittag, T.W., and Danias, J. (2010). Gene expression changes in areas of focal loss of retinal ganglion cells in the retina of DBA/2J mice. Invest. Ophthalmol. Vis. Sci. *51*, 2024-2034.

Prinz, M., Priller, J., Sisodia, S.S., and Ransohoff, R.M. (2011). Heterogeneity of CNS myeloid cells and their roles in neurodegeneration. Nat. Neurosci. *14*, 1227-1235.

Rivest, S. (2009). Regulation of innate immune responses in the brain. Nat. Rev. Immunol. *9*, 429-439.

Saederup, N., Cardona, A.E., Croft, K., Mizutani, M., Cotleur, A.C., Tsou, C.L., Ransohoff, R.M., and Charo, I.F. (2010). Selective chemokine receptor usage by central nervous system myeloid cells in CCR2-red fluorescent protein knock-in mice. PLoS One *5*, e13693.

Schlamp, C.L., Li, Y., Dietz, J.A., Janssen, K.T., and Nickells, R.W. (2006). Progressive ganglion cell loss and optic nerve degeneration in DBA/2J mice is variable and asymmetric. BMC Neurosci. *7*, 66.

Sennlaub, F., Auvynet, C., Calippe, B., Lavalette, S., Poupel, L., Hu, S.J., Dominguez, E., Camelo, S., Levy, O., Guyon, E.*, et al.* (2013). CCR2(+) monocytes infiltrate atrophic lesions in age-related macular disease and mediate photoreceptor degeneration in experimental subretinal inflammation in Cx3cr1 deficient mice. EMBO Mol. Med. *5*, 1775-1793.

Soto, I., Oglesby, E., Buckingham, B.P., Son, J.L., Roberson, E.D.O., Steele, M.R., Inman, D.M., Vetter, M.L., Horner, P.J., and Marsh-Armstrong, N. (2008). Retinal

Ganglion Cells Downregulate Gene Expression and Lose Their Axons within the Optic Nerve Head in a Mouse Glaucoma Model. J. Neurosci. *28*, 548-561.

Streit, W.J., and Xue, Q.S. (2014). Human CNS immune senescence and neurodegeneration. Curr. Opin. Immunol. *29*, 93-96.

Vagaja, N.N., Chinnery, H.R., Binz, N., Kezic, J.M., Rakoczy, E.P., and McMenamin, P.G. (2012). Changes in murine hyalocytes are valuable early indicators of ocular disease. Invest. Ophthalmol. Vis. Sci. *53*, 1445-1451.

van der Mark, V.A., Elferink, R.P., and Paulusma, C.C. (2013). P4 ATPases: Flippases in Health and Disease. Internatl. J. Mol. Sci. *14*, 7897-7922.

Wang, K., Peng, B., and Lin, B. (2014). Fractalkine receptor regulates microglial neurotoxicity in an experimental mouse glaucoma model. Glia *62*, 1943-1954.

Welsbie, D.S., Yang, Z., Ge, Y., Mitchell, K.L., Zhou, X., Martin, S.E., Berlinicke, C.A., Hackler, L., Jr., Fuller, J., Fu, J.*, et al.* (2013). Functional genomic screening identifies dual leucine zipper kinase as a key mediator of retinal ganglion cell death. Proc. Natl. Acad. Sci. USA *110*, 4045-4050.

Wolf, Y., Yona, S., Kim, K.W., and Jung, S. (2013). Microglia, seen from the CX3CR1 angle. Front. Cell. Neurosci. *7*, 26.

Zhang, Y., Chen, K., Sloan, S.A., Bennett, M.L., Scholze, A.R., O'Keeffe, S., Phatnani, H.P., Guarnieri, P., Caneda, C., Ruderisch, N.*, et al.* (2014). An RNA-sequencing transcriptome and splicing database of glia, neurons, and vascular cells of the cerebral cortex. J. Neurosci. *34*, 11929-11947.

Zhu, X., Libby, R.T., de Vries, W.N., Smith, R.S., Wright, D.L., Bronson, R.T., Seburn, K.L., and John, S.W. (2012). Mutations in a P-type ATPase gene cause axonal degeneration. PLoS Gen. *8*, e1002853.

CHAPTER 3

NEURODEGENERATION SEVERITY IS ANTICIPATED BY EARLY MICROGLIA ALTERATIONS MONITORED IN VIVO IN A MOUSE MODEL OF CHRONIC GLAUCOMA

Dis. Model. Mech. 2015 **10**, 1242. Neurodegeneration severity is anticipated by early microglia alterations monitored in vivo in a mouse model of chronic glaucoma. Alejandra Bosco, Cesar O. Romero, Kevin T. Breen, Alexis A. Chagovetz, Michael R. Steele, Balamurali K. Ambati, and Monica L. Vetter. © 2015. Published by The Company of Biologists Ltd. This is an Open Access article distributed under the terms of the Creative Commons Attribution License (http://creativecommons.org/licenses/by/3.0), which permits unrestricted use, distribution and reproduction in any medium provided that the original work is properly attributed.

Credits

Alejandra Bosco originally conceived of the idea to use in vivo confocal microscopy to monitor microglial activation and relate it to later optic nerve degeneration as well as the idea to use binary masks of glia and extracellular matrix as a proxy for axon loss in the optic nerve. I was crucial to this process by generating these masks and

gathering the data that was critical in establishing a strong correlation between early microglial activation and later optic nerve degeneration (Fig. 3.5). I was also instrumental in validating the use of CD169/Sialoadhesin as a marker of infiltrating macrophages in LPS intravitreally injected tissue as well as aged DBA/2J mice (Fig 3.6). I also quantified the co-localization between CD169 and the GFP expression marking all myeloid cells in the CX3CR1 $^{gfp/+}$ DBA/2J mice (Fig. 3.6). All in all I generated and quantified key data to the pivotal point of the paper and I was heavily involved in establishing the GFP+ cells as resident microglia.

© 2015. Published by The Company of Biologists Ltd | Disease Models & Mechanisms (2015) 8, 443-455 doi:10.1242/dmm.018788

RESEARCH ARTICLE

Neurodegeneration severity can be predicted from early microglia alterations monitored *in vivo* in a mouse model of chronic glaucoma

Alejandra Bosco[1,*], Cesar O. Romero[1], Kevin T. Breen[1], Alexis A. Chagovetz[2], Michael R. Steele[1], Balamurali K. Ambati[3] and Monica L. Vetter[1]

ABSTRACT

Microglia serve key homeostatic roles, and respond to neuronal perturbation and decline with a high spatiotemporal resolution. The course of all chronic CNS pathologies is thus paralleled by local microgliosis and microglia activation, which begin at early stages of the disease. However, the possibility of using live monitoring of microglia during early disease progression to predict the severity of neurodegeneration has not been explored. Because the retina allows live tracking of fluorescent microglia in their intact niche, here we investigated their early changes in relation to later optic nerve neurodegeneration. To achieve this, we used the DBA/2J mouse model of inherited glaucoma, which develops progressive retinal ganglion cell degeneration of variable severity during aging, and represents a useful model to study pathogenic mechanisms of retinal ganglion cell decline that are similar to those in human glaucoma. We imaged CX3CR1$^{+/GFP}$ microglial cells *in vivo* at ages ranging from 1 to 5 months by confocal scanning laser ophthalmoscopy (cSLO) and quantified cell density and morphological activation. We detected early microgliosis at the optic nerve head (ONH), where axonopathy first manifests, and could track attenuation of this microgliosis induced by minocycline. We also observed heterogeneous and dynamic patterns of early microglia activation in the retina. When the same animals were aged and analyzed for the severity of optic nerve pathology at 10 months of age, we found a strong correlation with the levels of ONH microgliosis at 3 to 4 months. Our findings indicate that live imaging and monitoring the time course and levels of early retinal microgliosis and microglia activation in glaucoma could serve as indicators of future neurodegeneration severity.

KEY WORDS: Microglia activation, Microgliosis, Retinal ganglion cells, Confocal ophthalmoscopy, Live image analysis, *Cx3cr1*$^{GFP/+}$ DBA/2J

INTRODUCTION

The ability to detect and monitor a neurodegenerative disease soon after its onset and to anticipate its future progression is a fundamental step towards uncovering early pathogenic mechanisms and developing targeted therapies. Such an early diagnostic and prognostic strategy depends on the detection of cellular and/or molecular markers dynamically linked with the pathogenic process of neurodegeneration. Growing evidence indicates that a wide range of neurodegenerative diseases are associated with innate immune responses from microglia, and in certain contexts, from recruitment of blood-derived monocytes or macrophages (Amor et al., 2014, 2010; Block et al., 2007; Cunningham, 2013; Perry and Teeling, 2013).

Microglia are long-lived myeloid cells that stably inhabit the adult CNS within parenchymal and perivascular niches (Kettenmann et al., 2011; Lawson et al., 1990, 1992; Prinz et al., 2011). Functionally, they constantly interact with surrounding neurons, blood-brain barrier cells and other glia (Davalos et al., 2005; Nimmerjahn et al., 2005; Ransohoff and Cardona, 2010; Ransohoff and Perry, 2009; Tremblay et al., 2010; Wake et al., 2009). Stress or damage to surrounding cells causes rapid microglial activation (Kettenmann et al., 2011; Kreutzberg, 1996), as identified by complex molecular, functional and cellular changes, as well as microgliosis, which refers to the expansion of microglial cell numbers by local self-renewal and/or recruitment of monocytes and/or macrophages from the blood-stream or, potentially, from latent progenitors (Ajami et al., 2007; Elmore et al., 2014; Lawson et al., 1992; Ransohoff and Cardona, 2010; Solomon et al., 2006; Streit et al., 1999). Thus, microglia, as ubiquitous, dynamic sensors of CNS damage and dyshomeostasis, are ideally suited to detect and indicate the progression of pathogenic processes.

Microgliosis and microglial activation mirror the course of neurodegeneration in both clinical and animal model studies of multiple diseases, such as Alzheimer's, Parkinson's and Huntington's disease (Ajami et al., 2011; Maeda et al., 2011; Ouchi et al., 2005; Sapp et al., 2001). Moreover, live imaging studies that have monitored microglial alterations have found evidence for their involvement at preclinical disease stages (Ajami et al., 2011; Davalos et al., 2012; Fuhrmann et al., 2010; Maeda et al., 2011; Ouchi et al., 2005; Sapp et al., 2001). Thus, CNS-resident microglia and infiltrating monocytes and macrophages are emerging as promising sensitive indicators of neuronal decline; however, their ability to predict later disease is not well defined, particularly at early stages of disease. Detection of microglial distribution and activation by molecular imaging of the brain using positron emission tomography has underscored the relevance of microglial activation as a relevant biomarker of disease in multiple neurological and psychiatric conditions (Jacobs and Tavitian, 2012; Politis et al., 2012; Venneti et al., 2013). The actual behavior of microglia at the cellular level during health, acute injury and chronic neurodegeneration has been studied in animal models over the course of minutes, and for up to 4 months, by direct observation of fluorescently labeled cells using two-photon confocal imaging of the brain, retina and spinal cord (Davalos et al., 2005, 2012;

[1]Department of Neurobiology and Anatomy, University of Utah, Salt Lake City, UT 84132, USA. [2]Department of Human Genetics, University of Utah, Salt Lake City, UT 84132, USA. [3]Department of Ophthalmology and Visual Sciences, University of Utah, Salt Lake City, UT 84132, USA.

*Author for correspondence (alejandra.bosco@neuro.utah.edu)

This is an Open Access article distributed under the terms of the Creative Commons Attribution License (http://creativecommons.org/licenses/by/3.0), which permits unrestricted use, distribution and reproduction in any medium provided that the original work is properly attributed.

Received 14 October 2014; Accepted 26 February 2015

RESEARCH ARTICLE Disease Models & Mechanisms (2015) 8, 443-455 doi:10.1242/dmm.018788

TRANSLATIONAL IMPACT

Clinical issue

Specific neuronal populations progressively deteriorate in neurodegenerative diseases. Early detection is key for slowing or halting neuronal decline and loss, underscoring the importance of defining reliable indicators of disease onset and progression. The course of neurodegeneration is mirrored by innate immune responses of CNS-resident microglia and infiltrating monocytes. Live imaging studies have detected early microglial alterations in animal models and humans, suggesting that they have potential value as sensitive indicators of disease progression. However, whether the early changes of innate immune cells are related to and can predict later neurodegeneration is unknown. Glaucoma results in progressive neurodegeneration of retinal ganglion cells (RGCs) and their axons in the optic nerve and retina. The disease is mostly asymptomatic at early stages and is detectable only once vision is irreversibly compromised. Despite this, the possibility of live monitoring retinal microglia to predict future neurodegeneration severity in glaucoma has not yet been explored. Confocal ophthalmoscopy (cSLO) allows for direct and repeated visualization and tracking of the microglial alterations that precede neurodegeneration in the intact retinal niche.

Results

Here, the authors use a mouse model of inherited glaucoma that, as in the human condition, develops age-dependent and variably severe neurodegeneration, coupled with innate immune responses. To assess the kinetics of early microgliosis (accumulation of microglia at the site of injury) and microglia activation, they used a DBA/2J reporter substrain in which microglia and infiltrating monocytes express green fluorescent protein (GFP) under the control of the fractalkine receptor locus (*Cx3cr1*), and imaged young mice at 1 to 5 months of age by cSLO to monitor early microglial changes. The authors then aged the mice to 10 months and analyzed optic nerve pathology *ex vivo*. Across individual eyes, live images collected at pre-pathological ages revealed dynamic patterns of retinal microglial activation and an unexpected diversity in the levels of microgliosis at the optic nerve head (ONH), which was attenuated by minocycline. Notably, they identified a significant correlation between early microgliosis at the ONH and the late severity of nerve pathology.

Implications and future directions

This study establishes microglia as indicators and early predictors of late optic nerve degeneration in a model of chronic glaucoma. This live imaging approach is the first to visualize, quantify and monitor microglial cellular changes during early stages of a neurodegenerative disease. The findings are broadly relevant to the field of neurodegeneration because they link microglial changes to future disease progression. Moreover, this study developed a non-invasive strategy to monitor visual biomarkers that is applicable to tracking and managing glaucoma and other chronic CNS diseases that affect RGCs.

Dibaj et al., 2011; Evans et al., 2014; Fuhrmann et al., 2010; Kozlowski and Weimer, 2012; Nayak et al., 2012; Nimmerjahn et al., 2005; Tremblay et al., 2010; Wake et al., 2009), and by confocal scanning laser ophthalmoscopy (cSLO) of the retina (Maeda et al., 2014; Seeliger et al., 2005). Given that *in vivo* imaging of the retina using cSLO is non-invasive, this technique has been used to directly visualize GFP-labeled retinal microglia in the mouse eye, and in some cases to monitor changes in a single animal over a limited period of time (Alt et al., 2012; Eter et al., 2008; Liu et al., 2012; Paques et al., 2010, 2006). Although these previous studies have detected changes in microgliosis in response to acute injury, what remains to be determined is whether this approach can be used in a chronic, progressive, age-related model of retinal disease to detect and quantify early changes in microglia that would predict the later course of neurodegeneration.

A relevant neurodegenerative disease of the retina with unresolved pathogenesis is glaucoma. The ability to detect and monitor glaucoma at early stages would offer the potential for early intervention in this disease. As a model of inherited, age-dependent glaucoma, we use DBA/2J mice, which like human patients undergo slow, asynchronous and chronic decline and loss of retinal ganglion cells (RGCs) and their axons in the optic nerve and retina (Casson et al., 2012; Nickells et al., 2012; Quigley, 1999, 2011; Weinreb and Khaw, 2004). Axonopathy first manifests at the optic nerve head (ONH), where unmyelinated axons exit the eye, and progressively expands across asymmetrical areas of the retina (Buckingham et al., 2008; Howell et al., 2007a; Inman et al., 2006; Schlamp et al., 2006; Soto et al., 2008), offering remarkable spatial resolution to track disease progression. Microglia activation has been associated with human glaucoma (Gramlich et al., 2013; Neufeld, 1999), and early alterations in retinal microglia, and potentially monocyte infiltration, precede detectable neuronal pathology in DBA/2J mice (Bosco et al., 2012, 2011; Fan et al., 2010; Howell et al., 2011). However, a predictive link between early microglia and/or peripheral monocyte alterations and later disease progression has not been defined.

To address this, our current approach took advantage of the remarkable variability of neurodegeneration severity across DBA/2J eyes (Anderson et al., 2001; Chang et al., 1999). To track retinal and ONH microglia and recruited monocytes *in vivo* with single-cell resolution, we generated DBA/2J mice carrying the microglia and monocyte reporter CX3CR1-GFP and applied recently optimized cSLO imaging and automated morphometric cell analysis to quantitatively monitor microgliosis and microglia activation from 1 to 5 months of age in a large cohort of young mice (Bosco et al., 2015). After allowing these same mice to age, we analyzed optic nerve pathology *ex vivo*. We provide evidence that microglial alterations are selectively detectable in eyes that progress to glaucoma at later stages, and establish that early microgliosis has a strong correlation with the severity of optic nerve degeneration. Taken together, these findings provide the first evidence that *in vivo* monitoring of the time course and dynamics of early microglia might serve as sensitive predictors of late chronic neurodegeneration.

RESULTS

Microglia can be visualized and tracked *in vivo* throughout the retina and ONH preceding neurodegeneration in *Cx3cr1*$^{GFP/+}$ DBA/2J mice

To allow the long-term monitoring and quantification of the kinetics of microgliosis and microglia activation during chronic glaucoma in live DBA/2J mice, we performed backcrossing to generate a substrain carrying a knock-in allele that expresses GFP under the control of the fractalkine receptor promoter (*Cx3cr1*; Jung et al., 2000). This reporter not only labels resident microglia but also peripheral monocytes and macrophages that can infiltrate the diseased or injured CNS (Ajami et al., 2011; Broux et al., 2012; Jung et al., 2000). Using cSLO in *Cx3cr1*$^{GFP/+}$ DBA/2J mice aged 1 to 5 months, we imaged individual eyes to track GFP$^+$ cells localized to the ONH and central retina (Bosco et al., 2015). At monthly intervals, we collected single and multiple *xy*-point confocal images centered on the optic disc in fundus images, and spanning approximately the central 1.5 mm or 1.5×3 to 4 mm of each retina, respectively, and its inner 30 to 40 µm in depth (Fig. 1A,B; supplementary material Fig. S1A). These live confocal images provided enough cellular resolution to visualize cell somata, and in some cases arbor dimensions (Fig. 1C), and to recognize three distinct subsets of GFP$^+$ cells of microglial or macrophage origin: (1) a large population of parenchymal cells tiling the retina (200 to

RESEARCH ARTICLE Disease Models & Mechanisms (2015) 8, 443-455 doi:10.1242/dmm.018788

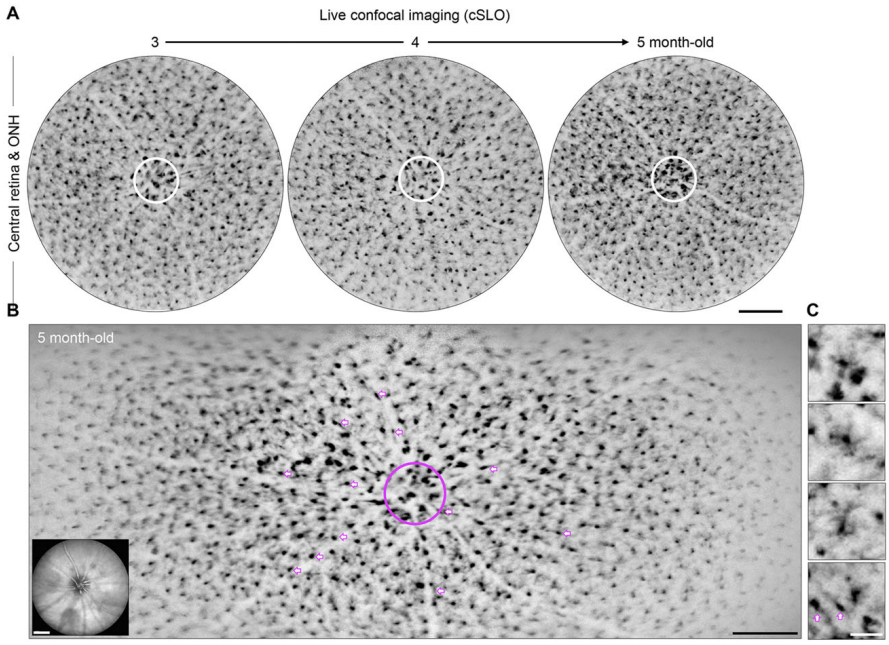

Fig. 1. *In vivo* monthly imaging of retinal and ONH microglia and/or peripheral monocytes during early stages of chronic glaucoma. (A) Monthly cSLO image sequence of the same eye, showing GFP$^+$ cells within ~2 mm^2 of retina around the ONH (circle) in young *Cx3cr1*$^{GFP/+}$ DBA/2J mice. The original greyscale was inverted to improve observation. (B) Multipoint cSLO image spanning approximately one third of the same retina when the mouse was 5 months old. There is a cluster of GFP-labeled cells localized to the ONH (circle), and radial rows of perivascular cells with bipolar shape along vessels (arrows), which interrupt the regular mosaic of parenchymal microglia. Live infrared fundus images of vasculature and optic disc (inset) were acquired for each fluorescence image, to facilitate the alignment of sequential images. (C) High-magnification view of parenchymal and perivascular GFP$^+$ cells (arrows). For parenchymal cells, the microglial soma size is readily identifiable, whereas process number and length are better resolved in larger cells. Scale bars: 250 µm (A,B), 50 µm (C).

300 cells), (2) a central cluster of microglia and/or blood-derived monocytes or macrophages localized to the ONH area, and (3) perivascular cells radiating from the ONH (Fig. 1B). We compared live and *ex vivo* confocal images of individual eyes collected less than 3 days apart, and confirmed that cSLO detects individual GFP$^+$ cells throughout the inner retinal layers (supplementary material Fig. S1B-E). Therefore, cSLO live imaging allows the tracking of cellular changes in retinal microglia and infiltrating monocytes that are localized adjacent to RGC somata, dendrites and unmyelinated axons across the inner retinal surface and ONH (Bosco et al., 2011).

We applied cell segmentation and morphometry to cSLO images of the central 1.5-1.7 mm^2 of retina to identify activated parenchymal microglia (Bosco et al., 2015). Briefly, using intensity-threshold-based morphometric analysis, we identified activated parenchymal microglia as cells with large somal areas (>50-60 µm^2) and a few short processes, and non-activated parenchymal and perivascular microglia as cells with somata that were 2-3 times smaller in area and had visibly extensive and complex arbors. Microglial soma size has been shown to increase with Iba1 upregulation, and provides a metric to determine the activation status of individual GFP$^+$ cells in live image analysis (Bosco et al., 2008; Kozlowski and Weimer, 2012). In sequential images of the same retinas collected at 3 and 4 months of age, we mapped and quantified numbers of activated and non-activated microglia across eight sectors radiating from the optic disc (supplementary material Fig. S2A,B), and at each age detected variable numbers of activated microglia between sectors and retinas, which were uncoupled from the concurrent changes in total GFP$^+$ cell density (supplementary material Fig. S2B,C). For most of the individual retinas monitored over 2 months, numbers and distribution of GFP$^+$ cells and activated microglia were dynamic (supplementary material Fig. S2C, left), although some retinas maintained relatively static levels and/or patterns of activation (supplementary material Fig. S2C, right).

Induced changes in retinal microgliosis can be monitored over time by cSLO

Previous live imaging studies of retinal GFP$^+$ microglia and macrophages have tracked changes in cell numbers in response to acute optic nerve injury (Eter et al., 2008; Liu et al., 2012). To determine the sensitivity of our methods to detect longitudinal changes in microgliosis in a chronic model, we induced a subtle reduction in microgliosis during early disease progression by treating young DBA/2J mice with minocycline, which we have previously shown decreases both the number and activated phenotype of retinal microglia and/or peripheral monocytes (Bosco et al., 2008). First, we identified a subset of 2-month-old

RESEARCH ARTICLE Disease Models & Mechanisms (2015) 8, 443-455 doi:10.1242/dmm.018788

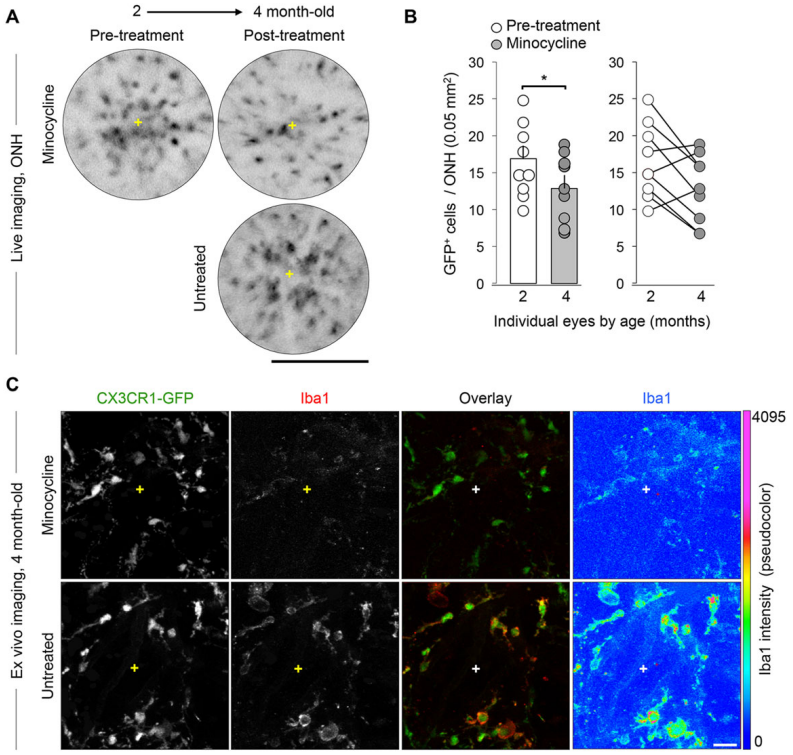

Fig. 2. Induced decreases in local microgliosis are detectable by live imaging. (A) Live cSLO images of the same ONH before and after oral minocycline treatment (mouse was 2 and 4 months old, respectively) showing a reduction in GFP$^+$ cell clustering, compared to an age-matched untreated control representing moderate microgliosis. (B) Total number of cells per ONH at 2 and 4 months of age (n=9 eyes represented by circles) plotted before and after minocycline treatment showing a significant mean reduction post-treatment (*P<0.05; Student's t-test). Bars indicate mean±s.e.m. at each age (16.9±1.65 cells per 0.05 mm^2 and 13±1.53, respectively). The graph to the right depicts with lines the drop in microgliosis in 6/9 individual ONHs. (C) *Ex vivo* immunostaining of the same 4-month-old ONHs shown in A revealing that there is a noticeable downregulation of Iba1 expression, but not of GFP, after minocycline treatment, as visible in the single-channel view of Iba1 and its pseudocolor coding by expression intensity. Each image shows a maximum intensity projection of 50 µm and represents the ONH area. Scale bars: 250 µm (A), 25 µm (C).

mice with relatively high ONH microgliosis by cSLO imaging, then administered systemic minocycline (120 mg/kg body weight for 6 weeks), and collected cSLO images after treatment at 4 months of age (Fig. 2A). The quantification of GFP$^+$ cell numbers within the ONH area showed that there were significant decreases in cell clustering in the treated eyes (P<0.05, n=9 eyes, Student's t-test; Fig. 2B). The ONH GFP$^+$ cells also displayed a manifest reduction in Iba1 expression relative to untreated eyes (Fig. 2C), consistent with the microglial deactivation reported for minocycline in this model (Bosco et al., 2008). Thus, live retinal imaging can track an induced attenuation in early microgliosis.

Young DBA/2J mice show highly variable levels of ONH microgliosis

Previous studies have established that DBA/2J mice typically lack histologically detectable retinal and optic nerve pathology in the first 6 months of age (John et al., 1998); however, young mice show clustering, activation and proliferation of Iba1+ microglia and/or peripheral monocytes at the ONH in some eyes (Bosco et al., 2012, 2011). Given that the age of glaucoma onset and progression are diverse in this model (Anderson et al., 2001; Chang et al., 1999), it was unclear whether these early microglia and infiltrating monocyte changes were linked to later neurodegeneration. To track the presence and levels of early ONH microgliosis prior to RGC degeneration, we analyzed cSLO retinal images collected between 1 and 5 months of age with preferential imaging at 3 months of age (Fig. 3A; supplementary material Fig. S1), when microgliosis in the DBA/2J retina peaks (Bosco et al., 2011). We detected a significant increase in the mean number of GFP$^+$ cells localized to the ONH at 3 months (P<0.01, n=19 to 59 eyes; Student's t-test), which persisted through 5 months (Fig. 3B), in agreement with *ex vivo* studies (Bosco et al., 2011). Furthermore, statistical analysis controlling for the potential effect of repeated imaging on individual eyes confirmed this result (linear mixed model; http://CRAN.R-project.org/package=lme4;

RESEARCH ARTICLE Disease Models & Mechanisms (2015) 8, 443-455 doi:10.1242/dmm.018788

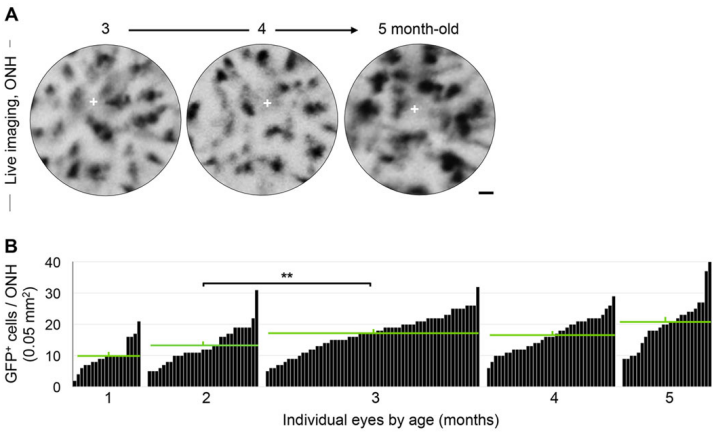

Fig. 3. Eyes show large variability in their levels of ONH microgliosis at pre-neurodegenerative ages. (A) Sequential imaging of the same ONH area at 3, 4 and 5 months revealed dynamic changes in GFP$^+$ cell numbers and size; the cross indicates the ONH center. (B) Total number of GFP$^+$ cells per ONH at 1, 2, 3, 4 and/or 5 months of age (n=19-59 images per age). Data with eye identification and late nerve pathology are presented in supplementary material Fig. S3. Each bar represents an individual ONH and green bars indicate mean±s.e.m. at each age group (10±1.06, 13.17±1.07, 16.85±0.77, 16.46±0.94 to 19.93±1.53, respectively). The average number of GFP$^+$ cells per ONH rises with age and significantly increases between 2 and 3 months (**P<0.01; Student's t-test). Scale bar: 25 µm.

P<0.0001), demonstrating that the effect of repeated observations on individual eyes is negligible (P=0.0942). Notably, we observed that eyes of the same age displayed widely variable GFP$^+$ cell density, ranging from 5 to 30 cells per 0.05 mm^2.

Early ONH microgliosis precedes late optic nerve degeneration

The diversity in levels of ONH microgliosis raised the question as to whether it reflects early, differential progression towards disease in a subset of eyes. To address this possibility, we assessed optic nerve pathology *ex vivo* in the same eyes at 10 months of age, when glaucomatous degeneration is evident in many DBA/2J mice (Fig. 4A-C). Glaucoma onset and the severity of neurodegeneration are highly variable in DBA/2J mice, thus axonal pathology can manifest with variable levels and distribution in individual optic nerves (Buckingham et al., 2008; Howell et al., 2007a; Inman et al., 2006; Jakobs et al., 2005; John et al., 1998; Libby et al., 2005; Schlamp et al., 2006; Soto et al., 2008). Using an established damage scoring system (Anderson et al., 2005; Howell et al., 2007a; Libby et al., 2005), high-resolution light microscopy images of 1-µm-thick cross-sections of individual nerves were categorized at one of three levels of damage based on qualitative parameters of pathology (Fig. 4C; see Materials and Methods). Next, the numbers of GFP$^+$ cells per ONH at 1 through to 5 months of age were plotted for nerves in each damage category (Fig. 4D). All 1-month-old mice showed similarly low GFP$^+$ cell densities in the ONH, but this analysis revealed a distinct trend to increase from 2 to 5 months of age, where nerves with severe late damage showed the highest levels of microgliosis, whereas nerves with moderate damage were preceded by more intermediate and variable levels of microgliosis. A Kruskal–Wallis rank ordered test showed that the median GFP$^+$ cell density per ONH for each level of severity of optic nerve pathology was significantly different at 3 months (χ^2=07.84, P=0.0199) and 4 months of age (χ^2=16.27, P=0.0003), and marginally significant at 5 months of age (Fig. 4E). This initial analysis shows a significant relationship between the early number of GFP-labeled cells at the ONH and the extent of late optic nerve degeneration.

Early ONH microgliosis correlates with future optic nerve pathology

To thoroughly define the correlation between ONH microgliosis at a young age and the susceptibility to develop glaucoma at an older age, we established a quantitative measure of optic nerve pathology based on the magnitude of gliosis and gliotic scaring associated with nerve degeneration (Crish et al., 2010; Libby et al., 2005; Schlamp et al., 2006). It is well documented that as axons are lost in the optic nerve, the area is replaced by reactive glia (hypertrophic and proliferative), and by a glial scar at the end stages of neurodegeneration (Burda and Sofroniew, 2014; Crish et al., 2010; Dai et al., 2012; Hernandez, 2000; Lye-Barthel et al., 2013; Qu and Jakobs, 2013; Sofroniew, 2009; Son et al., 2010; Sun and Jakobs, 2012; Sun et al., 2009). Therefore, the reduction of the non-axonal area at the expense of expanding glial territories in late stages of glaucoma was used as readout of nerve pathology severity. For this, we applied threshold-based segmentation of glial cells and scar tissue to high-resolution light images of entire optic nerve sections from 10-month-old mice (Fig. 5A, see Materials and Methods). Consistent with the variability in glaucoma onset and progression in DBA/2J mice, individual optic nerves showed large variability in the relative area occupied by glial cells or scar, which was consistently increased in nerves with widespread axonal damage and loss. According to the quantification of non-axonal area, individual *Cx3cr1*$^{GFP/+}$ DBA/2J nerves were classified as healthy if their total glial territory occupied less than 20% of the nerve, which is comparable to *Gpnmb*$^{+/SjJ}$ DBA/2J nerves (A.B., K.T.B., S.R.A., M.R.S., D.J.C. and M.L.V., unpublished data), the congenic control strain that carry a wild-type *Gpnmb* allele and do not undergo RGC degeneration (Howell et al., 2007b). Glaucomatous nerves with increased glial coverage were classified as having medium (20-40%) or high (>40%) gliosis (Fig. 5B). To confirm this classification, we compared the average glial area in each category and observed a significant increase from low to medium and then to high gliosis (P<0.001, n=41 eyes; Student's t-test). We thus used the expansion of gliosis and gliotic scar throughout areas devoid of RGC axons as a novel and objective measure of nerve degeneration severity.

Plotting the levels of early ONH microgliosis versus the magnitude of late nerve gliosis for each individual eye (Fig. 5C) revealed that nerves with low glial area or mild damage at

RESEARCH ARTICLE Disease Models & Mechanisms (2015) 8, 443-455 doi:10.1242/dmm.018788

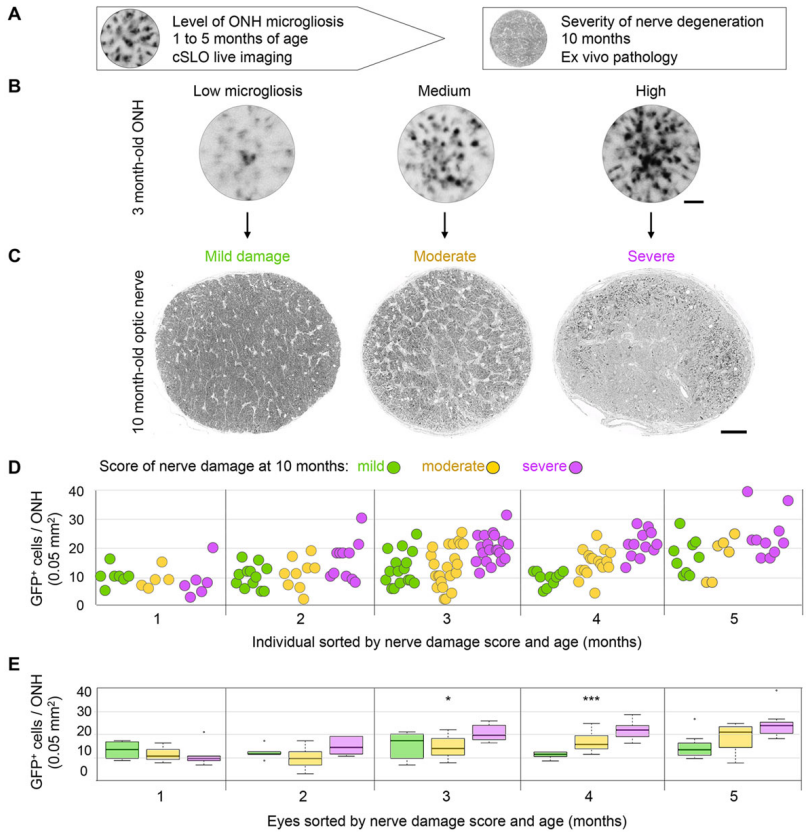

Fig. 4. Late nerve damage is preceded by early microgliosis at the ONH. (A) Experimental design. (B) Live cSLO images of GFP$^+$ cells localized to the ONH at 3 months of age in *Cx3cr1*$^{+/GFP}$ DBA/2J mice showing examples of low, medium and high levels of microgliosis. (C) Light-microscopy images of optic nerve cross-sections at 10 months of age for these same eyes, representative of mild, moderate and severe damage, as assessed by visual scoring. (D) Microgliosis level, quantified as total number of GFP$^+$ cells per ONH at 1 to 5 months of age (n=19, 31, 60, 36 and 25 eyes per respective age group), plotted for individual eyes and categorized by their corresponding optic nerve damage score at 10 months of age (color-coded as indicated). (E) Box plots of the same dataset illustrate significant changes at 3 and 4 months of age (*P<0.05 and ***P<0.001, respectively; Kruskal–Wallis rank ordered test), most notably in the severe nerves at both ages, and in the moderate nerves at 4 months. Plots indicate the median (thick line), interquartile range (IQR; box height), and data within 1.5 times the IQR (whiskers) or greater (outliers, circles). Scale bars: 250 µm (A) and 50 µm (C).

10 months showed low ONH microgliosis at 3 months. In contrast, eyes with moderate or severe nerve degeneration, evident by extensive gliosis or glial scaring, were preceded by intermediate and high levels of early ONH microgliosis, respectively. The comparison of the mean ONH microgliosis for eyes grouped by late nerve pathology revealed significant increases across the three levels of gliosis (P<0.001 and P<0.05, n=41 eyes; Student's t-test). A Spearman's rank-ordered correlation showed that nerve glial area at 10 months was significantly correlated with the number of microglial cells observed at 3 or 4 months (*rho*=0.56, P=0.0001; Fig. 5D). These analyses establish a predictive link between early microglia and/or peripheral monocyte alterations and later disease progression.

Resident microglia are main components of early ONH and retinal microgliosis

The selective increase in microgliosis detected prior to optic nerve degeneration in DBA/2J mice could involve resident microglia and/or proinflammatory monocyte entry to the ONH, as recently suggested (Howell et al., 2012). To address whether the early microgliosis detected by cSLO can be attributed to infiltrating cells, we assessed *ex vivo* the expression of sialoadhesin (Siglec-1 or CD169), which identifies infiltrating monocytes and macrophages, as well as vitreal hyalocytes and dendritic cells, but is absent in resident microglia (Butovsky et al., 2012; Davies et al., 2013; Vagaja et al., 2012). Sialoadhesin-expressing cells are absent in the brain and retina under physiological conditions, where the blood-

RESEARCH ARTICLE Disease Models & Mechanisms (2015) 8, 443-455 doi:10.1242/dmm.018788

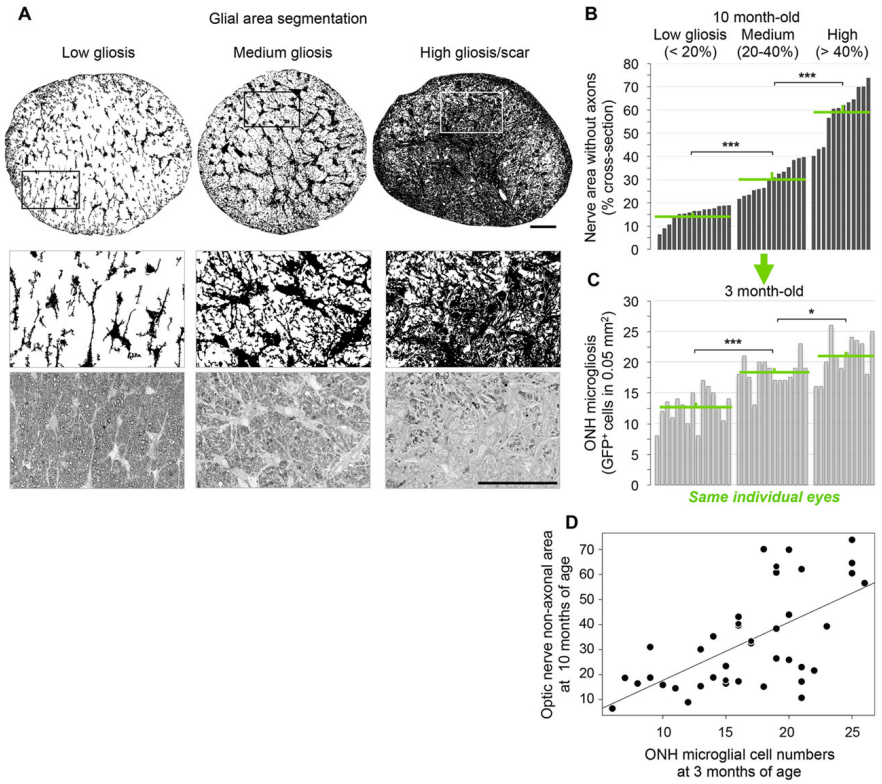

Fig. 5. Severity of nerve pathology and early microgliosis show a positive correlation. (A) Threshold analysis of the nerve area occupied by glial cells or scar for the cross-sections in Fig. 4C, and high-magnification views of framed areas. (B) Plot of individual optic nerves from 10-month-old mice sorted by relative glial area and ascending coverage, and classified as low, medium and high gliosis (15.24±0.96, 30.38±1.67 and 59.05±3.22 mean±s.e.m. non-axonal area, respectively). Nerves show a spectrum of glaucomatous damage, with significant increases in mean gliosis across groups (***P<0.001; Student's t-test). (C) Corresponding microgliosis level or total GFP$^+$ cell number per ONH at 3 months, plotted by their glial area at 10 months (i.e. same order as in B). Microgliosis is categorized by level as low, medium and high microgliosis (12.63±0.70, 18.43±0.62 and 21.08±0.97 mean cells per ONH, respectively). The mean ONH microgliosis shows significant increases across levels of nerve gliosis (***P<0.001 and *P<0.05; n=41 eyes; Student's t-test). Green lines indicate means and s.e.m. per group. (D) There is significant correlation between the optic nerve glial relative area at 10 months (non-axonal area) and their ONH microgliosis at 3 months (P=0.0001; Spearman's rank test). Scale bars: 50 µm.

brain or blood-retina barrier is intact (Hartnell et al., 2001; Linnartz-Gerlach et al., 2014; Perry et al., 1992; Sancho-Pelluz et al., 2008). Immunostaining of retinal whole mounts at 4 months of age detected only scarce sialoadhesin-expressing cells, and their numbers were independent of the relative levels of ONH microgliosis detected by live imaging at 3 months (Fig. 6A,B). Furthermore, quantification of cells expressing sialoadhesin in the ONH area at 4 months of age (n=10 retinas; Fig. 6C) detected no sialoadhesin in 86.60% of CX3CR1-GFP$^+$ cells, colocalization of GFP and sialoadhesin in 7.39% of cells, and 0.58% of cells expressing sialoadhesin but not GFP (in only two out of ten retinas). Consistent with previous reports of monocyte infiltration (Howell et al., 2012), we detected an increased presence of cells that were positive for both sialoadhesin and GFP throughout the central retina in 17-month-old DBA/2J mice (n=4); these cells were localized to the ONH, the retinal parenchyma and along blood vessels; however, such cells were infrequent at 4 months of age (Fig. 6D,E). Overall, these results reveal the presence of a small subset of peripheral monocytes confined to the ONH area in young DBA/2J mice, and point to resident microglia as the main cells underlying microgliosis during early stages of glaucoma progression.

DISCUSSION

Activation of microglia and innate immunity responses have been linked to the early stages of neurodegeneration (Ajami et al., 2011; Amor et al., 2014, 2010; Block et al., 2007; Cunningham, 2013; Davalos et al., 2012; Fuhrmann et al., 2010; Maeda et al., 2011; Ouchi et al., 2005; Perry and Teeling, 2013; Sapp et al., 2001). In

RESEARCH ARTICLE Disease Models & Mechanisms (2015) 8, 443-455 doi:10.1242/dmm.018788

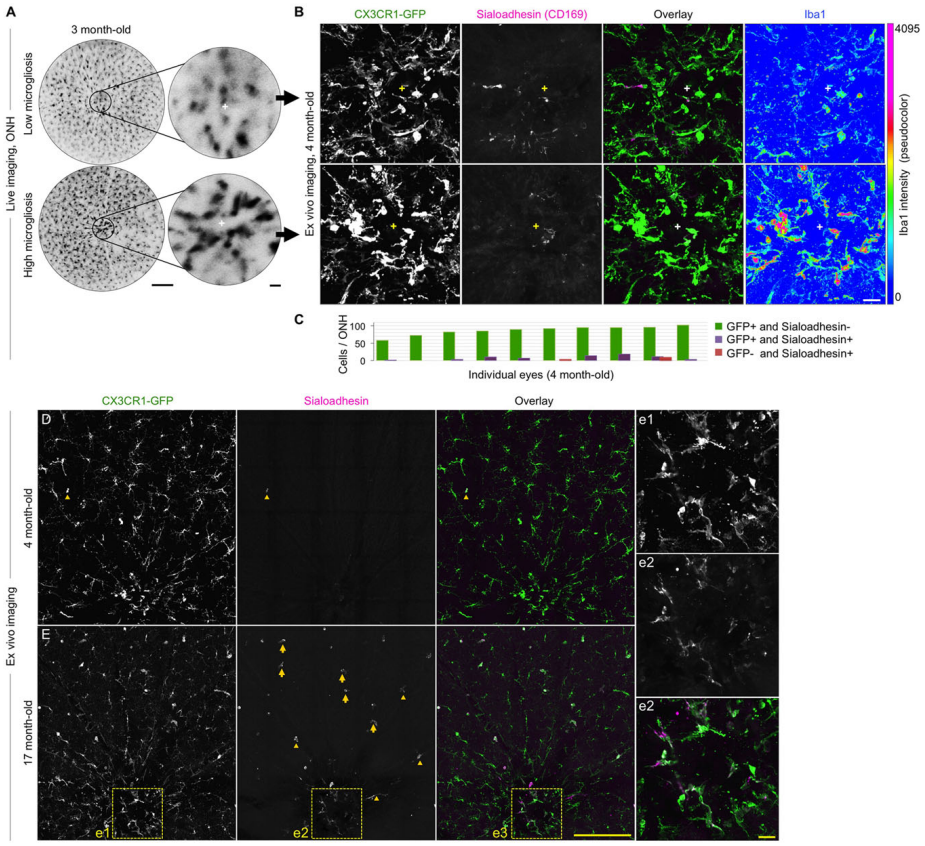

Fig. 6. Early microgliosis is mainly driven by microglia resident in the ONH. (A) Live cSLO images of two 3-month-old retinas (left) and their ONHs (right, cross indicating its center), representative of low and high microgliosis. (B) *Ex vivo* confocal images of the same ONHs at 4 months of age, shown as maximal intensity projection of the inner 30 µm. Triple-immunostaining detects few cells that are positive for both GFP and sialoadhesin within the ONH, regardless of their different levels of microgliosis and activation, revealed by upregulated Iba1 expression in the ONH with increased microgliosis. (C) Number of cells expressing GFP and/or sialoadhesin per ONH area at 4 months of age. Single- and double-stained cells were quantified in confocal images spanning the central 200 µm of retinal whole mounts, throughout the inner 60 µm (0.8-µm *z*-slices). (D) Low magnification, single-slice view of the same 4-month-old retina representative of high microgliosis (B, bottom row). (E) Comparable view of a 17-month-old retina, showing sialoadhesin expression in perivascular (arrowheads), parenchymal (arrows) and ONH cells (frame). The ONH area is shown at higher magnification in corresponding insets. Scale bars: 250 µm (A,B,D and E), 25 µm (insets in A, and e).

the retina, microglia activation is also associated with early stages of disease in animal models of chronic glaucoma (Bosco et al., 2012, 2011; Howell et al., 2011), as well as age-related macular degeneration (Combadière et al., 2007; Gupta et al., 2003; Karlstetter and Langmann, 2014; Sennlaub et al., 2013). However, it has been unclear whether these early responses are indicative of later severity or patterns of neurodegeneration. Here, we addressed this using the DBA/2J model of glaucoma, a chronic model of retinal neurodegeneration that is variable in onset and progression (Anderson et al., 2001; Chang et al., 1999). Building upon previous studies of direct *in vivo* imaging of CX3CR1-GFP^{+} retinal microglia and infiltrating monocytes using cSLO in models of acute injury (Alt et al., 2012; Eter et al., 2008; Liu et al., 2012; Paques et al., 2010, 2006), and morphometric quantification of microglia activation in live confocal images (Bosco et al., 2015; Kozlowski and Weimer, 2012), we performed live imaging at early disease stages, then allowed the animals to age and assessed late RGC pathology in the optic nerve.

We found that early microgliosis within the ONH is strongly correlated with later severity of optic nerve degeneration. The detection of early microgliosis is consistent with previous *ex vivo* studies that have reported microglia and/or peripheral monocyte clustering, activation and proliferation at the ONH prior to detectable neuronal pathology in this model (Bosco et al., 2011),

RESEARCH ARTICLE Disease Models & Mechanisms (2015) 8, 443-455 doi:10.1242/dmm.018788

as well as early infiltration of proinflammatory monocytes (Howell et al., 2012). Gene expression studies have also identified the activation of pathways related to innate immune responses and monocyte recruitment during early progression of chronic glaucoma (Fan et al., 2010; Howell et al., 2012; Steele et al., 2006). Previous studies tracking GFP^+ microglia by cSLO after induction of acute damage to RGCs, by optic nerve crush or intraocular pressure elevation, have detected increases in retinal microgliosis that were associated with reduced survival of RGCs (Alt et al., 2012; Liu et al., 2012). Here, using a chronic model of glaucoma, we found early microgliosis clustered at the ONH, and were able to link this to the later severity of optic nerve degeneration. Our findings suggest that ONH microgliosis might be an early indicator of RGC stress or damage, consistent with the localization of the earliest axonal damage to the retina-nerve interface (Howell et al., 2007a; Soto et al., 2008).

Microglia resident in the unmyelinated optic nerve and central retina initiate focal microgliosis

Proinflammatory, circulating monocytes infiltrate the DBA/2J ONH and have been observed in 10.5-month-old animals (Howell et al., 2012). At young ages, our preliminary analysis suggests that microglia represent the majority of the CX3CR1-GFP^+ cell population contributing to early microgliosis within the ONH and central retina, because there are few cells that express sialoadhesin (Siglec-1 or CD169), a marker of peripheral monocytes and/or macrophages, as well as of dendritic cells (Asano et al., 2011; Butovsky et al., 2012; Hartnell et al., 2001; O'Neill et al., 2013), although it is possible that sialoadhesin expression only identifies a subset of retinal and ONH peripheral monocytes. Interestingly, we find in 17-month-old DBA/2J retinas that sialoadhesin is expressed in the majority of amoeboid monocyte-lineage cells that are abundant within the ONH and throughout the retina, and which have been attributed to monocyte infiltration in previous studies (Howell et al., 2012). Thus, we suggest that early microgliosis is mainly driven by changes in resident microglia, both in the ONH and retina. Given the importance of proinflammatory monocyte infiltration in neurodegeneration (Conductier et al., 2010; Howell et al., 2012; Naert and Rivest, 2013; Perry and Teeling, 2013; Ransohoff and Cardona, 2010; Schwartz et al., 2013), it will be important to explore the crosstalk between microglia and infiltrating monocytes and/or macrophages during early versus late disease progression in glaucoma.

The pigmentary form of glaucoma in DBA/2J mice depends upon mutations in the two melanosomal proteins TYRP1 (tyrosinase-related protein 1) and GPNMB (glycoprotein nmb) (Anderson et al., 2001). We have previously shown that early clustering and activation of microglia was not evident in mice of the congenic substrain DBA/2J *Gpnmb*$^{+/SjJ}$ (Howell et al., 2007b). Notably, GPNMB is also expressed in cells of the macrophage and microglia lineage, and functions as a repressor of inflammation (Huang et al., 2012; Libby et al., 2005; Mo et al., 2003; Ripoll et al., 2007; Zhou et al., 2005). Thus, the early microglial changes documented in the DBA/2J mouse (Bosco et al., 2015, 2012, 2011; Fan et al., 2010) could reflect intrinsic immune components, or immune responses to early stress or damage in RGCs that might contribute to glaucoma pathogenesis. Nevertheless, ONH and central retinal microglial alterations represent the earliest retinal change evident in the DBA/2J mouse, and are strongly correlated with later disease. Although intraocular pressure is not consistently elevated at young ages in DBA/2J mice, progressive functional decreases have been detected after 3 months of age (Saleh et al., 2007). Thus early changes in RGC function are apparent, consistent with the early changes that we see in microglia at these ages.

Live, long-term visualization of microglial changes during neurodegeneration progression and treatment

We conclude that monitoring microglia activation and microgliosis at prepathological stages might be a powerful tool for detecting the onset and tracking progression of neurodegenerative disease. The retina is an ideal region of the CNS to achieve this because specific cell populations can be directly and repeatedly visualized in the intact organism by the use of cSLO and cell-selective transgenic labels (Alt et al., 2012; Chauhan et al., 2012; Eter, 2010; Eter et al., 2008; Kumar and Zhuo, 2010; Leung et al., 2008a,b; Leung and Weinreb, 2009; Liu et al., 2012; Nakano et al., 2011; Paques et al., 2010, 2006; Schallek et al., 2013; Schön et al., 2012; Seeliger et al., 2005). Previous live imaging studies have used the *Cx3cr1*$^{GFP/+}$ transgenic label for cSLO imaging in acute models of induced RGC injury (Alt et al., 2012; Liu et al., 2012). Here, we applied this to a chronic progressive neurodegenerative disease, and provided quantitative analysis of cell changes in the context of chronic neurodegeneration, by extending the period of tracking for microglial and/or peripheral monocytic changes over 5 months, and then analyzing disease progression at 10 months. The tracking of early microglial changes in young DBA/2J mice offers the possibility of optimizing the use of this chronic model by allowing the selection of young animals in which one or both eyes will likely progress to severe glaucoma at advanced ages, thus reducing the inter-individual variability in disease progression within experimental samples. This strategy should advance the already intense studies aimed at elucidating the complex cellular and molecular mechanisms that underlie neurodegeneration in chronic glaucoma (Anderson et al., 2006; Howell et al., 2011; Jakobs, 2014; Nair et al., 2014; Rieck, 2013; Steele et al., 2006), and identify initiating events associated with disease onset or early progression potentially relevant to glaucoma patients.

Other imaging modalities allow quantitative detection of regional microglia activation *in vivo* in chronic CNS pathologies, including positron emission tomography of radioligands for microglia and astrocyte translocator protein (TSPO) receptors, as well as magnetic resonance and bioluminescence imaging of neuroinflammation (Jacobs and Tavitian, 2012; Trapani et al., 2013; Venneti et al., 2013). However, *in vivo* visualization of microglia by cSLO provides cellular resolution, which enables quantitative analysis of microglia activation based on somal size (Bosco et al., 2015), similar to analysis of brain microglial activation in two-photon confocal images (Kozlowski and Weimer, 2012). We observed highly dynamic and sectorial patterns of microglia activation within the retinal parenchyma, suggesting that microglia might be responsive to local changes within the retina during early disease stages. Given that these changes are complex, this possibility will be addressed in future studies using early markers of neuronal stress or dysfunction. Our assessment of microglial behavior near glaucoma onset demonstrates the power of *in vivo* retinal imaging to detect early progression of neurodegeneration at the cell level, with high spatial and temporal resolution.

We also establish the feasibility of visually tracking induced changes in retinal microglia activation to assess therapies, in this case by administering minocycline to decrease activation. With the development of non-genetic labels for microglia, this could be a potential tactic applicable to both glaucoma management and treatment evaluation. Future studies could also evaluate the possibility of detecting retinal microglia and/or peripheral monocyte

RESEARCH ARTICLE Disease Models & Mechanisms (2015) 8, 443-455 doi:10.1242/dmm.018788

changes resulting from diverse pathologies because the retina and optic nerve are targeted for neurodegeneration in diseases such as Alzheimer's, Parkinson's and multiple sclerosis (Chan, 2012; Frost et al., 2010; Guo et al., 2010; Ikram et al., 2012; Kersten et al., 2014; Kesler et al., 2011). In line with this, the use of live detection of retina and ONH pathology for early Alzheimer's disease management is under intense study (Ikram et al., 2012; Petzold et al., 2010; Satue et al., 2014). Overall, our findings suggest that retinal microglia might serve as sensitive neuroimaging biomarkers to detect early and/or unidentified stages of disease onset and progression in glaucoma, and potentially in other neurodegenerative diseases that impact the retina and optic nerve.

MATERIALS AND METHODS

Mice

Heterozygote *Cx3cr1*$^{GFP/+}$ DBA/2J mice were derived by backcrossing homozygous C57BL/6.129P-*Cx3cr1*^{tm1Litt}/J mice, which express GFP under the control of the fractalkine receptor locus, for more than ten generations (Jung et al., 2000) with DBA/2J mice (Jackson Laboratories, Bar Harbor, ME). All mice were bred in-house, introducing new breeders every 3 to 4 generations. This study used females only. Mice were maintained and imaged in pathogen-free facilities, using protocols approved by the Institutional Animal Care and Use Committee at the University of Utah.

cSLO *in vivo* imaging of GFP$^+$ cells in the retina and ONH

Retinal and ONH GFP$^+$ microglial and/or peripheral monocyte cells were monitored using confocal scanning laser ophthalmoscope (cSLO) images collected at monthly intervals in mice aged 1 to 5 months (±1 week), following a recently reported protocol (Bosco et al., 2015). Eyes with corneal or iris defects detectable by fundus imaging were excluded from this study, and imaging was discontinued after 5 months of age, when corneal and/or iris defects prevented effective pupil dilation and reliable imaging. Briefly, mice anesthetized by intraperitoneal injection of Avertin (1.3% 2,2,2-tribromoethanol and 0.8% tert-amyl alcohol, Sigma-Aldrich, St Louis, MO) and fitted with PMMA contact lenses (Cantor & Nissel Ltd., Northants, UK), were imaged unrestrained with a cSLO system equipped with a 55° wide-field lens and real-time eye tracker (Spectralis HRA+OCT, Heidelberg Engineering). The central retina was visualized in single-point images spanning an area of ∼1.5 mm in diameter, or in composite images spanning 40 to 60% of the retina (∼1.5×3-4 mm), both across the inner planes of the retina and ONH (30-40 µm axial depth; 55-60° focus), using by 820-nm or 488-nm laser excitation (460-490 nm barrier filter set) to produce fundus and fluorescence images, respectively.

Live image analysis of cell density and morphological activation

To analyze ONH microgliosis, we manually identified and counted total GFP$^+$ cells within a ∼250-µm-diameter circle centered on the optic disc in cSLO images. In the surrounding central retina, we performed automated cell and somal segmentation followed by morphometric analysis using intensity-based thresholding in cSLO images of the central retina (∼1.5 mm^2) (Bosco et al., 2015). Briefly, individual somal areas were automatically measured, sorted into groups of activated microglia (>50-60 µm^2), non-activated microglia (10-50 µm^2) and manually identified cells <10 µm^2) and mapped to eight radial sectors (∼200 µm^2) that subdivided the central retina and excluded the ONH.

Minocycline treatment

A subset of mice that showed high ONH microgliosis by cSLO imaging at 2 months old (n=9), was administered systemic minocycline (120 mg/kg body weight, Sigma-Aldrich) on weekdays (Monday-Friday) for 6 weeks, from 2.5 to 4 months of age, by oral gavage (Bosco et al., 2011).

Mouse tissue collection

Mouse eyes were collected as previously described (Bosco et al., 2011). Briefly, under full anesthesia induced by inhalation of 2% (vol) Isoflurane in 2 liter/min oxygen, mice were transcardially perfused with 5 ml PBS followed by 20 ml 4% paraformaldehyde (PFA; Electron Microscopy Sciences, Hatfield, PA) in 0.1 M PBS circulated with a peristaltic pump (Dynamax, Rainin, Oakland, CA). Eyes with optic nerves were isolated from the brain and post-fixed for 2 h in PFA at 4°C, and nerves were dissected and further fixed overnight in 1.2% PFA and 0.8% glutaraldehyde in PB (Electron Microscopy Sciences).

Retinal histology

Retinas, with the dorsal pole of the eyes marked with a cauterizer, were processed as previously described (Bosco et al., 2012, 2008, 2011). Whole-mount retinas were immunostained using mouse anti human phospho-neurofilament (pNF, Dako, Carpinteria, CA), rabbit anti-human Iba1 (Wako, Richmond, VA), goat anti-GFP (Abcam, Cambridge, MA), and rat anti-mouse CD169 (sialoadhesin) conjugated to Alexa Fluor 647 (MOMA-1 clone, AbD Serotec, Bio-Rad, Raleigh, NC) primary antibodies, which were detected with Alexa-Fluor-conjugated donkey anti-IgG secondary antibodies (Invitrogen, La Jolla, CA).

Ex vivo confocal imaging

Confocal images spanning entire retinal flat mounts were generated as previously described (Bosco et al., 2012, 2011) using a confocal imaging system equipped with a 20× lens and a resonant scanner (A1R confocal, Eclipse Ti inverted microscope and NIS-Elements C, Nikon). Multipoint images (625 *xy* positions) were acquired at high resolution (0.41 µm/px), then stitched and projected as maximal intensity of the inner 30-40 µm of retina (0.8-µm step). To allow image analysis and quantification, the parameters of image acquisition were maintained constant between retinal samples, and, for illustration, images had their brightness and contrast minimally edited. Counts of ONH cells expressing GFP and/or sialoadhesin where manually performed in the central 200×200 µm around the optic disc, visualizing each channel independently in maximum-intensity projections, and verifying colocalization in slice view, through the *z* plane.

Optic nerve histopathology

Nerves from 10-month-old *Cx3cr1*$^{GFP/+}$ DBA/2J mice including the retro-orbital, myelinated segment (1-1.5 mm post-lamina), were prepared as 1-µm-thick plastic cross-sections, and stained with a modified paraphenylenediamine (PPD) protocol and Toluidine Blue (Anderson et al., 2005; Calkins et al., 2005; Inman et al., 2006; Sappington et al., 2003). High-resolution multipoint (36 *xy*) images were generated using a compound light-microscope and a 60× lens (BX51 and cellSens software, Olympus, Center Valley, PA).

Quantification of nerve gliosis

By direct visual inspection of high-resolution multipoint images obtained from entire optic nerve cross-sections, we identified glial cells and the gliotic scar as areas lacking dystrophic or intact axons, as well as meninges and vascular lumen. To segment glial areas and vascular spaces, we applied automatic thresholds to the red RGB channel to generate a binary overlay representing axon-free nerve areas (FluoRender, University of Utah). To quantify the relative area occupied by glial cells and/or the gliotic scar, we measured the cross-sectional area of the nerve and subtracted the area corresponding to blood vessels and meninges. Random samples independently segmented and measured by two investigators showed <5% variation in measured glial area (n=10).

Statistics

Statistical significance was calculated by a Student's post-hoc *t*-test (unpaired, two tailed; Fig. 2B, Fig. 3B and Fig. 5B,C), by a linear mixed model (http://CRAN.R-project.org/package=lme4; Fig. 3B) or Kruskal–Wallis rank-ordered test (Fig. 4E), and is indicated in the graphs as: *P<0.05, **P<0.01 and ***P<0.001. Correlation analysis was performed by Spearman's rank-ordered test (Fig. 5D). Analyses were conducted in R: A language and environment for statistical computing 2014 (R Core Team, R Foundation for Statistical Computing, Vienna, Austria) or Excel v. 14.4.6 (Microsoft, Redmond, WA).

Acknowledgements
We thank the Glaucoma Research Foundation Catalyst for a Cure Scientific Advisory Board, David J. Calkins (Vanderbilt University) for advice on optic nerve histopathology, Shelley Morandi Clark for superb technical support for confocal imaging and analysis, and at the University of Utah, Brian F. Codding for expert statistical advice, Kathryn B. Moore for manuscript critique, and the Scientific Computing and Imaging Institute for use of FluoRender software.

Competing interests
The authors declare no competing or financial interests.

Author contributions
A.B. conceived the project; A.B. and M.L.V. designed the experiments; B.K.A. contributed the cSLO; A.B., C.O.R., A.A.C. M.R.S. and K.T.B. performed the experiments; A.B. and K.T.B. analyzed and interpreted the data; A.B. and M.L.V. wrote the paper.

Funding
This work was supported by grants from the Glaucoma Research Foundation; the Melsa M. and Frank Theodore Barr Foundation; the US National Institutes of Health [grant numbers R01EY020878, R01EY023621 to M.L.V., R01EY017182, R01EY017950 to B.K.A., R01GM09815 to the Scientific Computing and Imaging Institute], and the University of Utah Vision Core [grant number 5P30EY014800].

Supplementary material
Supplementary material available online at
http://dmm.biologists.org/lookup/suppl/doi:10.1242/dmm.018788/-/DC1

References

Ajami, B., Bennett, J. L., Krieger, C., Tetzlaff, W. and Rossi, F. M. V. (2007). Local self-renewal can sustain CNS microglia maintenance and function throughout adult life. *Nat. Neurosci.* **10**, 1538-1543.

Ajami, B., Bennett, J. L., Krieger, C., McNagny, K. M. and Rossi, F. M. V. (2011). Infiltrating monocytes trigger EAE progression, but do not contribute to the resident microglia pool. *Nat. Neurosci.* **14**, 1142-1149.

Alt, C., Runnels, J. M., Teo, G. S. L. and Lin, C.P. (2012). In vivo tracking of hematopoietic cells in the retina of chimeric mice with a scanning laser ophthalmoscope. *Intravital* **1**, 132-140.

Amor, S., Puentes, F., Baker, D. and van der Valk, P. (2010). Inflammation in neurodegenerative diseases. *Immunology* **129**, 154-169.

Amor, S., Peferoen, L. A. N., Vogel, D. Y. S., Breur, M., van der Valk, P., Baker, D. and van Noort, J. M. (2014). Inflammation in neurodegenerative diseases–an update. *Immunology* **142**, 151-166.

Anderson, M. G., Smith, R. S., Hawes, N. L., Zabaleta, A., Chang, B., Wiggs, J. L. and John, S. W. M. (2001). Mutations in genes encoding melanosomal proteins cause pigmentary glaucoma in DBA/2J mice. *Nat. Genet.* **30**, 81-85.

Anderson, M. G., Libby, R. T., Gould, D. B., Smith, R. S. and John, S. W. M. (2005). High-dose radiation with bone marrow transfer prevents neurodegeneration in an inherited glaucoma. *Proc. Natl. Acad. Sci. USA* **102**, 4566-4571.

Anderson, M. G., Libby, R. T., Mao, M., Cosma, I. M., Wilson, L. A., Smith, R. S. and John, S. W. M. (2006). Genetic context determines susceptibility to intraocular pressure elevation in a mouse pigmentary glaucoma. *BMC Biol.* **4**, 20.

Asano, K., Nabeyama, A., Miyake, Y., Qiu, C.-H., Kurita, A., Tomura, M., Kanagawa, O., Fujii, S.-i. and Tanaka, M. (2011). CD169-positive macrophages dominate antitumor immunity by crosspresenting dead cell-associated antigens. *Immunity* **34**, 85-95.

Block, M. L., Zecca, L. and Hong, J.-S. (2007). Microglia-mediated neurotoxicity: uncovering the molecular mechanisms. *Nat. Rev. Neurosci.* **8**, 57-69.

Bosco, A., Inman, D. M., Steele, M. R., Wu, G., Soto, I., Marsh-Armstrong, N., Hubbard, W. C., Calkins, D. J., Horner, P. J. and Vetter, M. L. (2008). Reduced retina microglial activation and improved optic nerve integrity with minocycline treatment in the DBA/2J mouse model of glaucoma. *Invest. Ophthalmol. Vis. Sci.* **49**, 1437-1446.

Bosco, A., Steele, M. R. and Vetter, M. L. (2011). Early microglia activation in a mouse model of chronic glaucoma. *J. Comp. Neurol.* **519**, 599-620.

Bosco, A., Crish, S. D., Steele, M. R., Romero, C. O., Inman, D. M., Horner, P. J., Calkins, D. J. and Vetter, M. L. (2012). Early reduction of microglia activation by irradiation in a model of chronic glaucoma. *PLoS ONE* **7**, e43602.

Bosco, A., Romero, C. O., Ambati, B. K. and Vetter, M. L. (2015). *In vivo* dynamics of retinal microglial activation during neurodegeneration: confocal ophthalmoscopic imaging and cell morphometry in mouse glaucoma. *J. Vis. Exp.* (in press). doi:10.3791/52731.

Broux, B., Pannemans, K., Zhang, X., Markovic-Plese, S., Broekmans, T., Eijnde, B. O., Van Wijmeersch, B., Somers, V., Geusens, P., van der Pol, S. et al. (2012). CX(3)CR1 drives cytotoxic CD4(+)CD28(–) T cells into the brain of multiple sclerosis patients. *J. Autoimmun.* **38**, 10-19.

Buckingham, B. P., Inman, D. M., Lambert, W., Oglesby, E., Calkins, D. J., Steele, M. R., Vetter, M. L., Marsh-Armstrong, N. and Horner, P. J. (2008). Progressive ganglion cell degeneration precedes neuronal loss in a mouse model of glaucoma. *J. Neurosci.* **28**, 2735-2744.

Burda, J. E. and Sofroniew, M. V. (2014). Reactive gliosis and the multicellular response to CNS damage and disease. *Neuron* **81**, 229-248.

Butovsky, O., Siddiqui, S., Gabriely, G., Lanser, A. J., Dake, B., Murugaiyan, G., Doykan, C. E., Wu, P. M., Gali, R. R., Iyer, L. K. et al. (2012). Modulating inflammatory monocytes with a unique microRNA gene signature ameliorates murine ALS. *J. Clin. Invest.* **122**, 3063-3087.

Calkins, D. J., Sappington, R. M. and Hendry, S. H. C. (2005). Morphological identification of ganglion cells expressing the alpha subunit of type II calmodulin-dependent protein kinase in the macaque retina. *J. Comp. Neurol.* **481**, 194-209.

Casson, R. J., Chidlow, G., Wood, J. P. M., Crowston, J. G. and Goldberg, I. (2012). Definition of glaucoma: clinical and experimental concepts. *Clin. Exp. Ophthalmol.* **40**, 341-349.

Chan, J. W. (2012). Recent advances in optic neuritis related to multiple sclerosis. *Acta Ophthalmol.* **90**, 203-209.

Chang, B., Smith, R. S., Hawes, N. L., Anderson, M. G., Zabaleta, A., Savinova, O., Roderick, T. H., Heckenlively, J. R., Davisson, M. T. and John, S. W. M. (1999). Interacting loci cause severe iris atrophy and glaucoma in DBA/2J mice. *Nat. Genet.* **21**, 405-409.

Chauhan, B. C., Stevens, K. T., Levesque, J. M., Nuschke, A. C., Sharpe, G. P., O'Leary, N., Archibald, M. L. and Wang, X. (2012). Longitudinal in vivo imaging of retinal ganglion cells and retinal thickness changes following optic nerve injury in mice. *PLoS ONE* **7**, e40352.

Combadière, C., Feumi, C., Raoul, W., Keller, N., Rodéro, M., Pézard, A., Lavalette, S., Houssier, M., Jonet, L., Picard, E. et al. (2007). CX3CR1-dependent subretinal microglia cell accumulation is associated with cardinal features of age-related macular degeneration. *J. Clin. Invest.* **117**, 2920-2928.

Conductier, G., Blondeau, N., Guyon, A., Nahon, J.-L. and Rovère, C. (2010). The role of monocyte chemoattractant protein MCP1/CCL2 in neuroinflammatory diseases. *J. Neuroimmunol.* **224**, 93-100.

Crish, S. D., Sappington, R. M., Inman, D. M., Horner, P. J. and Calkins, D. J. (2010). Distal axonopathy with structural persistence in glaucomatous neurodegeneration. *Proc. Natl. Acad. Sci. USA* **107**, 5196-5201.

Cunningham, C. (2013). Microglia and neurodegeneration: the role of systemic inflammation. *Glia* **61**, 71-90.

Dai, C., Khaw, P. T., Yin, Z. Q., Li, D., Raisman, G. and Li, Y. (2012). Structural basis of glaucoma: the fortified astrocytes of the optic nerve head are the target of raised intraocular pressure. *Glia* **60**, 13-28.

Davalos, D., Grutzendler, J., Yang, G., Kim, J. V., Zuo, Y., Jung, S., Littman, D. R., Dustin, M. L. and Gan, W.-B. (2005). ATP mediates rapid microglial response to local brain injury in vivo. *Nat. Neurosci.* **8**, 752-758.

Davalos, D., Ryu, J. K., Merlini, M., Baeten, K. M., Le Moan, N., Petersen, M. A., Deerinck, T. J., Smirnoff, D. S., Bedard, C., Hakozaki, H. et al. (2012). Fibrinogen-induced perivascular microglial clustering is required for the development of axonal damage in neuroinflammation. *Nat. Commun.* **3**, 1227.

Davies, L. C., Jenkins, S. J., Allen, J. E. and Taylor, P. R. (2013). Tissue-resident macrophages. *Nat. Immunol.* **14**, 986-995.

Dibaj, P., Steffens, H., Zschüntzsch, J., Nadrigny, F., Schomburg, E. D., Kirchhoff, F. and Neusch, C. (2011). In Vivo imaging reveals distinct inflammatory activity of CNS microglia versus PNS macrophages in a mouse model for ALS. *PLoS ONE* **6**, e17910.

Elmore, M. R. P., Najafi, A. R., Koike, M. A., Dagher, N. N., Spangenberg, E. E., Rice, R. A., Kitazawa, M., Matusow, B., Nguyen, H., West, B. L. et al. (2014). Colony-stimulating factor 1 receptor signaling is necessary for microglia viability, unmasking a microglia progenitor cell in the adult brain. *Neuron* **82**, 380-397.

Eter, N. (2010). Molecular imaging in the eye. *Br. J. Ophthalmol.* **94**, 1420-1426.

Eter, N., Engel, D. R., Meyer, L., Helb, H.-M., Roth, F., Maurer, J., Holz, F. G. and Kurts, C. (2008). In vivo visualization of dendritic cells, macrophages, and microglial cells responding to laser-induced damage in the fundus of the eye. *Invest. Ophthalmol. Vis. Sci.* **49**, 3649-3658.

Evans, T. A., Barkauskas, D. S., Myers, J. T., Hare, E. G., You, J. Q., Ransohoff, R. M., Huang, A. Y. and Silver, J. (2014). High-resolution intravital imaging reveals that blood-derived macrophages but not resident microglia facilitate secondary axonal dieback in traumatic spinal cord injury. *Exp. Neurol.* **254**, 109-120.

Fan, W., Li, X., Wang, W., Mo, J. S., Kaplan, H. and Cooper, N. G. (2010). Early involvement of immune/inflammatory response genes in retinal degeneration in DBA/2J mice. *Ophthalmol. Eye Dis.* **1**, 23-41.

Frost, S., Martins, R. N. and Kanagasingam, Y. (2010). Ocular biomarkers for early detection of Alzheimer's disease. *J. Alzheimers Dis.* **22**, 1-16.

Fuhrmann, M., Bittner, T., Jung, C. K. E., Burgold, S., Page, R. M., Mitteregger, G., Haass, C., LaFerla, F. M., Kretzschmar, H. and Herms, J. (2010). Microglial Cx3cr1 knockout prevents neuron loss in a mouse model of Alzheimer's disease. *Nat. Neurosci.* **13**, 411-413.

Gramlich, O. W., Beck, S., von Thun und Hohenstein-Blaul, N., Boehm, N., Ziegler, A., Vetter, J. M., Pfeiffer, N. and Grus, F. H. (2013). Enhanced insight into the autoimmune component of glaucoma: IgG autoantibody accumulation

and pro-inflammatory conditions in human glaucomatous retina. *PLoS ONE* **8**, e57557.
Guo, L., Duggan, J. and Cordeiro, M. F. (2010). Alzheimer's disease and retinal neurodegeneration. *Curr. Alzheimer Res.* **7**, 3-14.
Gupta, N., Brown, K. E. and Milam, A. H. (2003). Activated microglia in human retinitis pigmentosa, late-onset retinal degeneration, and age-related macular degeneration. *Exp. Eye Res.* **76**, 463-471.
Hartnell, A., Steel, J., Turley, H., Jones, M., Jackson, D. G. and Crocker, P. R. (2001). Characterization of human sialoadhesin, a sialic acid binding receptor expressed by resident and inflammatory macrophage populations. *Blood* **97**, 288-296.
Hernandez, M. R. (2000). The optic nerve head in glaucoma: role of astrocytes in tissue remodeling. *Prog. Retin. Eye Res.* **19**, 297-321.
Howell, G. R., Libby, R. T., Jakobs, T. C., Smith, R. S., Phalan, F. C., Barter, J. W., Barbay, J. M., Marchant, J. K., Mahesh, N., Porciatti, V. et al. (2007a). Axons of retinal ganglion cells are insulted in the optic nerve early in DBA/2J glaucoma. *J. Cell Biol.* **179**, 1523-1537.
Howell, G. R., Libby, R. T., Marchant, J. K., Wilson, L. A., Cosma, I. M., Smith, R. S., Anderson, M. G. and John, S. W. M. (2007b). Absence of glaucoma in DBA/2J mice homozygous for wild-type versions of Gpnmb and Tyrp1. *BMC Genet.* **8**, 45.
Howell, G. R., Macalinao, D. G., Sousa, G. L., Walden, M., Soto, I., Kneeland, S. C., Barbay, J. M., King, B. L., Marchant, J. K., Hibbs, M. et al. (2011). Molecular clustering identifies complement and endothelin induction as early events in a mouse model of glaucoma. *J. Clin. Invest.* **121**, 1429-1444.
Howell, G. R., Soto, I., Zhu, X., Ryan, M., Macalinao, D. G., Sousa, G. L., Caddle, L. B., MacNicoll, K. H., Barbay, J. M., Porciatti, V. et al. (2012). Radiation treatment inhibits monocyte entry into the optic nerve head and prevents neuronal damage in a mouse model of glaucoma. *J. Clin. Invest.* **122**, 1246-1261.
Huang, J.-J., Ma, W.-J. and Yokoyama, S. (2012). Expression and immunolocalization of Gpnmb, a glioma-associated glycoprotein, in normal and inflamed central nervous systems of adult rats. *Brain Behav.* **2**, 85-96.
Ikram, M. K., Cheung, C. Y., Wong, T. Y. and Chen, C. P. L. H. (2012). Retinal pathology as biomarker for cognitive impairment and Alzheimer's disease. *J. Neurol. Neurosurg. Psychiatry* **83**, 917-922.
Inman, D. M., Sappington, R. M., Horner, P. J. and Calkins, D. J. (2006). Quantitative correlation of optic nerve pathology with ocular pressure and corneal thickness in the DBA/2 mouse model of glaucoma. *Invest. Ophthalmol. Vis. Sci.* **47**, 986-996.
Jacobs, A. H. and Tavitian, B. (2012). Noninvasive molecular imaging of neuroinflammation. *J. Cereb. Blood Flow Metab.* **32**, 1393-1415.
Jakobs, T. C. (2014). Differential gene expression in glaucoma. *Cold Spring Harb. Perspect. Med.* **4**, a020636.
Jakobs, T. C., Libby, R. T., Ben, Y., John, S. W. M. and Masland, R. H. (2005). Retinal ganglion cell degeneration is topological but not cell type specific in DBA/2J mice. *J. Cell Biol.* **171**, 313-325.
John, S. W., Smith, R. S., Savinova, O. V., Hawes, N. L., Chang, B., Turnbull, D., Davisson, M., Roderick, T. H. and Heckenlively, J. R. (1998). Essential iris atrophy, pigment dispersion, and glaucoma in DBA/2J mice. *Invest. Ophthalmol. Vis. Sci.* **39**, 951-962.
Jung, S., Aliberti, J., Graemmel, P., Sunshine, M. J., Kreutzberg, G. W., Sher, A. and Littman, D. R. (2000). Analysis of fractalkine receptor CX(3)CR1 function by targeted deletion and green fluorescent protein reporter gene insertion. *Mol. Cell. Biol.* **20**, 4106-4114.
Karlstetter, M. and Langmann, T. (2014). Microglia in the aging retina. *Adv. Exp. Med. Biol.* **801**, 207-212.
Kersten, H. M., Roxburgh, R. H. and Danesh-Meyer, H. V. (2014). Ophthalmic manifestations of inherited neurodegenerative disorders. *Nat. Rev. Neurol.* **10**, 349-362.
Kesler, A., Vakhapova, V., Korczyn, A. D., Naftaliev, E. and Neudorfer, M. (2011). Retinal thickness in patients with mild cognitive impairment and Alzheimer's disease. *Clin. Neurol. Neurosurg.* **113**, 523-526.
Kettenmann, H., Hanisch, U.-K., Noda, M. and Verkhratsky, A. (2011). Physiology of microglia. *Physiol. Rev.* **91**, 461-553.
Kozlowski, C. and Weimer, R. M. (2012). An automated method to quantify microglia morphology and application to monitor activation state longitudinally in vivo. *PLoS ONE* **7**, e31814.
Kreutzberg, G. W. (1996). Microglia: a sensor for pathological events in the CNS. *Trends Neurosci.* **19**, 312-318.
Kumar, S. and Zhuo, L. (2010). Longitudinal in vivo imaging of retinal gliosis in a diabetic mouse model. *Exp. Eye Res.* **91**, 530-536.
Lawson, L. J., Perry, V. H., Dri, P. and Gordon, S. (1990). Heterogeneity in the distribution and morphology of microglia in the normal adult mouse brain. *Neuroscience* **39**, 151-170.
Lawson, L. J., Perry, V. H. and Gordon, S. (1992). Turnover of resident microglia in the normal adult mouse brain. *Neuroscience* **48**, 405-415.
Leung, C. K.-S. and Weinreb, R. N. (2009). Experimental detection of retinal ganglion cell damage in vivo. *Exp. Eye Res.* **88**, 831-836.
Leung, C. K.-S., Lindsey, J. D., Crowston, J. G., Ju, W.-K., Liu, Q., Bartsch, D.-U. and Weinreb, R. N. (2008a). In vivo imaging of murine retinal ganglion cells. *J. Neurosci. Methods* **168**, 475-478.
Leung, C. K.-S., Lindsey, J. D., Crowston, J. G., Lijia, C., Chiang, S. and Weinreb, R. N. (2008b). Longitudinal profile of retinal ganglion cell damage after optic nerve crush with blue-light confocal scanning laser ophthalmoscopy. *Invest. Ophthalmol. Vis. Sci.* **49**, 4898-4902.
Libby, R. T., Anderson, M. G., Pang, I.-H., Robinson, Z. H., Savinova, O. V., Cosma, I. M., Snow, A., Wilson, L. A., Smith, R. S., Clark, A. F. et al. (2005). Inherited glaucoma in DBA/2J mice: pertinent disease features for studying the neurodegeneration. *Vis. Neurosci.* **22**, 637-648.
Linnartz-Gerlach, B., Kopatz, J. and Neumann, H. (2014). Siglec functions of microglia. *Glycobiology* **24**, 794-799.
Liu, S., Li, Z.-W., Weinreb, R. N., Xu, G., Lindsey, J. D., Ye, C., Yung, W.-H., Pang, C.-P., Lam, D. S. C. and Leung, C. K.-S. (2012). Tracking retinal microgliosis in models of retinal ganglion cell damage. *Invest. Ophthalmol. Vis. Sci.* **53**, 6254-6262.
Lye-Barthel, M., Sun, D. and Jakobs, T. C. (2013). Morphology of astrocytes in a glaucomatous optic nerve. *Invest. Ophthalmol. Vis. Sci.* **54**, 909-917.
Maeda, J., Zhang, M.-R., Okauchi, T., Ji, B., Ono, M., Hattori, S., Kumata, K., Iwata, N., Saido, T. C., Trojanowski, J. Q. et al. (2011). In vivo positron emission tomographic imaging of glial responses to amyloid-beta and tau pathologies in mouse models of Alzheimer's disease and related disorders. *J. Neurosci.* **31**, 4720-4730.
Maeda, A., Palczewska, G., Golczak, M., Kohno, H., Dong, Z., Maeda, T. and Palczewski, K. (2014). Two-photon microscopy reveals early rod photoreceptor cell damage in light-exposed mutant mice. *Proc. Natl. Acad. Sci. USA* **111**, E1428-E1437.
Mo, J.-S., Anderson, M. G., Gregory, M., Smith, R. S., Savinova, O. V., Serreze, D. V., Ksander, B. R., Streilein, J. W. and John, S. W. M. (2003). By altering ocular immune privilege, bone marrow-derived cells pathogenically contribute to DBA/2J pigmentary glaucoma. *J. Exp. Med.* **197**, 1335-1344.
Naert, G. and Rivest, S. (2013). A deficiency in CCR2+ monocytes: the hidden side of Alzheimer's disease. *J. Mol. Cell. Biol.* **5**, 284-293.
Nair, K. S., Barbay, J., Smith, R. S., Masli, S. and John, S. W. M. (2014). Determining immune components necessary for progression of pigment dispersing disease to glaucoma in DBA/2J mice. *BMC Genet.* **15**, 42.
Nakano, N., Ikeda, H. O., Hangai, M., Muraoka, Y., Toda, Y., Kakizuka, A. and Yoshimura, N. (2011). Longitudinal and simultaneous imaging of retinal ganglion cells and inner retinal layers in a mouse model of glaucoma induced by N-methyl-D-aspartate. *Invest. Ophthalmol. Vis. Sci.* **52**, 8754-8762.
Nayak, D., Zinselmeyer, B. H., Corps, K. N. and McGavern, D. B. (2012). In vivo dynamics of innate immune sentinels in the CNS. *Intravital* **1**, 95-106.
Neufeld, A. H. (1999). Microglia in the optic nerve head and the region of parapapillary chorioretinal atrophy in glaucoma. *Arch. Ophthalmol.* **117**, 1050-1056.
Nickells, R. W., Howell, G. R., Soto, I. and John, S. W. M. (2012). Under pressure: cellular and molecular responses during glaucoma, a common neurodegeneration with axonopathy. *Annu. Rev. Neurosci.* **35**, 153-179.
Nimmerjahn, A., Kirchhoff, F. and Helmchen, F. (2005). Resting microglial cells are highly dynamic surveillants of brain parenchyma in vivo. *Science* **308**, 1314-1318.
O'Neill, A. S. G., van den Berg, T. K. and Mullen, G. E. D. (2013). Sialoadhesin - a macrophage-restricted marker of immunoregulation and inflammation. *Immunology* **138**, 198-207.
Ouchi, Y., Yoshikawa, E., Sekine, Y., Futatsubashi, M., Kanno, T., Ogusu, T. and Torizuka, T. (2005). Microglial activation and dopamine terminal loss in early Parkinson's disease. *Ann. Neurol.* **57**, 168-175.
Paques, M., Simonutti, M., Roux, M. J., Picaud, S., Levavasseur, E., Bellman, C. and Sahel, J.-A. (2006). High resolution fundus imaging by confocal scanning laser ophthalmoscopy in the mouse. *Vision Res.* **46**, 1336-1345.
Paques, M., Simonutti, M., Augustin, S., Goupille, O., El Mathari, B. and Sahel, J.-A. (2010). In vivo observation of the locomotion of microglial cells in the retina. *Glia* **58**, 1663-1668.
Perry, V. H. and Teeling, J. (2013). Microglia and macrophages of the central nervous system: the contribution of microglia priming and systemic inflammation to chronic neurodegeneration. *Semin. Immunopathol.* **35**, 601-612.
Perry, V. H., Crocker, P. R. and Gordon, S. (1992). The blood-brain barrier regulates the expression of a macrophage sialic acid-binding receptor on microglia. *J. Cell Sci.* **101**, 201-207.
Petzold, A., de Boer, J. F., Schippling, S., Vermersch, P., Kardon, R., Green, A., Calabresi, P. A. and Polman, C. (2010). Optical coherence tomography in multiple sclerosis: a systematic review and meta-analysis. *Lancet Neurol.* **9**, 921-932.
Politis, M., Su, P. and Piccini, P. (2012). Imaging of microglia in patients with neurodegenerative disorders. *Front. Pharmacol.* **3**, 96.
Prinz, M., Priller, J., Sisodia, S. S. and Ransohoff, R. M. (2011). Heterogeneity of CNS myeloid cells and their roles in neurodegeneration. *Nat. Neurosci.* **13**, 1227-1235.

Disease Models & Mechanisms (2015) 8, 443-455 doi:10.1242/dmm.018788

Qu, J. and Jakobs, T. C. (2013). The time course of gene expression during reactive gliosis in the optic nerve. *PLoS ONE* **8**, e67094.
Quigley, H. A. (1999). Neuronal death in glaucoma. *Prog. Retin. Eye Res.* **18**, 39-57.
Quigley, H. A. (2011). Glaucoma. *Lancet* **377**, 1367-1377.
Ransohoff, R. M. and Cardona, A. E. (2010). The myeloid cells of the central nervous system parenchyma. *Nature* **468**, 253-262.
Ransohoff, R. M. and Perry, V. H. (2009). Microglial physiology: unique stimuli, specialized responses. *Annu. Rev. Immunol.* **27**, 119-145.
Rieck, J. (2013). The pathogenesis of glaucoma in the interplay with the immune system. *Invest. Ophthalmol. Vis. Sci.* **54**, 2393-2409.
Ripoll, V. M., Irvine, K. M., Ravasi, T., Sweet, M. J. and Hume, D. A. (2007). Gpnmb is induced in macrophages by IFN-gamma and lipopolysaccharide and acts as a feedback regulator of proinflammatory responses. *J. Immunol.* **178**, 6557-6566.
Saleh, M., Nagaraju, M. and Porciatti, V. (2007). Longitudinal evaluation of retinal ganglion cell function and IOP in the DBA/2J mouse model of glaucoma. *Invest. Ophthalmol. Vis. Sci.* **48**, 4564-4572.
Sancho-Pelluz, J., Wunderlich, K. A., Rauch, U., Romero, F. J., van Veen, T., Limb, G. A., Crocker, P. R. and Perez, M.-T. (2008). Sialoadhesin expression in intact degenerating retinas and following transplantation. *Invest. Ophthalmol. Vis. Sci.* **49**, 5602-5610.
Sapp, E., Kegel, K. B., Aronin, N., Hashikawa, T., Uchiyama, Y., Tohyama, K., Bhide, P. G., Vonsattel, J. P. and DiFiglia, M. (2001). Early and progressive accumulation of reactive microglia in the Huntington disease brain. *J. Neuropathol. Exp. Neurol.* **60**, 161-172.
Sappington, R. M., Pearce, D. A. and Calkins, D. J. (2003). Optic nerve degeneration in a murine model of juvenile ceroid lipofuscinosis. *Invest. Ophthalmol. Vis. Sci.* **44**, 3725-3731.
Satue, M., Seral, M., Otin, S., Alarcia, R., Herrero, R., Bambo, M. P., Fuertes, M. I., Pablo, L. E. and Garcia-Martin, E. (2014). Retinal thinning and correlation with functional disability in patients with Parkinson's disease. *Br. J. Ophthalmol.* **98**, 350-355.
Schallek, J., Geng, Y., Nguyen, H. and Williams, D. R. (2013). Morphology and topography of retinal pericytes in the living mouse retina using in vivo adaptive optics imaging and ex vivo characterization. *Invest. Ophthalmol. Vis. Sci.* **54**, 8237-8250.
Schlamp, C. L., Li, Y., Dietz, J. A., Janssen, K. T. and Nickells, R. W. (2006). Progressive ganglion cell loss and optic nerve degeneration in DBA/2J mice is variable and asymmetric. *BMC Neurosci.* **7**, 66.
Schön, C., Hoffmann, N. A., Ochs, S. M., Burgold, S., Filser, S., Steinbach, S., Seeliger, M. W., Arzberger, T., Goedert, M., Kretzschmar, H. A. et al. (2012). Long-term in vivo imaging of fibrillar tau in the retina of P301S transgenic mice. *PLoS ONE* **7**, e53547.
Schwartz, M., Kipnis, J., Rivest, S. and Prat, A. (2013). How do immune cells support and shape the brain in health, disease, and aging? *J. Neurosci.* **33**, 17587-17596.
Seeliger, M. W., Beck, S. C., Pereyra-Muñoz, N., Dangel, S., Tsai, J.-Y., Luhmann, U. F. O., van de Pavert, S. A., Wijnholds, J., Samardzija, M., Wenzel, A. et al. (2005). In vivo confocal imaging of the retina in animal models using scanning laser ophthalmoscopy. *Vision Res.* **45**, 3512-3519.
Sennlaub, F., Auvynet, C., Calippe, B., Lavalette, S., Poupel, L., Hu, S. J., Dominguez, E., Camelo, S., Levy, O., Guyon, E. et al. (2013). CCR2(+) monocytes infiltrate atrophic lesions in age-related macular disease and mediate photoreceptor degeneration in experimental subretinal inflammation in Cx3cr1 deficient mice. *EMBO Mol. Med.* **5**, 1775-1793.
Sofroniew, M. V. (2009). Molecular dissection of reactive astrogliosis and glial scar formation. *Trends Neurosci.* **32**, 638-647.
Solomon, J. N., Lewis, C.-A. B., Ajami, B., Corbel, S. Y., Rossi, F. M. V. and Krieger, C. (2006). Origin and distribution of bone marrow-derived cells in the central nervous system in a mouse model of amyotrophic lateral sclerosis. *Glia* **53**, 744-753.
Son, J. L., Soto, I., Oglesby, E., Lopez-Roca, T., Pease, M. E., Quigley, H. A. and Marsh-Armstrong, N. (2010). Glaucomatous optic nerve injury involves early astrocyte reactivity and late oligodendrocyte loss. *Glia* **58**, 780-789.
Soto, I., Oglesby, E., Buckingham, B. P., Son, J. L., Roberson, E. D. O., Steele, M. R., Inman, D. M., Vetter, M. L., Horner, P. J. and Marsh-Armstrong, N. (2008). Retinal ganglion cells downregulate gene expression and lose their axons within the optic nerve head in a mouse glaucoma model. *J. Neurosci.* **28**, 548-561.
Steele, M. R., Inman, D. M., Calkins, D. J., Horner, P. J. and Vetter, M. L. (2006). Microarray analysis of retinal gene expression in the DBA/2J model of glaucoma. *Invest. Ophthalmol. Vis. Sci.* **47**, 977-985.
Streit, W. J., Walter, S. A. and Pennell, N. A. (1999). Reactive microgliosis. *Prog. Neurobiol.* **57**, 563-581.
Sun, D. and Jakobs, T. C. (2012). Structural remodeling of astrocytes in the injured CNS. *Neuroscientist* **18**, 567-588.
Sun, D., Lye-Barthel, M., Masland, R. H. and Jakobs, T. C. (2009). The morphology and spatial arrangement of astrocytes in the optic nerve head of the mouse. *J. Comp. Neurol.* **516**, 1-19.
Trapani, A., Palazzo, C., de Candia, M., Lasorsa, F. M. and Trapani, G. (2013). Targeting of the translocator protein 18 kDa (TSPO): a valuable approach for nuclear and optical imaging of activated microglia. *Bioconjug. Chem.* **24**, 1415-1428.
Tremblay, M.-È., Lowery, R. L. and Majewska, A. K. (2010). Microglial interactions with synapses are modulated by visual experience. *PLoS Biol.* **8**, e1000527.
Vagaja, N. N., Chinnery, H. R., Binz, N., Kezic, J. M., Rakoczy, E. P. and McMenamin, P. G. (2012). Changes in murine hyalocytes are valuable early indicators of ocular disease. *Invest. Ophthalmol. Vis. Sci.* **53**, 1445-1451.
Venneti, S., Lopresti, B. J. and Wiley, C. A. (2013). Molecular imaging of microglia/macrophages in the brain. *Glia* **61**, 10-23.
Wake, H., Moorhouse, A. J., Jinno, S., Kohsaka, S. and Nabekura, J. (2009). Resting microglia directly monitor the functional state of synapses in vivo and determine the fate of ischemic terminals. *J. Neurosci.* **29**, 3974-3980.
Weinreb, R. N. and Khaw, P. T. (2004). Primary open-angle glaucoma. *Lancet* **363**, 1711-1720.
Zhou, X., Li, F., Kong, L., Tomita, H., Li, C. and Cao, W. (2005). Involvement of inflammation, degradation, and apoptosis in a mouse model of glaucoma. *J. Biol. Chem.* **280**, 31240-31248.

CHAPTER 4

DISCUSSION

Research summary

Alterations to myeloid immune cells have been recorded for over a hundred years in cases of neurodegeneration, yet the roles these cells play in pathogenesis remains a mystery. The rapid and remarkable plasticity of the myeloid system in response to CNS injury or disease make answering this question a still formidable task, yet with the newly characterized lineages of myeloid cells, it has become increasingly possible. Since the myeloid immune system is so plastic and reactive to stress and injury, genetic and age-related chronic models are good systems to study it. For this reason, I examined changes to myeloid cells in the DBA/2J mouse, a chronic and genetic mouse model of the neurodegenerative disease glaucoma.

Since different parts or compartments of a neuron degenerate at different times, models that grant access to these compartments are necessary in order to understand the biology of neurodegeneration, and to not overlook potential contributions to pathology within different compartments. By comparing degeneration in one compartment with another, very surprising discoveries have been made. For example, it has been shown that an RGC disconnected from its central targets will persist in the retina for up to 1 month (Soto et al., 2008), begging the question of whether these RGCs can be prompted to

regenerate. Furthermore, in DBA/2J mice null for the pro-apoptotic gene Bax, it has been shown that the axon still degenerates despite preservation of the cell soma within the retina (Libby et al., 2005). However, it remains rare for investigators to compare degeneration in multiple compartments in a progressive model of neurodegeneration as in Schlamp et al. (2006) and even more rare to examine multiple compartments in each individual sample. In so doing, my data have revealed selective changes to RGCs within the retina that are uncoupled from optic nerve degeneration at that time point. This observation raises the question about how functional RGCs might be if only axonal injury signaling mechanisms are targeted during the course of disease.

In addition to the issue of which compartments of a neuron are degenerating, there has recently also arisen the question of which lineage of myeloid cell is affecting any given aspect of neurodegeneration. Yet there remains a paucity of neurodegenerative models wherein the myeloid innate immune system is manipulated and compartmentalized neurodegeneration tracked. The DBA/2J mouse is an excellent model to examine this issue because changes to both yolk sac derived microglia and hematopoietically-derived macrophages occur with disease progression (Bosco et al., 2011; Bosco et al., 2012; Bosco et al., 2015; Howell et al., 2012). In this dissertation, I have described how loss of the neuron to myeloid cell communication system, the fractalkine (FKN) system, affected retinal ganglion cell (RGC) compartmentalized neurodegeneration and myeloid cell recruitment in the DBA/2J. Additionally, I have identified the lineage of myeloid cells both early and later in the DBA/2J thus beginning to catalog, in a myeloid lineage-specific manner, changes to these cells throughout glaucoma progression in this chronic model.

Loss of CX3CR1 signaling differentially worsens RGC compartmentalized degeneration

The fractalkine signaling system has been used as a tool to manipulate neuron to myeloid cell communication that has resulted in context- or model-dependent interpretations as to whether or not this system is neurotoxic or neuroprotective. In Chapter 2, I determined in the DBA/2J mouse model of glaucoma that loss of the fractalkine receptor (CX3CR1) differentially affected RGC compartmentalized degeneration in a manner that was much more subtle than has been reported in more acute models of CNS injury/neurodegeneration (Cardona et al., 2006), with selective effects on axon transport. This fact highlights the need to analyze multiple neuronal compartments using multiple readouts, especially in chronic models of neurodegeneration.

My data suggest that loss of CX3CR1 worsened axonal transport deficits as measured by an increase in RGCs that had accumulated axonal proteins, phosphorylated neurofilaments (somal pNF+ RGCs) around the cell soma and dendrites, as well as by reduced mRNA for the anterograde motor protein Kif1b (25%). The reduction in Kif1b is significant because it was also reduced in sectors of DBA/2J retina depleted of RGCs labeled with a retrograde axonal tracer (Panagis et al., 2010), suggesting that reduction of Kif1b is reflecting loss of axonal transport specifically in RGCs. Further, the reduction found in my study likely is an underestimate since it was derived from whole retinas, and might have been greater if analyzed in RGCs specifically. The effect of loss of CX3CR1 was compartmentalized since RGC transcriptional dysregulation and optic nerve degeneration were unaffected. Together, these data support the idea of a novel retina-

specific degeneration pathway where myeloid cells lacking FKN signaling first disrupt RGC axonal transport. This finding is important for two reasons. First, it suggests that categorizing DBA/2J samples based solely on optic nerve degeneration, which is typically done, may miss some potentially early changes to RGCs. Second, the data suggest that in order to prevent glaucoma or restore function, the myeloid innate immune system of the retina may need to be targeted. Third, it suggests that different mechanisms may drive neurodegeneration in different compartments, possibly including loss of axonal transport by disrupted neuron to myeloid cell signaling.

Analyzing all neuronal compartments also allowed me to propose a sequence of RGC degeneration, with loss of Brn3 expression happening earlier than accumulation of somal pNF or optic nerve degeneration. This result argues that immunostaining for Brn3 may reveal early stages of glaucoma progression. Indeed, reductions in Brn3+ nuclei in DBA/2J have recently been shown at 7 months (Domenici et al., 2014), which is significantly earlier than the 10-11 month time point used in this study. In the future, it will be interesting to determine at what timepoint the population of Brn3+ somal pNF+ cell discovered here initially appears.

In addition to demonstrating how CX3CR1 affects RGC compartmentalized degeneration, my study showed that expression of the phosphatidyl-serine flippase Atp8a2 was also reduced. These results are consistent with those of (Zhu et al., 2012) who showed that loss of Atp8a2 results in disrupted axonal transport marked by increased numbers of RGCs that accumulate somal pNF without showing enhanced optic nerve degeneration. I showed by qRT-PCR experiments from whole retina that there was a significant reduction (15%) in Atp8a2 mRNA in CX3CR1 null versus control DBA/2J

retinas, a reduction that may be understated since whole retinas were used. Another limitation of this study was that many of the samples might have been depleted of RGCs (as measured by depletion of the RGC specific marker gamma-synuclein) in both the control and CX3CR1-deficient retinas thus reducing any potential difference between them. Nonetheless, these data implicate loss of Atp8a2 in the process of neurodegeneration. To further examine the role of Atp8a2 in this disease model, I would monitor its expression at earlier time points, especially since loss of axonal transport occurs relatively earlier in the DBA/2J (Crish et al., 2010). Since gene expression profiling data from cortex indicates that Atp8a2 can be expressed by neurons or microglia (Zhang et al., 2014), it will also be important to determine which cells in the retina express Atp8a2. If Atp8a2 is expressed in microglia, then it supports the hypothesis that loss of function in microglia causes a specific RGC pathology (loss of axonal transport). This would be an impactful finding because there is currently a lack of direct evidence that a loss of function in microglia contributes to neurodegeneration. Conversely, if Atp8a2 is expressed in RGCs, then it would implicate phosphatidyl-serine and the receptors that bind it as a molecular mechanism for early axonal transport deficits that are seen in many models of neurodegeneration such as Alzheimer's disease, multiple sclerosis, and ALS (Morfini et al., 2009). A third option would be a combination of these two.

Future experiments examining how loss of CX3CR1 affects RGC compartmentalized degeneration

While my data demonstrated compartmental changes that are consistent with reductions in axonal transport, I did not measure this directly. To more directly assess RGC axonal transport, we will use intravitreal injection of Cholera-toxin B (CTB) conjugated to fluorophores, since CTB requires uptake and active transport from RGCs to the superior colliculus. Since Crish et al. (2010) showed that axonal transport deficits can happen very early in the DBA/2J, we will analyze CTB levels in the superior colliculus at the 8-month time point, when they first noticed a majority of animals had anterograde axonal transport deficits, to determine if loss of CX3CR1 affects this readout. Another limitation of my study was the use of whole retina in qRT-PCR experiments that might have masked a greater reduction in gene expression in candidate genes such as Kif1b in RGCs. Since anterograde transport is disrupted early in the DBA/2J (Crish et al., 2010), and Kif1b carries important neuronal cargos such as mitochondria and synaptic vesicles (Zhao et al., 2001), getting a more precise answer as to the levels of Kif1b down-regulation in RGCs from CX3CR1 null DBA/2J retinas would be insightful. This could be accomplished by purifying RGCs through immunopanning and RNA extraction (Ivanov et al., 2006). Additionally, while my data show no effects on optic nerve degeneration at this stage, I assessed this only in the proximal optic nerve. I selected this region because it is thought to be the initial site of damage to RGC axons. However, as Crish et al. (2010) demonstrate, there are a greater number of dystrophic axonal profiles more distally in the DBA/2J optic nerve. Thus, it is possible that loss of CX3CR1 affected degeneration more distally first and that the proximal location simply had not

been affected at the 10-month timepoint. Therefore, now that we have developed better tools to assess optic nerve degeneration, it will be interesting to examine the degeneration of the optic nerve and optic tract past the chiasm at several more distal points at 10 months. At the same time, since we do not understand the relationship between myeloid cells and axon degeneration, we will sample for dystrophic profiles and examine myeloid activation in these areas. These future experiments will give a more complete answer to the question: did loss of CX3CR1 uncouple retinal from optic nerve degeneration, or did it just do so in the proximal optic nerve?

All together, these data demonstrate that loss of CX3CR1 affects neurodegeneration in a compartmentalized rather than general manner, and links the myeloid system to axonal transport deficits frequently seen in neurodegeneration. My findings also urge caution when extrapolating results from acute models to chronic ones, since loss of CX3CR1 in acute contexts has much more dramatic effects (Cardona et al., 2006). My findings also suggest that earlier pathways that potentially affect RGC function might be found by profiling RGCs according to pathology in the retina rather than the optic nerve.

Loss of CX3CR1 signaling increases macrophage infiltration but not myeloid activation overall

One of the major issues with determining the role of the myeloid innate immune system in neurodegeneration is that few investigators have manipulated it and examined how compartmentalized neurodegeneration was affected. In order to address this issue, I analyzed myeloid cells in the DBA/2J retina and determined that rather than increasing

microglial activation across all myeloid cells, loss of FKN signaling increased macrophage infiltration. I showed that amoeboid Iba1+ cells were CCR2+ and localized to the surface of the retina, as is the case for macrophages infiltrating in response to injury (Garcia-Valenzuela and Sharma, 1999) or screening the vitreous (Vagaja et al., 2012). However, despite this increase in amoeboid Iba1+ cells, the numbers of these macrophages did not correlate with RGC pathology. Lastly, numbers of presumed resident microglia were unchanged, total levels of Iba1 mRNA were unaffected, and there was no difference in microglia morphology after loss of CX3CR1, suggesting that microglia activation was not increased. However, I cannot rule out specific molecular changes to microglia that affect their function. All together, these data demonstrate that loss of CX3CR1 increases macrophage infiltration rather than overall myeloid activation, consistent with the findings of Sennlaub et al. (2013) in a mouse model of age-related macular degeneration. However, in contrast to the finding of Sennlaub et al. (2013), who showed that infiltrating macrophages on a CX3CR1 background increased neuronal apoptosis, I found that the numbers and distribution of infiltrating macrophages were not correlated to the RGC pathology that I measured. To determine whether microglia or infiltrating macrophages are contributing to RGC pathology, it will be important to determine the effect of loss of CX3CR1 in a myeloid lineage specific manner. My data are consistent with the hypothesis that a loss of function in resident microglia led to a reduction in RGC axonal transport, but so far the role of either resident microglia or macrophages has not been directly tested (see Figure 4.1A).

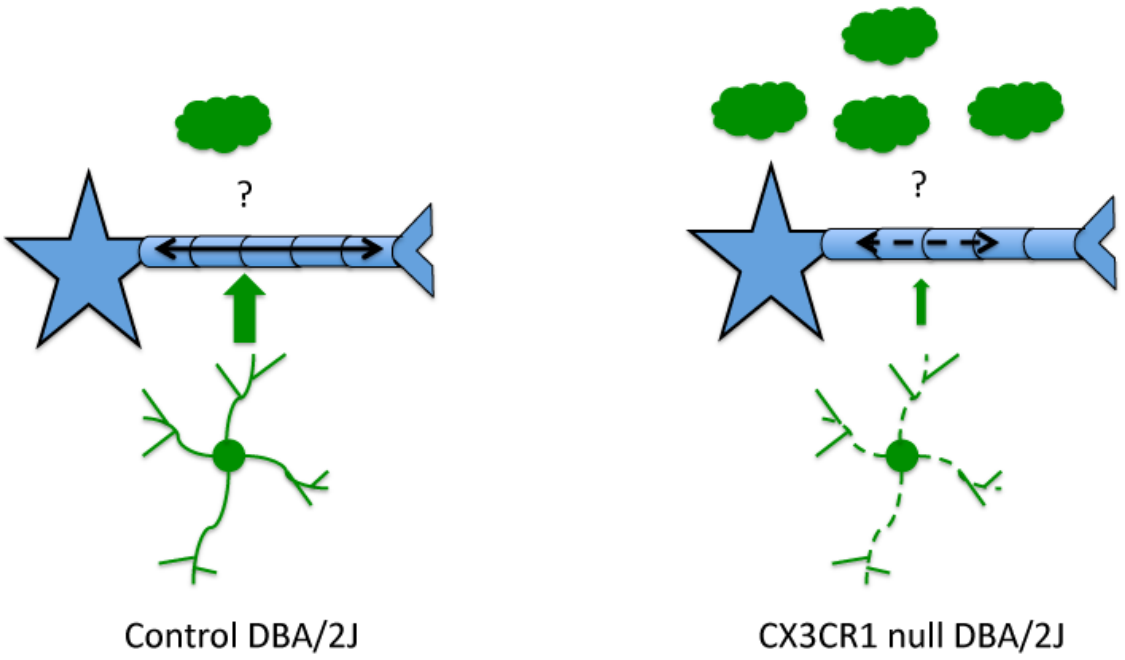

Figure 4.1: Proposed model for how loss of CX3CR1 affects retinal ganglion cell axonal transport, resident microglia, and CCR2+ infiltrating macrophages in the DBA/2J. (A) Overall the data are consistent with a loss of function model amongst resident microglia (branched green cell) that reduced axonal transport in retinal ganglion cells. Macrophage (green clouds) infiltration is increased but it is unclear what relation this has to neuronal degeneration

Future experiments examining how loss of CX3CR1 affects myeloid function and lineage specific roles in RGC neurodegeneration

While my data did show an increase in infiltrating macrophages, I did not stain branched microglia with a verified resident microglial marker such as CD39 or P2Y12. It remains possible, then, that peripheral macrophages infiltrated, downregulated CCR2, and adopted a branched shape as resident microglia, although the literature in other neurodegenerative diseases suggests this does not happen (Ajami et al., 2011). Some antibodies to these resident microglia markers exist, but another approach would be to intravenously inject EdU to label the more quickly proliferating monocytes as in Sennlaub et al. (2013). Other authors have noted upregulation of pro-inflammatory cytokines with loss of CX3CR1, which I did not address in my study. In particular, Il-1β and Tnf-α have been shown in multiple studies to be upregulated (Cardona et al., 2006; Mizutani et al., 2012; Zujovic et al., 2000). It would be important to quantify these in CX3CR1 null DBA/2J retinas, because upregulation of these cytokines would be consistent with a neurotoxic gain of function in myeloid cells.

An interesting question raised by my study is what are the direct roles of macrophages or resident microglia in RGC compartmentalized pathology? Manipulating these cells in a myeloid lineage-specific manner is the only way to untangle their contributions to pathology and answer whether a loss, a gain of function, or some combination contributed to neurodegeneration. Further, since the contributions of myeloid cells can vary wildly from being pro-regenerative to degenerative, it is crucial to more carefully tease apart their contributions (Block et al., 2007; Cui et al., 2009).

Until there is a more mechanistic understanding of these different myeloid

lineages, ablation experiments can be utilized to test their contributions to pathology. For example, macrophages can be ablated as in El Khoury et al. (2007), who showed that macrophages did not accumulate in a mouse model of Alzheimer's disease on a CCR2 genetically ablated background. In order to directly test the role of macrophages in glaucoma, existing CCR2 knock out mice could be backcrossed onto the DBA/2J background and tested for the RGC pathology measured here. Alternatives to this genetic approach include injecting clodronate liposomes to eliminate infiltrating macrophages at times selected based on the appearance of CCR2+ macrophages in the DBA/2J, although repeated injections may be necessary due to the variable age of onset and prolonged course of disease.

In contrast to infiltrating macrophages, it remains challenging to ablate resident microglia. Since microglia are dependent on CSF1R signaling for survival, administration of a CSF1R antagonist (Elmore et al., 2014) can be used to ablate microglia with apparently minimal effect on macrophage numbers (Mok et al., 2014). As Elmore et al. (2014) demonstrated, there might be a microglial stem cell that repopulates the CNS with microglia after ablation, such that chronic dosing of this drug may be necessary. However, since RGCs also express the CSF1R, there is concern that the drug may have direct effects on the RGCs (Lindqvist et al., 2010). An alternative option for microglia ablation would be to use existing mice with a floxed CSF1R allele crossed with mice expressing a tamoxifen inducible Cre driven by the CX3CR1 promoter (Goldmann et al., 2013). In these mice, specific ablation of microglia may be achieved in adult mice after administration of tamoxifen, without injury to the eye. It would be necessary in these mice to monitor levels of macrophages to measure the potential confound of

toxicity to these cells. If this strategy proves too toxic, AAVs that express Cre driven from an F4/80 promoter that target microglia (Cucchiarini et al., 2003) can be injected intravitreally in mice expressing the floxed CSF1R.

Ultimately all myeloid ablation experiments suffer from a potential interference with myeloid cell homeostatic functions. In addition, if injury is required for the ablation, there may be confounding effects from toxic gain of functions. Thus, it would be more ideal to selectively excise the CX3CR1 gene in circulating monocytes or resident microglia and measure how this affects RGC pathology such as axonal transport. These experiments are also more consistent with potential therapies than cell lineage ablation paradigms. To date, the existing tools disrupt the CX3CR1 gene throughout the entire animal whether by GFP or Cre insertion at the CX3CR1 locus (Goldmann et al., 2013). In the absence of more specific tools, carefully controlled bone marrow chimerism experiments alongside measures of RGC pathology may address whether resident microglia or macrophages drive RGC degeneration. With shielding the head, the roles of these two myeloid lineages cells can be assessed by grafting wild type marrow into CX3CR1 null DBA/2J and CX3CR1 null marrow into wild type DBA/2J mice, respectively, and measuring RGC pathology. If resident microglia are responsible for an increase in somal pNF+ RGCs as Chapter 2 suggests, then there will be more somal pNF+ RGCs in the CX3CR1 null animal reconstituted with wild type marrow than the converse.

The most useful experiment would be to conditionally and genetically inactivate CX3CR1 using a floxed allele that would only be excised by resident microglia or macrophages. Currently, we lack the specific Cre drivers to accomplish this inactivation,

but there is an increasing list of resident microglia and peripheral macrophage specific markers that may soon allow this experiment to be accomplished (Butovsky et al., 2014; Butovsky et al., 2012; Hickman et al., 2013; Saederup et al., 2010; Zhang et al., 2014). With these tools, the direct role of FKN function in either resident microglia or macrophages can be assessed in terms of their effect on RGC pathology.

All together, my findings implicate myeloid cells in neurodegeneration, and demonstrates to the field that loss of CX3CR1 in a chronic neurodegenerative context increases macrophage infiltration but not myeloid cell activation overall. The lack of correlation between infiltrating macrophages and RGC pathology is inconsistent with the model of a neurotoxic macrophage, and hints that resident microglia may have been responsible for the apparent disrupted axonal transport in the DBA/2J glaucoma model, and possibly in other neurodegenerative diseases. Interestingly, this lack of correlation, in combination with the apparent lack of change to resident microglia, raises the question of whether a loss of homeostatic myeloid function can contribute to neurodegeneration. A possible candidate gene for this mentioned above is Atp8a2. If a loss of function is found, it would be the first direct link between microglial function and neuronal pathology that has long been suggested but not shown by the literature. Additionally, any toxic gain of functions found in resident microglia would help to develop new therapies.

Early microgliosis correlates with later optic nerve degeneration and is composed of resident microglia

Although microglial activation had been demonstrated to occur in a subset of DBA/2J mice at 3 months in the retina (Bosco et al., 2011), it was unclear whether there

was any relationship to glaucoma progression. Additionally, given the findings that macrophages do infiltrate the DBA/2J retina (Howell et al., 2012), whether these CX3CR1+ cells were resident microglia or macrophages was a relevant question. This study (Bosco et al., 2015), described in Chapter 3, used confocal scanning laser ophthalmoscopy (cSLO) in vivo imaging at 3 months, assessment of optic nerve pathology at 10 months, and immunostaining using myeloid lineage-specific markers to answer these questions. We determined that early microgliosis is a strong predictor of later optic nerve pathology. We also determined that this early microgliosis was composed of resident microglia.

I contributed in crucial ways to both of these questions. Pathology in the optic nerves was scored by a novel analysis technique using binary masks to determine the percentage of optic nerve composed of non-axonal elements being glia and extracellular matrix. I created these masks and quantified the % non-axonal elements from these masks in order to establish the key correlation between early microgliosis and later optic nerve pathology. I also determined that there were very few peripheral macrophages (CD169/Sialoadhesin+ cells) in 3-month-old DBA/2J mice and validated the use of CD169 in LPS intravitreally injected mice, as well as in older DBA/2J animals. This demonstrated that microgliosis at 3 months was composed of resident microglia, confirmed earlier reports of macrophage infiltration in the DBA/2J (Howell et al., 2012), and was the first study to show CD169+ cells entering the retina in a model of glaucoma. One caveat to this study is that resident microglial markers were not used to positively identify the resident microglia. Recently, some options such as antibodies to P2Y12 and CD39 have been generated and could be validated in an LPS intravitreal injection

paradigm with markers of peripheral macrophages such as CCR2 and the resulting whole mounts analyzed for co-localization. The data predict there will not be co-localization, but the expression of these resident microglial markers remains unknown in the context of injury or within the retina. Alternatively, an existing CX3CR1 promoter-driven estrogen receptor-inducible Cre mouse exists that when crossed to a rosa26-driven lox-stop lox YFP mouse can label resident microglia. This double transgenic mouse takes advantage of the fact microglia are a stable population while monocytes proliferate and turn over. This mouse has already been used to stably label microglia with YFP at 5 to 7 weeks, while after 1 week of tamoxifen exposure less than 0.2% of circulating Ly6c^{lo} monocytes were labeled (Goldmann et al., 2013). These two constructs could be bred onto the DBA/2J background or used in Bl6 mice to verify resident microglia-specific markers.

One model in the field suggests that neuronal damage activates microglia which then become chronically activated, setting up a vicious cycle further damaging neurons (Block et al., 2007). The finding that microglial activation at 3 months in the DBA/2J retina correlates with later optic nerve degeneration, in combination with the beneficial effect of head-only irradiation at 3 months to ablate proliferating microglia, supports this model (Bosco et al., 2012; Howell et al., 2012). However, this model remains to be directly tested and has not been examined in a compartmental manner. Perhaps early microgliosis is beneficial for RGC compartments within the retina but not the nerve. It also will be important to determine the time course of RGC pathology in mice that have early microgliosis versus those that do not.

Future experiments generating a time course of RGC degeneration in the DBA/2J

The existing tools that I have used and helped verify in Chapter 2 could be used to answer these questions. cSLO imaging could be used to identify retinas with intense microglial activation and these could be stained with the RGC transcription factor Brn3 and phosphorylated neurofilament alongside histologic analysis of optic nerve degeneration as was done in Bosco et al. (2015). In particular, since Brn3 can be reduced as early as 7 months in some DBA/2J retinas (Domenici et al., 2014), it would be interesting to answer the question of how this loss of RGC transcription factors relates to microglial activation at 3 months. To date, establishing a true time course of pathology in the DBA/2J has been technically challenging because of the variability of the phenotype, resulting in large numbers of mice needed for analysis, and the assumption that pathology was not apparent until 10 months in most animals (Schlamp et al., 2006). However, with our new technique of imaging the eye to detect microgliosis at young ages, a sample could be enriched for sick retinas, potentially allowing better analysis of the time course. Further by comparing mice with different timings of microglial activation, it could be determined if there is a stereotyped sequence of pathology or whether different mice progress differently in the retina or optic nerve. These investigations might implicate new genes in glaucoma and neurodegeneration.

In addition to RGC pathology, using cSLO live imaging would allow us to ask how microglia in an activated retina are different from a quiescent retina. Since we know that the microglial activation at 3 months is composed of resident microglia that in $Cx3CR1^{gfp/+}$ animals express GFP, it would be simple to use flow cytometry to isolate

them and then profile them by RNAseq or qRT-PCR for candidate genes.

In addition to profiling microglia, with the cSLO imaging tool we could determine whether early microglia activation correlates with other early RGC pathology readouts that have been noted in the DBA/2J. For example, Crish et al. (2010) noted disrupted anterograde axonal transport in some DBA/2J mice at 3 months, and Saleh et al. (2007) found a reduction in pattern electro-retinogram amplitude (PERG, a measure of RGC electrical activity) at this same time point. Animals with intense microgliosis at 3 months could then be identified by cSLO, PERG amplitude measured, and anterograde axonal transport determined directly by fluorophore conjugated CTB intravitreal injection. If early microgliosis correlates with either of these readouts, it could then more directly be manipulated through ablation experiments or pharmacologically with minocycline as in Bosco et al. (2008), and the affect on pathology measured.

Conclusions

My work provides the framework necessary to evaluate the contributions of the myeloid innate immune system to chronic neurodegeneration. Models such the DBA/2J are critical to the neurodegenerative field, despite the technical limitations such as sample size and time constraints, because they provide a genetic, spontaneously arising neurodegenerative phenotype. However, if these models are not assessed in a compartmentalized manner, selective impacts to neurodegeneration may be missed. The case of loss of CX3CR1 exemplifies these principles. If my analysis of CX3CR1 null DBA/2J mice had solely focused on the integrity of the optic nerve, then the conclusion would have been that fractalkine signaling has no role in glaucoma progression. In

contrast, I found a retina-specific contribution of myeloid cells to RGC degeneration. Additionally, my work on microglial changes at 3 months in the DBA/2J has laid the groundwork for a study of compartmentalized time course of RGC pathology that could put forth a strong sequence of degeneration.

My work also begins to lay the foundation for determining how myeloid lineage specific cells contribute to neurodegeneration. These cells are crucial because they not only drive neurodegeneration, but also may be harnessed to ameliorate it as peripheral macrophages have been shown to do for amyloid-β deposition. However, it has been challenging to study them, since they are so rapidly plastic, derive from different myeloid lineages, and may therefore play different roles in neurodegeneration. My work demonstrates that the DBA/2J retina is a good model to study these cells because both resident myeloid cells and macrophages are involved. Further, I have shown that these infiltrating macrophages can be labeled without the need for genetic markers. Already the tools I have helped develop have suggested that these macrophages may be playing a different role, rather than driving pathology. With these markers and knowledge of which pathology to score, more direct tests of the role(s) that resident microglia and macrophage play in neurodegeneration can be performed. Studies targeting one myeloid population or the other may discover unknown genes that operate within the immune system to alter neurodegenerative progression. Furthermore, investigators can begin to ask how does one arm of the myeloid system alter the other? The contribution of resident microglia to neuronal pathogenesis, whether for good or ill, has also long intrigued investigators. If resident microglia do contribute to axonal transport deficits in a loss of function manner, this might suggest a positive homeostatic role played by microglia. Ultimately, my work

should help answer the question of whether a gain or loss of function within resident microglia or macrophages contributes to neurodegeneration, information that will be important not only for glaucoma but for many other neurodegenerative diseases. Further, studying microglia in age-related diseases may reveal how the function of these constant gardeners change over time and shed light on the reasons why some individuals become sick with age while others remain resilient.

References

Ajami, B., Bennett, J.L., Krieger, C., McNagny, K.M., and Rossi, F.M. (2011). Infiltrating monocytes trigger EAE progression, but do not contribute to the resident microglia pool. Nat. Neurosci. *14*, 1142-1149.

Block, M.L., Zecca, L., and Hong, J.-S. (2007). Microglia-mediated neurotoxicity: uncovering the molecular mechanisms. Nat. Neurosci. *8*, 57-69.

Bosco, A., Crish, S.D., Steele, M.R., Romero, C.O., Inman, D.M., Horner, P.J., Calkins, D.J., and Vetter, M.L. (2012). Early reduction of microglia activation by irradiation in a model of chronic glaucoma. PLoS One *7*, e43602.

Bosco, A., Inman, D.M., Steele, M.R., Wu, G., Soto, I., Marsh-Armstrong, N., Hubbard, W.C., Calkins, D.J., Horner, P.J., and Vetter, M.L. (2008). Reduced retina microglial activation and improved optic nerve integrity with minocycline treatment in the DBA/2J mouse model of glaucoma. Invest. Ophthalmol. Vis. Sci. *49*, 1437-1446.

Bosco, A., Romero, C.O., Breen, K.T., Chagovetz, A.A., Steele, M.R., Ambati, B.K., and Vetter, M.L. (2015). Neurodegeneration severity is anticipated by early microglia alterations monitored in vivo in a mouse model of chronic glaucoma. Dis. Mod. & Mech. *8*, 443-455.

Bosco, A., Steele, M.R., and Vetter, M.L. (2011). Early microglia activation in a mouse model of chronic glaucoma. J. Comp. Neurol. *519*, 599-620.

Butovsky, O., Jedrychowski, M.P., Moore, C.S., Cialic, R., Lanser, A.J., Gabriely, G., Koeglsperger, T., Dake, B., Wu, P.M., Doykan, C.E.*, et al.* (2014). Identification of a unique TGF-beta-dependent molecular and functional signature in microglia. Nat. Neurosci. *17*, 131-143.

Butovsky, O., Siddiqui, S., Gabriely, G., Lanser, A.J., Dake, B., Murugaiyan, G., Doykan,

C.E., Wu, P.M., Gali, R.R., Iyer, L.K.*, et al.* (2012). Modulating inflammatory monocytes with a unique microRNA gene signature ameliorates murine ALS. J. Clin. Invest. *122*, 3063-3087.

Cardona, A.E., Pioro, E.P., Sasse, M.E., Kostenko, V., Cardona, S.M., Dijkstra, I.M., Huang, D., Kidd, G., Dombrowski, S., Dutta, R.*, et al.* (2006). Control of microglial neurotoxicity by the fractalkine receptor. Nat. Neurosci. *9*, 917-924.

Crish, S.D., Sappington, R.M., Inman, D.M., Horner, P.J., and Calkins, D.J. (2010). Distal axonopathy with structural persistence in glaucomatous neurodegeneration. Proc. Natl. Acad. Sci. USA *107*, 5196-5201.

Cucchiarini, M., Ren, X.L., Perides, G., and Terwilliger, E.F. (2003). Selective gene expression in brain microglia mediated via adeno-associated virus type 2 and type 5 vectors. Gene Therapy *10*, 657-667.

Cui, Q., Yin, Y., and Benowitz, L.I. (2009). The role of macrophages in optic nerve regeneration. Neuroscience *158*, 1039-1048.

Domenici, L., Origlia, N., Falsini, B., Cerri, E., Barloscio, D., Fabiani, C., Sanso, M., and Giovannini, L. (2014). Rescue of retinal function by BDNF in a mouse model of glaucoma. PLoS One *9*, e115579.

El Khoury, J., Toft, M., Hickman, S.E., Means, T.K., Terada, K., Geula, C., and Luster, A.D. (2007). Ccr2 deficiency impairs microglial accumulation and accelerates progression of Alzheimer-like disease. Nat. Med. *13*, 432-438.

Elmore, M.R., Najafi, A.R., Koike, M.A., Dagher, N.N., Spangenberg, E.E., Rice, R.A., Kitazawa, M., Matusow, B., Nguyen, H., West, B.L.*, et al.* (2014). Colony-stimulating factor 1 receptor signaling is necessary for microglia viability, unmasking a microglia progenitor cell in the adult brain. Neuron *82*, 380-397.

Garcia-Valenzuela, E., and Sharma, S.C. (1999). Laminar restriction of retinal macrophagic response to optic nerve axotomy in the rat. J. Neurobiol. *40*, 55-66.

Goldmann, T., Wieghofer, P., Muller, P.F., Wolf, Y., Varol, D., Yona, S., Brendecke, S.M., Kierdorf, K., Staszewski, O., Datta, M.*, et al.* (2013). A new type of microglia gene targeting shows TAK1 to be pivotal in CNS autoimmune inflammation. Nat. Neurosci. *16*, 1618-1626.

Hickman, S.E., Kingery, N.D., Ohsumi, T.K., Borowsky, M.L., Wang, L.C., Means, T.K., and El Khoury, J. (2013). The microglial sensome revealed by direct RNA sequencing. Nat. Neurosci. *16*, 1896-1905.

Howell, G.R., Soto, I., Zhu, X., Ryan, M., Macalinao, D.G., Sousa, G.L., Caddle, L.B., MacNicoll, K.H., Barbay, J.M., Porciatti, V.*, et al.* (2012). Radiation treatment inhibits

monocyte entry into the optic nerve head and prevents neuronal damage in a mouse model of glaucoma. J. Clin. Invest. *122*, 1246-1261.

Ivanov, D., Dvoriantchikova, G., Nathanson, L., McKinnon, S.J., and Shestopalov, V.I. (2006). Microarray analysis of gene expression in adult retinal ganglion cells. FEBS Letters *580*, 331-335.

Libby, R.T., Li, Y., Savinova, O.V., Barter, J., Smith, R.S., Nickells, R.W., and John, S.W.M. (2005). Susceptibility to Neurodegeneration in a Glaucoma Is Modified by Bax Gene Dosage. PLoS Gen. *1*, e4.

Lindqvist, N., Lonngren, U., Agudo, M., Napankangas, U., Vidal-Sanz, M., and Hallbook, F. (2010). Multiple receptor tyrosine kinases are expressed in adult rat retinal ganglion cells as revealed by single-cell degenerate primer polymerase chain reaction. Upsala J. Med. Sci. *115*, 65-80.

Mizutani, M., Pino, P.A., Saederup, N., Charo, I.F., Ransohoff, R.M., and Cardona, A.E. (2012). The fractalkine receptor but not CCR2 is present on microglia from embryonic development throughout adulthood. J. Immunol. *188*, 29-36.

Mok, S., Koya, R.C., Tsui, C., Xu, J., Robert, L., Wu, L., Graeber, T.G., West, B.L., Bollag, G., and Ribas, A. (2014). Inhibition of CSF-1 receptor improves the antitumor efficacy of adoptive cell transfer immunotherapy. Cancer Res. *74*, 153-161.

Morfini, G.A., Burns, M., Binder, L.I., Kanaan, N.M., LaPointe, N., Bosco, D.A., Brown, R.H., Jr., Brown, H., Tiwari, A., Hayward, L.*, et al.* (2009). Axonal transport defects in neurodegenerative diseases. J. Neurosci. *29*, 12776-12786.

Panagis, L., Zhao, X., Ge, Y., Ren, L., Mittag, T.W., and Danias, J. (2010). Gene expression changes in areas of focal loss of retinal ganglion cells in the retina of DBA/2J mice. Invest. Ophthalmol. Vis. Sci. *51*, 2024-2034.

Saederup, N., Cardona, A.E., Croft, K., Mizutani, M., Cotleur, A.C., Tsou, C.L., Ransohoff, R.M., and Charo, I.F. (2010). Selective chemokine receptor usage by central nervous system myeloid cells in CCR2-red fluorescent protein knock-in mice. PLoS One *5*, e13693.

Saleh, M., Nagaraju, M., and Porciatti, V. (2007). Longitudinal Evaluation of Retinal Ganglion Cell Function and IOP in the DBA/2J Mouse Model of Glaucoma. Invest. Ophthalmol. Vis. Sci. *48*, 4564-4572.

Schlamp, C.L., Li, Y., Dietz, J.A., Janssen, K.T., and Nickells, R.W. (2006). Progressive ganglion cell loss and optic nerve degeneration in DBA/2J mice is variable and asymmetric. BMC Neurosci. *7*, 66.

Sennlaub, F., Auvynet, C., Calippe, B., Lavalette, S., Poupel, L., Hu, S.J., Dominguez, E.,

Camelo, S., Levy, O., Guyon, E.*, et al.* (2013). CCR2(+) monocytes infiltrate atrophic lesions in age-related macular disease and mediate photoreceptor degeneration in experimental subretinal inflammation in Cx3cr1 deficient mice. EMBO Mol. Med. *5*, 1775-1793.

Soto, I., Oglesby, E., Buckingham, B.P., Son, J.L., Roberson, E.D.O., Steele, M.R., Inman, D.M., Vetter, M.L., Horner, P.J., and Marsh-Armstrong, N. (2008). Retinal Ganglion Cells Downregulate Gene Expression and Lose Their Axons within the Optic Nerve Head in a Mouse Glaucoma Model. J. Neurosci. *28*, 548-561.

Vagaja, N.N., Chinnery, H.R., Binz, N., Kezic, J.M., Rakoczy, E.P., and McMenamin, P.G. (2012). Changes in murine hyalocytes are valuable early indicators of ocular disease. Invest. Ophthalmol. Vis. Sci. *53*, 1445-1451.

Zhang, Y., Chen, K., Sloan, S.A., Bennett, M.L., Scholze, A.R., O'Keeffe, S., Phatnani, H.P., Guarnieri, P., Caneda, C., Ruderisch, N.*, et al.* (2014). An RNA-sequencing transcriptome and splicing database of glia, neurons, and vascular cells of the cerebral cortex. J. Neurosci. *34*, 11929-11947.

Zhao, C., Takita, J., Tanaka, Y., Setou, M., Nakagawa, T., Takeda, S., Yang, H.W., Terada, S., Nakata, T., Takei, Y.*, et al.* (2001). Charcot-Marie-Tooth disease type 2A caused by mutation in a microtubule motor KIF1Bbeta. Cell *105*, 587-597.

Zhu, X., Libby, R.T., de Vries, W.N., Smith, R.S., Wright, D.L., Bronson, R.T., Seburn, K.L., and John, S.W. (2012). Mutations in a P-type ATPase gene cause axonal degeneration. PLoS Gen. *8*, e1002853.

Zujovic, V., Benavides, J., Vige, X., Carter, C., and Taupin, V. (2000). Fractalkine Modulates TNF-a Secretion and Neurotoxicity Induced by Microglial Activation. Glia *29*, 305-315.